Light Curves of Supernovae Type I

Inauguraldissertation

zur
Erlangung der Würde des Doktors der Philosophie
vorgelegt der
Philosophisch-Naturwissenschaftlichen Fakultät
der Universität Basel

von

Bruno Leibundgut

aus Affoltern i.E. (Bern)

Basel, 1988

Genehmigt von der Philosophisch-Naturwissenschaftlichen Fakultät

auf Antrag der

Herren Professoren Dr. G.A. Tammann und Dr. U.W. Steinlin

Basel, den 6. Dezember 1988

Prof. Dr. Werner A. Gallusser

Dekan

Table of Contents

1. Introduction

a) History

The phenomenon of supernovae (SNe) has, since they were recognised as an own class of objects apart from normal novae, risen to become a topic of many detailed studies (for reviews see e.g. Minkowski 1964, Trimble 1982, Rees and Stoneham 1982, Bartel 1985, Woosley and Weaver 1986). The separation from other explosive variable stars was forced by the very luminous "nova" S Andromedae which appeared 1885 in the spiral nebula M31 (the Andromeda nebula) and was about four magnitudes brighter than other novae observed in the same object. If S And would have been a normal nova, then it would have been clear evidence that the spiral nebulae found in the sky lie inside our Milky Way and the idea of Island Universes would have been wrong. But already at that time Lundmark (1920, as cited by Trimble 1982) mentions the possibility of a distinct "subclass" of very bright novae. The argumentation turned around after the discovery of cepheid stars in the Andromeda nebula by Hubble (1925a, 1925b). Now there was a superluminous object, that appeared last century in M31. This together with some observations of other extragalactic "novae" led Zwicky and Baade in the early thirties to introduce the new class of "super-novae" (e.g. Baade and Zwicky 1934a, 1934b). In a remarkable paper Zwicky (1938) foresaw many then yet unobserved features and outcomes of SNe. He predicted neutron stars whose existence was shown only 31 years later by the discovery of pulsars. He also mentioned topics like the problem of the energy production in the stars and the origin of cosmic rays. In this paper a first estimate of a supernova rate for "average" galaxies is made based on a search performed with a little 18-inch Schmidt telescope at Caltech. Further he draws the attention on the importance of studying light curves and spectroscopic observations of supernovae as sources of understanding the interiors of exploding stars.

Luckily, he and Baade had among their first discoveries the supernovae in IC 4182 and NGC 1003. These two supernovae, SN 1937C and SN 1937D, in modern nomenclature - again proposed by Zwicky (Zwicky et al. 1963) -, are among the best observed until today. SN 1937D reached a maximum brightness $m_{pg}^{max}=12^m.2$ and has an extraordinarily well observed light curve in the photographic magnitude system used in those days (Minkowski 1964) and SN 1937C ($m_{pg}^{max}=8^m.5$) was until SN 1986G and SN 1987A appeared the brightest supernova of this century and has one of the longest observed light curves (more than 400 days) until present (Minkowski 1964; his Figure 1). The extensive study of its spectral evolution (Minkowski 1939) is still used as a set of standard spectra for the comparison of supernovae (e.g. Kirshner et al. 1973a, Oke and Searle 1974).

Since supernovae are so elusive (for SNe rates see e.g. Tammann 1982, Branch 1986, McClure et al. 1987, van den Bergh 1987, Cappellaro and Turatto 1988) and are found very seldom, several supernova searches have been undertaken to broaden the

little knowledge. Zwicky himself was the first to start such a project and followed the search he initiated until the sixties, when colleagues from Caltech took over the programme (Zwicky 1964, Kowal and Sargent 1971). Several catalogues of SNe have been published. The most recent in 1984 (Barbon et al. 1984) lists 568 supernovae discovered between 1885 (S And) and the end of 1983. A new catalogue is planned which will include all SNe discovered until the end of 1988 (Barbon et al. 1988). Nowadays many searches are under way or have terminated recently, so that the number of SNe in the last years has increased rapidly. The determination of the supernova rate(s) has been refined from the crude estimates by Zwicky (1938) to extended studies of biasing influences on the detection possibilities in different galaxy types and for different SNe subclasses (see below).

Very soon it has been noted, that not all supernovae showed the same spectra nor the same spectral evolution and light curves. SN 1940B in NGC 4725 became the first supernova of what today is called Type II (Minkowski 1941). The bright ones earlier (SNe 1937C and 1937D) were of what now is known as Type I(a). Zwicky later introduced three more subclasses (Zwicky 1962) but Minkowski (1964) and others (Kirshner et al. 1973a, Oke and Searle 1974) returned to the separation into two groups. The main distinguishing spectral feature are the presence (SNe II) or the absence (SNe I) of hydrogen lines. This seemed by then the only secure way to define the subtype of an observed supernova event. All other proposed criteria could not separate unambiguously the two subclasses (e.g. Barbon et al. 1973a, Barbon et al. 1979, Doggett and Branch 1985 for light curves; van den Bergh 1983, van den Bergh 1988a for remnants). Nevertheless there are properties that suggest a possible supernova type. These are:

- SNe I show a surprisingly small scatter around a template curve (Cadonau 1986, Cadonau et al. 1985, Barbon et al. 1973a, Doggett and Branch 1985).

- light curves with a plateau are always Type II events (Barbon et al. 1979).

- a pulsar (neutron star) always is a sign that a massive star exploded (SN II, but see below for new developments).

- a non existing compact centre indicates type I SNe, but this does not apply for all known SN remnants. Crucial for this determination are theoretical models and the few historical SNe for which the remnant must be identified and the light curve estimated (with the problems cited above). These historical SNe are namely SN 1006, SN 1054, observed by Chinese astronomers and today as the Crab nebula, SN 1181, what today is the radio source 3C58, Tycho's supernova

(SN 1572), Kepler's supernova (SN 1604) and the bright radio source Cas A, which represents the remnant of a supernova around 1670 with no known observations (for a review of historical SNe see Clark and Stephenson 1977).

- radio detection of a supernova normally implies a SN II (but some SNe I have been detected, too; see below).

- the location in a young stellar population, e.g. near a HII region or in the disk of spiral galaxies, or in a region of old stars, e.g. galaxy halos, suggest SNe II and SNe I, respectively (Maza and van den Bergh 1976, Richter and Rosa 1984, Huang 1987, but see Oemler and Tinsley 1979, Tinsley and Oemler 1980). Here again, there is a new development described later.

- all SNe discovered in elliptical galaxies so far were SNe I.

With this set-up (two subclasses distinguished mainly by spectral features) the discussion on the observational side turned to the errors in the measurements and the trial to detect more differences between the individual members of the groups. For SNe II it was clear, that there was a broad scatter in the specific supernova features. This could be explained by theoretical models based on explosions of massive stars. The case of SNe I was distinct. The small deviations from (best observed) "standard" supernovae like SNe 1937C, 1937D, 1962L, 1972E, 1981B (for a complete list see Cadonau 1986) in almost all aspects, gave hope to provide a new standard candle for the determination of cosmological distances (e.g. Wheeler 1980, Bartel 1985). On the other hand this posed a difficult problem to theorists with models that did not always expect the same behaviour (e.g. Trimble 1982).

The state of the theory at the beginning of the eighties was (according to Trimble 1982) more or less as follows:
"All we need for a Type II is a kindly little genie willing to deposit $\geq 10^{51}$ erg at the base of a $\geq 5M_{\odot}$ envelope of solar composition and supergiant structure... And if the same genie will be good enough to put $\sim 1M_{\odot}$ of Ni^{56} in the portion of the hydrogen-poor star that is being disrupted by detonation or deflagration..." we will have a Type I. But she continues: "In both cases the genies have proven either uncooperative or inept."

Nevertheless the basics were known, as being:

- Type II:

A single massive star ($M \geq 7M_{\odot}$) explodes when the degenerate iron core, produced by stellar nucleo-synthesis during the evolution of the star, reaches the Chan-

drasekhar mass limit and collapses in a few microseconds, because of photodesintegration of the Fe and subsequent electron captures. This goes on to neutron star densities. There a process for the inversion of the implosion into an explosion of the envelope has to emerge. Two processes were proposed. One was the so called neutrino transport mechanism, i.e. neutrinos emitted from the collapsed core deposit their energy in the mantle that is freely falling onto the core and reverse the direction of the shock. The other was, a core bounce, where the densities in the core pass even nuclear densities and the core bounces back producing a pressure shock wave, that rushes through the infalling material.
Both ideas were burdened with several problems (Trimble 1982 and references therein).

- Type I:

There were three feasible models producing a clump of degenerate carbon and oxygen of Chandrasekhar mass:

1. a 4 - 8 $M_\odot$ main sequence star loosing the hydrogen envelope during its evolution, which then would explode in a carbon detonation or deflagration.

2. a 8 - 10 $M_\odot$ star with the same fate as before disrupted in the end by a carbon deflagration.

3. a star with 1.4 - 4 $M_\odot$ at the beginning of his life that would end in igniting carbon and oxygen.

But all these cases of single star models were less favoured against the double star scenario, in which almost every combination of initial conditions evolved into a reasonable progenitor of a supernova. Several groups agreed on the basic concepts of the evolution and produced detailed models containing a carbon-oxygen white dwarf accreting mass from its companion and eventually surpassing the Chandrasekhar limit. These stars would be disrupted completely, so that no relic star remained. (There were some other models producing a compact remnant even for SNe I). The most important feature of all these models is the production of radioactive Ni^{56} with a decay via electron capture and γ-emission to Co^{56} which in turn decays with various γ transitions to Fe^{56}. For the late time evolution of SNe I it has been shown, that the same process can power the light curve (Axelrod 1980, and references therein).

b) The discovery of SNe Ib

The progress in theory led to further refinement in these views, which will be described later. Observations of new SNe after 1982 revealed a new subtype in the class of type I supernovae which caused a dramatic change in the picture. SN 1983N in M83 (NGC 5236) was discovered early in its evolution (several days before maximum, Richtler and Sadler 1983) and had a moderately defined light curve (Cadonau 1986). A year later SN 1984L in NGC 991 started a little revolution, when Wheeler and Levreault (1985) found, that the spectrum of this supernova differed distinctly from the ones of normal SNe I in lacking a broad absorption feature at about 6150Å, while still resembling a type I spectrum as it did not show any hydrogen lines. They also cite a few cases with similar properties as SN 1984L, namely SNe 1962L, 1964L, and 1983N. SNe 1962L and 1964L (Bertola 1964, Bertola et al. 1965) were assigned already "peculiar I" supernovae because of exactly this abnormality in the (photographical) spectra. SN 1983N, because of its brightness, quickly evolved into the standard supernova of the new subclass nowadays called Type Ib (the old type I or normal type I became Ia). The ultraviolet behaviour did not digress much from other SNe I observations, but - as in the optical - the spectrum resembled more a supernova after than before maximum although the light curve was still rising (Panagia 1984). This object also was the first supernova type I with a measured radio emission (Sramek et al. 1984), the first SN in which a strong Fe emission was detected (Graham et al. 1986) and - maybe the strongest indication for being a distinct subclass of SNe I - its infrared light curve deviated strongly from standard Ia curves (Elias et al. 1985). Furthermore this new group of supernovae seemed to be "subluminous" in respect to their maximum light compared to normal SNe Ia, which threatened the proposition, that SNe I could be good standard candles. Yet another property of all these SNe Ib is their position close or even in HII regions, indicating, that the progenitor stars of these explosions were young, whereas SNe Ia were thought to be produced by old stars. A further discovery introduced another new aspect of these new objects: in a series of papers Filippenko and Sargent (1985, 1986) and Filippenko et al. (1986) described a supernova they discovered accidentally in an HII region in NGC 4618 (SN 1985F), which had a very peculiar appearance. They proposed, that it was a supernova several months after maximum light and, because of its non-detection near maximum, that it had been "subluminous". Soon afterwards a comparison of the late time spectra of SN 1983N and spectra of SN 1985F (Gaskell et al. 1986) showed, that SN 1985F was indeed a type Ib supernova. With this, the new subclass had been firmly established. As will be shown in this work, there are almost no differences in the shape of optical light curves between the type Ia and Ib. The main distinguishing properties are:

- the lack of the spectral absorption feature at 6150Å (near the maximum phase)

- a probable subluminosity in comparison to SNe Ia

- red colours (e.g. B-V)

- parent galaxy is a late spiral

- close neighbourhood to an HII region

- radio emission

- He emission lines in the spectra (Harkness et al. 1987)

- distinct infrared light curve (Elias et al. 1985).

A search through the list of all supernovae discovered in the past has been performed by several authors (e.g. Uomoto and Kirshner 1985, Panagia et al. 1986, Filippenko 1986, Porter and Filippenko 1987)

An actual list of known type Ib supernovae may include:

Supernova	Galaxy	remarks
SN 1962L	NGC 1073	
SN 1963J	NGC 3913	
SN 1964L	NGC 3968	
SN 1975B	anonymous	
SN 1976B	NGC 4402	
SN 1982R	NGC 1187	
SN 1983N	NGC 5236 (M83)	
SN 1983I	NGC 4051	
SN 1983V	NGC 1365	
SN 1984L	NGC 991	
SN 1985F	NGC 4618	
SN 1986M	NGC 7499	Filippenko and Shields 1986b
SN 1987K	NGC 4651	Filippenko 1988a
SN 1987M	NGC 2715	Filippenko 1987, Porter 1987
SN 1988L	NGC 5850	Filippenko 1988b, Graham 1988b

That in recent years more SNe Ib were discovered than earlier reflects the difficult detectability on a photometric basis. Only new detectors (especially for spectroscopy) allow to disentangle the details, that indicate a completely different event. Another remark has to be made here. Some years ago there was a suggestion, that SN I would have young progenitors (Oemler and Tinsley 1979, Tinsley and Oemler 1980), although most people thought SNe I would arise from an old population of stars (Tammann 1982, Maza and van den Bergh 1976). This problem was solved in a very natural way in assuming that SNe Ib stem from young stars and SNe Ia have an old stellar population providing the progenitors. The difficult task of determining separate explosion rates for Ia and Ib has been attempted (Branch 1986,

Tornambé and Matteucci 1987), but the data are still too scarce and any approach based on old SNe suffers from heavy biasing. The optical light curves of SNe Ib have not been described, because there is little or no deviation from the known standard Ia curves. Again the data available is not sufficient to draw strong conclusions. Taking this into account, theory has made astonishing progress in understanding SNe Ib. There have been hints in the literature like: "Extended helium envelopes are also possible,...but explosions inside them would look more like SN I's than SN II's." (Trimble 1982). So it is not surprising, that rapidly models with a massive core exploding under a large helium envelope ($M \geq 5M_\odot$) appeared (Harkness et al. 1987) or massive stars like Wolfe-Rayet stars ejecting their hydrogen envelope by a strong stellar wind and therefore resembling a highly evolved helium-oxygen star (Begelmann and Sarazin 1986, Gaskell et al. 1986, van den Bergh 1988b). Other ideas are hydrogen deficient binaries consisting of a helium supergiant and a hot main-sequence star (Uomoto 1986) or the off centre explosion of an accreting white dwarf in a binary system (Branch and Nomoto 1986, Iben et al. 1987). Some models leave compact relics (the massive star models) others disrupt the star totally. There is still much discussion on this topic. The observed radio emission is explained as an interaction with surrounding matter like shells ejected from the star earlier or interstellar matter.

c) SNe II models

A simplified view of the SN II theory today (based on Woosley and Weaver 1986) describes the evolution of massive stars ($M \geq 8M_\odot$) into explosive end phases as follows. A core of He, C, Ne is built up in smaller stars ($8M_\odot \leq M \leq 11M_\odot$) and collapses because of electron capture and subsequent loss of pressure to hold the envelope. More massive stars evolve into red supergiants containing an iron core, which contracts rapidly as photodesintegration and electron capture set in. In each case the core collapses to nuclear densities ($\sim 3 \cdot 10^{13}$ g cm^{-3}) in a short time (a few milliseconds). The model with a core bounce and an outgoing shock wave, as described above, works only for a small range of initial masses and cannot provide the mechanism for very massive stars. But a new model of "delayed" explosions has come up. The problem in the bounce theory was that the outgoing shock wave died out very fast, because of energy losses due to photodesintegration and neutrino emission. In the "delayed" explosion a neutrino energy transport takes place and refuels the shock. This happens as neutrinos, carrying $\sim 10^{53}$ erg of energy, deposit a small fraction ($\leq 5\%$) in the wave and strengthen it again. This model also allows the core to collapse into a black hole, if the star is massive enough. This leads to SN II with $\sim 10^{50}$ erg of optical energy output. Whether this really works is still a matter of dispute. The light curves of the p-type (plateau, cf. Barbon et al. 1979) can be described fairly well, with the additional assumption, that little Ni^{56} is produced to power the curves at the late times. The l-type

(linear) curves still lack a considerable amount of understanding, but seem again to depend on the mass of Ni^{56} produced during the explosion. As mentioned before, SNe II represent a very inhomogenous group of objects and resemble SNe Ia only in their energy output and luminosities. Another problem arose with SN 1987A, for which for the first time the progenitor star is known as being a blue supergiant of the spectral class B Ia contradicting the so far assumed red supergiants as precursors of SNe II. This supernova showed an unprecedented light curve and ultraviolet behaviour, but confirmed the predicted neutrino emission, as a neutrino burst was measured by two groups (cf. Danziger 1987), showing that, what can be seen in the optical is only a small fraction ($\sim 10^{-3}$) of all energy freed in a SN II explosion.

d) SNe I

Concerning SN I, there exists a general consent on a concept for the mechanism of the explosion of a white dwarf (cf. for a review Woosley and Weaver 1986). Emerging from the fact, that SNe I show a remarkable resemblance in almost all observable quantities, one was forced to look for what some people call "a fine tuned" bomb. Out of a number of proposed models, like the hydrodynamic explosion of stellar cores or pulsar-driven explosions, nowadays most people concentrate on the thermo-nuclear disruption of a white dwarf (Woosley and Weaver 1986 and references therein, but see also Lopez et al. 1986a, 1986b, Canal et al. 1988). Even with this decision there is room left for a variety of choices. Mainly discussed are models, where the white dwarf explodes by means of a detonation (either helium or carbon) or deflagration (carbon). The difference is that in a detonation the thermo-nuclear burning moves supersonic through the star increasing density and pressure in the wave, whereas in a deflagration the front propagates subsonic and diminishes the pressure and the density. These two main tracks lead to different ways of explosion and could provide a possibility to find a reasonable explanation for the above mentioned type Ib subclass. Despite all these alternatives a "standard model" for SNe Ia has emerges based on an idea worked out by Nomoto et al. (1984). Their best fitting model (W7) consists in a 1 $M_\odot$ white dwarf accreting hydrogen and helium in a binary system at a rate of $4 \cdot 10^{-8}$ $M_\odot$ yr^{-1}, which is a relatively high rate and speaks for a close system. The evolution of this system leads to a heating of the white dwarf and a mass increase until it reaches ~1.4 $M_\odot$ and the density near the centre is near $3 \cdot 10^9$g cm^{-3} and ignites the carbon in the core of the star. Because of the highly degenerate electrons, the principle flash in the core grows into a thermo-nuclear runaway building up elements until the nuclear statistical equilibrium is reached, i.e. producing mainly Ni^{56}. The energy generated is not high enough to produce a detonation wave, or if so the detonation dies out very soon, and a deflagration moves outwards. A total of $1.8 \cdot 10^{51}$erg of nuclear energy is set free, which goes

into $1.3 \cdot 10^{51}$ erg of kinematic energy and only a very small fraction into neutrinos. During the explosion ~0.6 $M_\odot$ Ni^{56} is produced, which is just right to power the observed light curve by means of radioactive decay of Ni^{56} to Co^{56} and to Fe^{56} (Axelrod 1980, Woosley and Weaver 1986, Woosley, Taam and Weaver 1986, Graham 1987). Furthermore the total mass of iron group elements is $\geq 0.86 M_\odot$ and in the outer layer, where the deflagration wave dies out and the material is only partially burned ~$0.27 M_\odot$ of elements between silicon and calcium is generated. The predicted spectra agree remarkably well with the observations (Branch et al. 1985, Axelrod 1980). Other observed features are reproduced as well. So these SNe originate from old stars, namely white dwarfs with accretion, inferred from the fact, that these supernovae occur in elliptical and are not confined to the disk or the spiral arms in spiral galaxies. There is, of course, no hydrogen in the explosion and only a weak neutrino flux is expected. The remnant contains no compact component, i.e. no neutron star (pulsar) or black hole, as the white dwarf is disrupted and there is no collapse.

As successful as the model is so far, it leaves several questions open. One problem is, that there is an over-production of iron group elements in comparison to what is found in the solar neighbourhood. This means, that if all heavy elements are produced by SNe I, we would expect much more iron and ironlike products. No fine tuning of the explosion and the subsequent evolution can bring relieve yet. Another problem are the number of possible progenitor systems for SNe Ia. The long-lasting believe, that a degenerate CO white dwarf, companion of a red supergiant, would be suitable, has been shown to fail (Iben and Tutukov 1985). The production rate of SNe Ia would be far too low for the observed number. The real problem is, how the white dwarf can accrete enough helium or even heavier elements without expelling it again in shell flashes and nova-like eruptions. This could be solved by a closed system of two degenerate white dwarfs, that looses gravitational energy by radiating gravitational waves and the two components eventually merge. But again, the difficulty arises, that an accretion disk would form rather than an accretion flow onto the star. Other models are even more specific in the choice of the components and therefore more unlikely.

Finally we might address the problem of SNe being standard candles. It is clear, that in the case of type II events there is no hope for a uniform behaviour and hence a common luminosity. The hope remains for the type I's. Here it turned out, that the subclass of Ia's still shows a very narrow range of intrinsic scatter around the template behaviour. The understanding of the theory has strengthened this view. Nevertheless the new subclass of Ib's contaminates the sample and such cases have to be sorted out very carefully, mainly by spectroscopic observations or infrared light curves. For the SNe Ia several groups attempted a calibration and a distance determination (Elias et al. 1981, 1985, infrared; Sandage and Tammann 1982, Tammann 1982, Branch 1982, 1985, Cadonau et al. 1985, optical). Most interestingly

there has been an speculation in calculating the Hubble parameter H_o in a theoretical approach by computing the mass of Ni^{56} produced in a SN Ia (Arnett et al. 1985, Wheeler and Sutherland 1985). A new caveat using SNe Ia as a distance indicator, i.e. their degrees as standard candles, has risen lately. There are indication, that differences in the expansion velocities of SNe Ia exist (Branch 1987, Schneider et al. 1987, Branch et al. 1988). Nevertheless this argument is based on two cases only, namely SN 1984A and SN 1987D. The latter having only one line differing substantially from "normal" velocities and SN 1984A is still contradictory (Pearce et al. 1988). For the distance scale also a supernova in a galaxy with primary calibrator (e.g. cepheids), distance would be needed for an absolute calibration. Because of this no absolute determination for H_o and q_o is possible (not mentioned is the problem of internal absorption in galaxies). Finally also in this subclass we have to mention a few cases of "peculiar" events (SNe 1971G, 1971I and 1974G). Then again SN 1984A, which seems to have a light curve dropping to fast (Graham 1988a). An even more intriguing case is SN 1986G, which by its spectrum is classified as a type Ia, but exhibits a much to narrow peak in the optical light curves and a very strange infrared behaviour, that does not follow any known template (Phillips et al. 1987, Frogel et al. 1987). Somehow it is suspect, that many of nearby occurred SNe show a strange, unexpected evolution in (optical) light curves. This includes SN 1987A (type II), SN 1986G, SN 1885 and SN 1604 (Kepler's).

In this work we focus on SNe I in the optical B, V and U and the infrared J, H and K filters. Chapter 2 is an overview on previous approaches. The light curves of SNe Ia and their implications are described in chapter 3. Two effects neglected so far in supernova observations are presented in the following sections (4 and 5). The case of SNe Ib is discussed next (chapter 6). Then we address the unique SN 1986G, which poses severe problems to the uniformity of the class of SNe Ia (chapter 7). In chapter 8 differences in two-colour diagrams, luminosities and bolometric light curves are discussed. Absolute magnitudes are derived in chapter 9, where also the character as standard candles of SNe Ia is investigated. The conclusions are given in chapter 10.

2. Light Curves of Supernovae Type I

Zwicky (1938) pointed out very early the importance of light curves for the understanding of supernovae. At the beginning of supernova research they were the most applicable and easiest method for the collecting of data of such objects. Spectroscopy had to fight low sensitivity and the broad often blended P Cygni type lines were hard to interpret. So photometry was the only technique to collect enough data for comparison between individual events. This changed with the advent of new instrumentation for spectroscopy and other regions of the electromagnetic spectrum than the optical. Nevertheless light curves still remain an important tool in determining an overall picture of what happens in an exploding star and also to connect older data with new observations and theories. Several groups have tried to classify distinct subclasses of curves and hitherto subtypes of supernovae (Barbon et al. 1973a, Pskovskii 1967, 1968, 1971, 1977, 1984, Younger and van den Bergh 1985, Doggett and Branch 1985, but see also Cadonau et al. 1985 and Cadonau 1986). In his review Minkowski (1964) shows curves of various SNe, but does not combine them. Many observations were published for individual supernovae (for a list of references for SNe until 1983 see Barbon et al. 1984 and Cadonau 1986, only for type I's). The first to join colours and magnitudes of different data sets into one diagram was Pskovskii (1967, 1968). He was followed by Barbon et al. (1973a). Further work was done by Pskovskii (1971, 1977, 1984), Barbon et al. (1979), Younger and van den Bergh (1985), Doggett and Branch (1985), Cadonau et al. (1985) and Cadonau (1986). All combining work fights a severe problem: the inhomogeneity of the available data. As it has been collected from many different observations by many observers with individual instruments and at different epoches, it is very difficult to normalise them in a reasonable manner. As a main problem we mention the conversion of eye witness magnitudes into the modern filter band luminosities (for all historical supernovae) and from photographic into photometric magnitudes. Let us add, that also the transformation of CCD magnitudes into the photoelectric system is not trivial. The search for subclasses with this data ended in the known subdivisions of type I and type II supernovae. In the class of SNe II a further distinction between plateau and linear type curves was found (Barbon et al. 1979, Doggett and Branch 1985). For the SNe I three approaches of a further classification exist.

A determination of several empirical parameters of the (B and pg) light curve was attempted by Pskovskii (1967, 1971, 1984, Branch 1982, Phillips et al. 1987). They are the rates of the increase of brightness before and the decrease shortly after maximum and in the final decay phase and the time of the so called "inflection" or "bending" point, when the slope changes between the early and late phases, as well as the magnitude difference between maximum light and the "bending" point. The often used and obviously most relevant parameter seems to be β, the rate of the decline during the steep decrease in the first

days after maximum (measured as Δm/100days). So every individual supernova I can be ascribed to a subclass with more or less distinctive parameters. We believe, that because of the inhomogeneities of the existing data and the often inaccurate measurements, this approach is too detailed to describe supernovae. We will also show, that the value of β depends on the degree of reddening of a supernova in the special cases of SNe Ia and, that a somewhat different parameter could suggest a distinction of the SNe Ib from SNe Ia.

Another attempt to classify SNe I was made by Barbon et al. (1973a) and Barbon (1980) with the subdivision into "fast" and "slow" decaying mode supernovae. This is again based on photographic and B photoelectric data. It has been shown, that this separation depends strongly on observations and does not hold for all SNe I (Cadonau et al. 1985, Cadonau 1986). Since a new subclass (SNe Ib) is established, we think that this subdivision is obsolete.

A third group tried to show, that there are no further subtypes in the class of SNe I (Tammann 1982, Cadonau et al. 1985, Cadonau 1986). This does not hold any longer, as SNe Ib have clearly been identified as a subgroup.

Our point of view will be, that there is indeed a distinct subclass of type I supernovae, namely the Sne Ib, which is clear by the arguments mentioned in chapter I, and we will try to show the real differences in the light curves of 6 filter bands (UBVJHK) by constructing "standard" curves for the subtypes of supernovae I in each filter. A third case will be considered: SN 1986G in Cen A (NGC 5128), which displayed very strange, uncommon light curves.

3. Light Curves of Supernovae Ia

a) Construction of the light curves and the set of standard SNe Ia

Since the contamination of SNe I by the "peculiar" SNe Ib has been recognised the nomenclature Ia is used for the "normal" SNe I. All studies of light curves before the separation of the Ib-subtype could only treat a combination of the two groups. Therefore all these studies support the view, that the subclass of SNe Ib differs little from the supernovae Ia, considering the optical curves (UBV). Although there is at least one SN Ib (SN1962L) in the sample for the determination of the standard light curves in B, V and U in the work of Cadonau (1986), we used only slightly modified curves. The modification consists in omitting "smoothing" points and simply joining the three segments of his light curves, being the rising phase, which was fitted by a linear equation, the peak, a polynom of 10th power, and the final decay, again a linear approximation. The parameters of the curves are given in Table 1. Furthermore we normalised the curves to have 0 magnitude at the time of the maximum brightness in B. Throughout this paper the time t_o will be fixed to this epoch of a supernova. Due to this normalisation both the V as well as the U have negative values at their maximum brightness, which occur at $t_o=2^d$ and $t_o=-3^d$ for V and U, respectively (Cadonau et al. 1985, Cadonau 1986). Figure 1 shows the resulting three optical curves. The break in the U is due to the mentioned procedure. The slopes in Table 1 agree very well with those given by Barbon et al. (1973a; their Table to Figure 1). Some small differences are present, but not larger than would be expected from the scatter in their Figure 1. For the infrared (JHK) curves we used data from Elias et al. (1981, 1985). They already derive light and colour curves for SNe Ia and Ib. To combine the data they had to rely on partially insecure maximum epoches in B to shift the observations in time and determine then an H brightness (H_{20}) at 20 days past the B maximum. This value depends of course of the choice of the phase. To improve the curves we decided to determine first the B maximum epoch from optical light curves of only well observed SNe Ia, thus fixing t_o, and adjust the data solely in brightness. This, of course, assumes that SNe Ia follow a standard behaviour and have a comparable evolution in time. Once the epoch was fixed, we shifted the infrared values of each filter in brightness to give a best eye fit. Then a polynom of 10th power was fitted to parametrise the early phases of the light curves. For the final decline a linear regression was fitted to a subset of the data chosen by eye. Joining the two parts simply at the intersection point provided the standard curves. Finally the magnitude at $t_o=0^d$ (B maximum) was set to 0 for the normalisation. Figure 2 displays the found infrared curves. The slopes at late phases (see Table 1) agree well with the values of Elias et al. (1985), whereas the early times differ strongly. However, this epoch is determined only by a few observations and the extrap-

olation beyond the first observed point lacks any physical significance. In respect to Elias et al. the epoch changed by about 5 days, so that the value H_{20} corresponds to $H(t_0 \approx 15^d)$. The main feature of these curves is the dip before a second maximum. The first maximum has never been observed, so that no information exists on how the supernovae reach the brightness level before they fade and brighten again. It would be very interesting to correlate this phase with the optical curves to find an explanation for the strange shape. A tabulated form of all standard light curves is given in Table 2. Also listed are the B-V, U-B, B-H, J-H, and H-K colours, which were calculated with the brightness curves. The supernovae used in the construction of the infrared curves were SN 1972E, 1980N, 1981B and 1981D. Two supernovae occurred in the same galaxy (SNe 1980N and 1981D) in NGC 1316 (Fornax A). Table 3 lists some properties of galaxies and SNe. The galaxy types, velocities and distances are taken from Kraan-Korteweg (1986). The velocities are corrected for the solar motion with respect to the centroid of the Local Group and the distances are given in units of the Virgo distance d_{vir} assuming an infall velocity of v_{vc}=220km s^{-1} and a Virgo velocity v_{vir}=967km s^{-1}. For galaxies with ambiguous distances we also give a second possible distance in parenthesis. A_B is the foreground absorption in the Galaxy as given by Sandage (1973). The determination of $t(B_{max})$ is described below. Also listed is SN 1983G, which has not been used to establish the standard curves. For a list of references for the optical observations of these supernovae see Cadonau (1986).

b) The optical curves

The quality of the curves is illustrated in Figures 3 and 4, where the observations of the four standard SNe are compared with the B and H curves respectively. The fitting procedures were the following. First we determined the maximum date $t(B_{max})$ of the B values by a least squares fit to the analytical solution of the light curve, then the sum of differences of the measured data and the expected tabulated values was used to normalise the observations in brightness. This gives equal weight to every observation and does not distinguish between good measurements (e.g. near maximum, where the supernova is bright) and late phase observation with its possible uncertainties (like photometric errors or contamination from background light of the underlying galaxy). For the fit of the magnitudes only measurements between $t_0 \geq -5^d$ and $t_0 \leq 110^d$ were used, because of the poorly determined curves at other times (though it is expected, that the linear decay continues, which was used in the fit for the maximum date) and the data become unreliable especially for fainter supernovae, as they already have faded by more than 4 magnitudes. Even with these limits one has to be cautious fitting infrared brightness at phases where $t_0 \leq 5^d$, as the curves are extended without observations beyond this phase. A standard deviation was calculated by admitting only differences in brightness. As is seen in Figures 3 and 4, the points

exhibit a very small scatter around the curves. In B this is achieved on a curve that was defined by 36 SNe (see Cadonau et al. 1985; Figures 1 and 2). This is endorsed by Table 4, that gives the standard deviations in magnitudes for the four standard SNe individually and combined in all colours. Additionally the values for SN 1983G are given. Also shown are the number of observations used to determine the deviations. The scatter for B and V (shown in Figure 5) is smaller than would be expected from photometric errors, whereas in U (see Figure 5) it reflects the difficulty of the observations in this filter (transformation problems can arise, as the filter is cut at the violet end by the atmosphere, which is slightly variable).

c) The infrared curves

Elias et al. (1981, 1985) already pointed out the small scatter around a fiducial curve for the infrared data, illustrated in Figure 4 for the H band and in Figure 6 for J and K. It has to be said here, that this curve was defined by the shown points, but the diagram demonstrates the small internal deviations from a standard behaviour, as the scatter is in the range of the photometric errors. J and H exhibit a larger scatter because of SN 1972E, which introduces this spread (Elias et al. 1985; Appendix, Lee et al. 1972). The more recent data scatter much less, especially SNe 1981B and 1981D. A remark on the accuracy should be made here. The quality of the fits depends on the determination of the maximum epoch. This means, a badly defined maximum in B always introduces some scatter into the data. We therefore claim, that especially the B maxima are well determined for these 4 standard SNe, despite the fact, that not all were observed during their maximum phase. The second distinguished point for the fit is the break from the steep slope after maximum and the late slow decay at $t_o \approx 35^d$ in B. With good observations during this period good maximum date and brightness can be determined by using the standard curve, as was the case for SN 1972E and (maybe) SN 1980N.

d) The epoches of the maxima

As standard candles SNe Ia should also show a fixed time difference between the maxima in different filters. To test this property (Cadonau et al. 1985, Cadonau 1986) we attempted to fit each light curve independently to find an individual maximum epoch. This method depends strongly on the quality of the data. A short inspection tells, that in the case of SN 1981D too few observations are available to obtain a significant value of the optical maxima. But SNe 1972E and 1981B seem very likely to give reasonable results. SN 1980N is useless for a U maximum, but can provide B and V dates. From this selection we derived the following values:

$$t_0^{B_{max}} - t_0^{U_{max}} \approx 2.^d8 \pm 0.^d2 \quad (2\ \text{SNe})$$

and

$$t_0^{V_{max}} - t_0^{B_{max}} \approx 2.^d5 \pm 1.^d0 \quad (3\ \text{SNe})$$

This at least reproduces the figures calculated by Cadonau (1986) based on 3 and on 6 SNe, respectively. No such investigation was made in the infrared because the data is too scarce. We just give the summary of the different epoches in Table 5. Surprisingly, the occurrence of the maxima is inverted in the infrared. In the optical the redder the filter band lies the *later* the maximum is reached, whereas in the infrared the redder the filter is the *earlier* the maximum occurs. The same can be observed for the minima in the infrared. This adds to the distinct pattern these curves exhibit, which continues in the I and somewhat weaker in the R bands (Elias et al. 1981 and references therein). To explain this with absorption or emission arising in the filter bands seems unlikely, because this evolution stretches over more than 10000Å. It might be possible to explain the strong variation in J by an intervening absorption, which has been seen in infrared spectroscopy of SN 1986G (Frogel et al. 1987), but the smoother H and K curves must result from another effect. Clearly non-thermal radiation is seen here.

e) SN 1983G - a test

An independent way to check the ability of the standard curves to describe observed light curves is provided by the observations of SN 1983G, which has reasonably well observed light curves and was determined spectroscopically to be of type Ia (Harris et al. 1983 and references therein). In Table 3 some information on this supernova is listed. Figure 7 shows the best fit. This supernova agrees fairly well with the given optical standard curves as the small deviations indicate in Table 4 and also in the infrared the scatter is comparable to the standard SNe in H and K, but differs strongly in J. This stems from the one observation at $t_o \approx 18^d$. Elias et al. (1985) give possible errors in the photometry of up to 0.3 mag. for the infrared observations, so that it is quite likely to have such a case here. Otherwise this large deviation is unexplained. Fits of more SNe I to optical light curves can be found in Cadonau (1986). There eye fits were made and the results do not differ significantly from those by the method used here.

f) Intrinsic colours

With the set of light curves it is easy to find the shapes of the colour evolution of SNe Ia. Due to the normalisation, however, the found colour curves do not yet represent the true intrinsic values. To determine this we have to calculate the intrinsic colours of SNe Ia at the normalisation point ($t_o=0^d$). Once this offset is known the real colour evolution can be determined. Normally the inherent colours of supernovae in the optical are measured from SNe in elliptical galaxies at high galactic latitudes, so that no or very little internal extinction in the parent galaxy and no galactic foreground absorption was expected. As no supernova in our sample occurred in an E galaxy, it is not possible to find this value here. Earlier

attempts have been made to measure this (Pskovskii 1968, Barbon et al. 1973a, Cadonau 1986). The results were $(B-V)_o{}^o=-0.^m2$ (Barbon et al.), $(B-V)_o{}^o=-0.^m26$ (Pskovskii) and $(B-V)_o{}^o=-0.^m27$ (Cadonau). The first two values were measured by determining the colour curve, while the last solution was found using two SNe in elliptical galaxies. The agreement is considerable concerning the uncertainties of the (B-V) curve and the small sample of Cadonau. In general one would expect, that the bluest measured values would indicate the intrinsic colour. Therefore we adopted here $(B-V)_o{}^o=-0.^m27$. The case of $(U-B)_o{}^o$ is more difficult, because the U observations are normally much less reliable. Furthermore there is no SN Ia in an elliptical galaxy with good U data. A determination was attempted by Cadonau, who found $(U-B)_o{}^o\approx-0.^m4\pm0.^m1$. (For another determination see Pskovskii, who derives $(U-B)_o{}^o\approx-0.^m58$). In the infrared the assumption, that these filters are only little absorbed by interstellar matter, leads to a simple measurement of the colours. Thus the differences in magnitudes should yield reasonable intrinsic colours. This provides a new test on the quality of SNe Ia as showing a standard behaviour. In Table 6 we list the magnitudes for $t_o=0^d$ for the standard SNe and SN 1983G. These values are corrected for foreground absorption. Also given are 6 colours. For the moment the infrared colours $(J-H)_o{}^o$ and $(H-K)_o{}^o$ are of main interest. $(H-K)_o{}^o$ shows only little scatter, that can be explained by photometrical errors. Averaging gives: $(H-K)_o{}^o=0.^m27\pm0.^m03$. The case of $(J-H)_o{}^o$ is ambiguous. Especially the value of SN 1981D is very high compared to SN 1980N in the same galaxy. A special investigation showed, that because of the distribution of the observations the J value of this supernova is strongly variable as a function of the maximum epoch. Shifting this value by one day results in a magnitude shift in J of $0.^m18$ (SN 1980N being the second worst case exhibits only $0.^m08$, all other SNe have a shift smaller than $0.^m02$). Therefore we omit this supernova for the averaging of $(J-H)_o{}^o$, which leads $(J-H)_o{}^o\approx-1.^m36\pm0.^m10$. Two comments regarding this result are given. First, because of the steep slope of the J curve at early phases this curve is very sensitive to uncertainties of the epoches. Second, as was mentioned above, Frogel et al. (1987) found, that the J filter is strongly influenced by an absorption feature. This explains partially the strong changes in the J curve and has been proposed earlier (Elias et al. 1985). If this absorption changes because of some unknown reason $(J-H)_o{}^o$ is affected. The colours $(V-K)_o{}^o$ and $(B-H)_o{}^o$ are sensitive to reddening of the optical and no single value can be expected. We adopt here a value of $(B-H)_o{}^o=-0.^m85$ with the argument, that the bluest supernova (SN 1972E) is closest to the intrinsic colour.

Figure 8 shows a 3-dimensional plot of all Ia light curves now shifted according to the colours adopted above. The break between V and J is clearly visible and that the J curve lies lower for $t_o\geqq5^d$ than any other filter supports the view, that this band suffers of an absorption at all times. This Figure proves also, that no black body can fit the data at early phases ($t_o\leqq50^d$). Another obvious feature is the fact, that the

infrared maxima occur earlier at larger wavelengths. This means, that some contribution of a non thermal radiation governs the early times of a supernova type Ia.

g) The two-colour diagram

It is now also possible to construct a two-colour diagram with the evolutionary tracks of SNe Ia. This is shown in Figure 9 for intrinsic optical colours ($(U-B)_o$ and $(B-V)_o$). The fast evolution during the first days brings the supernova from very blue colours close to the black body line at a temperature around T=5000K. The ultraviolet flux is very deficient during this period due to many Fe lines, which depress the fluxes at small wavelengths (Panagia 1982, 1985, Branch and Venkatakrishna 1986, Wheeler et al. 1986). The loop of the curve between $t_o=25^d$ and $t_o=40^d$ is probably artificial, because in the standard curves the transition from the polynomial to the linear equation takes place during that period, but in each curve at a different epoch. They are comparable again only for times with $t_o \geq 40^d$, when all curves are in the final decay. The prediction is that the supernova stays close to the black body for several days. This is supported by direct calculations of the colour temperatures, which give values around T=5000K between $t_o=20^d$ and $t_o=40^d$ for $(B-V)_o$ **and** $(U-B)_o$. It seems as if the radiation thermalises as the atmosphere becomes optically thinner. The first days could be a combination of the overlaying, expelled envelope, which is obviously very small, and the burned core material. At the end of this phase only burned (heated) matter is seen, which radiates the continuum. As the photosphere expands rapidly it cools and so the relatively low temperature is reached. The phase for $t_o \geq 40^d$ is powered by the Ni^{56} and Co^{56} decays (Axelrod 1980, Woosley et al. 1986, Woosley and Weaver 1986, Graham 1987). This diagram has been described by Cadonau (1986), who got the same result, and Pskovskii (1968, 1971), who found for the final decay a completely different slope, but does not give any interpretation. The discrepancy between this result here and his curve can be explained by the badly defined colour curve he was forced to use.

h) The colour temperatures

To achieve an overall picture of the evolution of SNe Ia two further investigations were carried out. It is possible to calculate a colour temperature of SNe by using the well known black body energy distribution. If the supernova would show thermal radiation all obtained temperatures would be equal. As can be seen form Figure 9 this is not true during the early phases ($t_o \leq 30^d$) and again after $t_o \approx 50^d$ in U. Nevertheless valuable insight in the nature of SNe can be gained by comparing colour temperatures of different colours. This has been attempted by Fu and Arnett (1986). The procedure depends strongly on the calibration of the black body colours (e.g. Matthews and Sandage 1963 for the optical bands). To determine the calibration

for the infrared we decided to use a star already used by Matthews and Sandage. 10Lac (HD 214680) is an O9 V star with the optical colours close to a black body at ~20000K. A combination of optical magnitudes and colours (Nicolet 1978) with infrared data (Gezari et al. 1984) allows the calculation of approximate zero points for the black body colours (Fu and Arnett 1986). Once these zero points are determined it is possible to get temperatures for a given colour. Figure 10 shows the evolution of different colour temperatures for the standard curves. A separation in three distinct groups of curves can be stated. The optical colours (B-V) and (U-B) lie lower than the curves including B and the highest temperatures are measured for colours with the V band. This is identical to what has been worked out by Fu and Arnett (1986). The separation only evolves after ≈20 days, when - as can be seen in the two-colour diagram - the supernova approaches the black body line. The strong deviation from that line is reflected in this diagram by the divergence of the optical colours after that epoch. Remarkably (B-V) follows in shape all other curves, although the temperature is always much lower than for the other colours. Also noticeable is, that between $t_o \approx 30^d$ and $t_o \approx 50^d$ the supernova shows a single colour temperature in the optical, whereas all colours combining an optical and an infrared magnitude exhibit a higher temperature. The reason for this could be diluted black bodies (Fu and Arnett 1986), but it is not clear, if it fully accounts for the effect. At early stages this diagram shows that the assumption of a black body does not hold as all colours show strong and seemingly independent variations, supporting the view, that the spectrum is constituted mainly by single lines and large depressions (Wheeler et al. 1986) and no thermalisation has evolved yet contradicting earlier findings (Kirshner et al. 1973b). At late phases of a supernova the temperature rises again, although no common temperature for the different colours emerges. Only the (U-B) temperature drops indicating that the U band is affected most strongly by absorption. No further interpretation of this situation has been attempted, but a mechanism explaining the different black body temperatures of the different colours at the same phase would definitely improve the insight into supernovae atmospheres.

To make the point that SNe Ia are not showing black body radiation at early times ($t_o \leqq 20^d$) and in late phases ($t_o \geqq 50^d$) we give Figure 11 displaying the measurements of the different bands. Also shown is the curve of a black body with the effective temperature of (B-V). It is obvious, that the J band (λ_{eff}=1.25 µm) is strongly absorbed at all times (cf. Figure 8). But it is also clear here that no single black body fits all points at the same time. Especially the evolution of the U flux is interesting. Being too low at phases $t_o \leqq 20^d$ it rises significantly until it fits the black body with the (B-V) colour temperature reasonably well to drop again after $t \approx 40^d$ suffering obviously from heavy absorption. The infrared H and K magnitudes always lie lower than a black body fitting the optical would suggest, hence indicating a lower temperature. This picture contradicts

the previous result, that a black body is a reasonable assumption for the continuum radiation (Kirshner et al. 1973b). This is so even in the optical region, where the U is strongly affected by absorption (Panagia 1987, Wheeler et al. 1986).

i) The bolometric light curve

Therefore it is clear, that for a bolometric light curve the simple use of a bolometric correction based on empirical data for main sequence stars cannot account for the real energy output of a supernova. One feasible way to obtain a bolometric light curve is to integrate the flux given either by spectra or photometry (Graham 1987). The numerical integration over all standard curves results in a smooth curve that resembles closely the V curve in shape, a hint that the main part of the energy received from SNe Ia stems from this section of the spectrum. Nevertheless, the maximum is wider as far as can be distinguished. No secure statements are possible for times before $t_o=5^d$ because no infrared observations for these epoches are available. A comparison with the light curve calculated using the bolometric corrections is shown in Figure 12. The strongest deviation appears shortly after maximum, where the supernova is very blue implying a strong bolometric correction. The assumption, that a bolometric correction can be applied breaks down at this time. But also later phases do not reproduce the integrated curve. Although it is not possible to integrate the totally emitted radiation of SNe Ia yet, as we are lacking the high energy parts, it seems as if the conventional bolometric correction as applied to normal stars cannot be used for SNe Ia. The bolometric light curve as shown in Figure 12 has no "observed" maximum, i.e. in the infrared no first maximum has ever been observed. The main contributions are as expected from the optical range, but a considerable amount of the energy is radiated between V and J. Because no information in the spectral range between 6000 and 12000 Angstroms has been used (R and I bands), this contribution is somewhat insecure. Nevertheless it has been stated earlier, that these bands show the same strange bump as the infrared filters, though too a lesser extent (Elias et al. 1981). The large base between these two integration points gives high weight to the V data. With these caveats we think this approximation still superior to any attempts using only optical data. A very important expansion of the data into the UV region is still missing as IUE spectra are available for only a short time around maximum (Benvenuti et al. 1982) an no SN Ia has been observed at higher energies yet.

The curve found is best characterised by two lines. The final decay after $t_o=40^d$ and a phase shortly before this smooth bend. The slopes at these two epoches are $\approx 0.^m055$ and $\approx 0.^m025$ per day for the times before and after the bending point, respectively. This corresponds to a half life time of ~14 and ~30 days of the decay of the light curve, respectively. For an independent check of the curve we compared our bolometric curve with directly integrated observations for SNe 1972E and 1981B (Graham

1987) adjusted to the time of the B maxima found in this work. Although the observed points are not integrated over the same spectral range as our light curves the main contributors to the energy, namely the optical part, are in common to both sets. The good correspondance in Figure 13 supports the statement that only little is contributed by infrared bands. It is also possible now to compare the empirical curve to a calculated bolometric light curve (Graham 1987). The used model is a deflagration in a white dwarf corresponding to the model W7 (Nomoto et al. 1984) modified to consist of three zones, an inner zone with stable elements, a shell of radioactive Ni^{56} and an outer layer of absorbing matter. This model fits the found curve surprisingly well, if one assumes, that the time difference between explosion and the maximum B brightness is around 16 days (Barbon et al. 1973a, Pskovskii 1977). An even better conformity can be achieved by assuming $\Delta t \approx 20$ days supporting a value given by Cadonau (1986). A comparison of the shapes of the two curves is given in Figure 14. Both curves were shifted in brightness to achieve the best correspondence. The discrepancies can probably be explained by the different approaches to the curves. The empirical curve is a composite of different sections, whereas the theoretical one emerges from an analytical model. We confined this discussion to the shapes of the curves, because a comparison of the radiated energies involves distances to the SNe and will be treated separately.

4. The effect of absorption on the shape of SNe Ia light curves

a) Derivation

Absorption - being foreground in our Galaxy or internal in the parent galaxy - has hindered every investigation of common properties of SNe. Especially internal absorption in the parent galaxy is difficult to determine (if at all possible) because of the little information on the properties of dust or other absorbing material. Therefore most determinations of intrinsic colours are based on SNe lying preferably in elliptical galaxies at high galactic latitudes, where no or only little absorption is expected. No corrections for absorption were ever applied to the shape of SNe light curves, but because absorption shows also a slight colour dependence for normal stars (Buser 1978, Schmidt-Kaler 1982) the light curves may suffer some deformation. The set of standard Ia curves provides a suitable tool for the determination of the size of the effect. We used the formulae given by Schmidt-Kaler (1982), which differ only little from the values given by Buser (1978) for stars:

$$A_B = (4.3 + 0.28(B-V)_0 + 0.04E_{B-V})E_{B-V}$$

where A_B is the absorption in B, $(B-V)_0$ the intrinsic colour of the object and E_{B-V} the colour excess in (B-V), defined as:

$$E_{B-V} = (B-V)_{obs} - (B-V)_0$$

Using the (B-V) standard colour curve as given in Table 2 as $(B-V)_0$ (the intrinsic colour) and assuming a constant E_{B-V} valid for the whole range that spans the colour curve, we can calculate the changes introduced by reddening. This assumes, that we have the same law of absorption, for foreground **and** internal reddening of the supernova. Dropping the constant terms in the first equation results in a change of the **shapes** of the light curves only.

The effect is supposed to be very small for the infrared bands because only little absorption is expected in this region. It is probably big in U, but this curve is defined so poorly, that the internal errors in U exceed the corrections. So we confined the investigation to the B and V bands. The resulting group of curves is shown in Figures 15 and 16 for B and V, respectively. Again the normalisation was at the B maximum ($t_0=0^d$), so that no changes at this point appear, but with the evolution in $(B-V)_0$ the curves fall below the unreddened template. Because the colour curve is not well established at late times the narrowing of the spread in this phase is not significant, but there is a real change in the first 40 days, that results in a relative magnitude difference of about $0.^m45$ at $t_0=40^d$ for the heavily reddened case of $E_{B-V}=1.^m5$. Such reddenings are extremely rare, but to illustrate this point we calculated Pskovskii's β-parameter for different reddenings. This β is

defined as the magnitude difference per 100 days of the initial decline of the supernova B light curve in the interval given by the maximums epoch and the intersecting point of the lines of the steepest slope during the first 30 days and the final decay phase (Pskovskii 1967, 1971, 1984). This point is normally referred to as t_{Bend}. The magnitude difference Δm is then the difference between the maximums brightness and this intersecting point, which always lies **below** the observed light curve (for an illustration see Phillips et al. 1987, Figure 3). Table 7 lists the values measured with this procedure for the different reddened B curves. What is striking is the strong dependence of β on the reddening. This effect should be considered, when a heavily reddened supernova (e.g. SN 1986G) is observed. To have some handle on the problem we propose to use the magnitude differences $\Delta m(t_o)$ between the brightness at maximum and at t_o, which follow the simple equations:

$$\Delta m(t_o=30^d) = 2.53 + 0.31 \cdot E_{B-V}$$

and

$$\Delta m(t_o=40^d) = 2.96 + 0.30 \cdot E_{B-V}$$

The U and $(U-B)_o$ are not defined well enough to allow this treatment at the moment, but in principle there is no difference to the applied procedure.

b) An example

Unfortunately we are not able to test the predictions with real data, because no supernova with a large colour excess E_{B-V} is in our sample. However, we show the case of SN 1983G, which had an E_{B-V} of $\sim 0.^m5$ (assuming $(B-V)_o{}^o = -0.^m27$) in Figure 17. The maximum date has been shifted by two days (to JD 2445429) and by $0.^m23$ in brightness (from $13.^m02$ to $12.^m79$) to achieve this picture. The scatter of the points around the curve with $E_{B-V}=0.^m5$ is the same as for the unreddened curve with maximum date JD 2445431, namely $0.^m10$. We get the same result for SN 1981D, which seems to be almost equally reddened. The case of SN 1986G in Cen A, which has suffered a strong absorption will be discussed below, because this supernova shows several features, that can not be handled in the picture of standard SNe Ia. Another test would be to find a correlation between the $(B-V)_{obs}$ colours and β. But the available data (Pskovskii 1976, 1984 for β and Cadonau 1986 for the colours) are not conclusive, as the scatter in β is extremely large and the range of $(B-V)_{obs}$ too small.

c) Kepler's SN 1604

It is also interesting to see how Kepler's supernova 1604 fits into this picture. This supernova was strongly absorbed ($A_V \approx 3.^m5$, Danziger and Goss 1980) and - if it was a type Ia su-

pernova - it should show this effect. The data available (Baade 1943, Xi Ze-zong and Po Shu-jen 1966, Clark and Stephenson 1977, Pskovskii 1978) are shown with the V curves in Figure 18. The points were fitted to agree with the rising slope (given by Cadonau 1986) and the maximum. As can be seen, the observations fall below the curves and would indicate an EB-V much bigger than 1! There is no way to accommodate the data in a proper manner on one of the curves. There exists, however, a discrepancy in the observations cited by Baade (1943) and Pskovskii (1978). The supernova became more brilliant than Mars during October-November 1604 and some sources compare it then to Venus. The brightness difference between Mars and Venus is at least 1.m5, so that it is difficult to estimate brightness in this interval because no objects in this apparent magnitude range are observable. Baade claims that the supernova reached maximum around October 15, whereas in estimates of magnitude including comparisons with Venus the maximum occurred later. Disregarding the measurements, which stem from comparisons to Venus, who was close to the sun (Pskovskii 1978) and following Baade we fitted the data again on the set of curves. No decisive result could be obtained, but the optically best fit is shown in Figure 19 with the maximum occurring around October 24, 1604. This is a week later than Baade's estimate, but only two days earlier than Pskovskii's determination including all comparisons of the supernova with Venus. The V magnitude at maximum was hence -2.m5 assuming a reddening of EB-Volm. This value lies somewhat higher than Baade's, but lower than other determinations (Stephenson and Clark 1977, Pskovskii 1978). Therefore the absolute magnitude using a distance of 5 kpc (Hughes and Helfand 1985, D'Odorico et al. 1986, see however Strom 1988) gives MVo-19.m5, which is only 0.m5 fainter than previous results (Tammann 1982). A somewhat smaller distance to Kepler's supernova remnant would imply a fainter absolute magnitude (MV=-19.m1 for r_{Kepler}=4.2 kpc). For a summary on distances to SN 1604 see van den Bergh (1988a). The supernova had a very steep rise and the observed maximum is several days earlier than the fitted one. To accommodate these observations one is forced to accept an exceedingly steep slope for the brightening of the supernova. After the maximum the scatter of the points is too large to distinguish which curve fits best. Nevertheless it seems, that a somewhat obscured curve would suit the data most. No definite determination can be drawn of this discussion, but assuming Kepler's SN 1604 was really a Type Ia event, the steep decline after maximum could be explained as a combined effect of inaccurate observations - the gap in brightness is too large for a fine scaled determination, the position on the sky was very low for European observers and the observations against twilight introduced further uncertainty (this is also true for the Korean and the Chinese observations) - and the strong absorption by interstellar matter, which steepens the decline after maximum.

5. The effect of redshift on the light curves of SNe Ia

a) Theory and calculations

Although SNe Ia are hoped to be good standard candles (e.g. Bartel 1985), it has never been attempted to derive a light curve expected for such an event at cosmological distances. This is surprising as several searches for supernovae at redshifts of $z \geq 0.1$ are planned or under way (Hansen et al. 1987). To determine the corrections caused by the shifting of the spectrum we chose a set of spectra observed in SN 1981B in NGC 4536 (Branch et al. 1983). Table 8 lists the used spectra, which were corrected for the redshift of the parent galaxy, but not for reddening due to absorption. The spectra were digitised and served as templates of SNe Ia spectra, which display very uniform spectral evolutions (Panagia 1987, Wheeler 1985, see also Canal et al. 1988, Branch et al. 1988, however). For these spectra we calculated K-corrections whenever possible. The corrections were determined using the formula

$$\Delta m(z) = -2.5 \log \left(\frac{\int_0^\infty F(\lambda(1+z)) S(\lambda)(1+z) d\lambda}{\int_0^\infty F(\lambda) S(\lambda) d\lambda} \right)$$

where $F(\lambda)$ is the flux of the unshifted and $F(\lambda(1+z))$ of the redshifted spectra and $S(\lambda)$ the response function of the filter band. This is equivalent to the definition given in Oke and Sandage (1968) and leads to a correction of the magnitude by

$$m(z) = m(z=0) + \Delta m(z)$$

The approach here is just inverted to the normal K-correction, which calculates the magnitudes in the rest frame of a receding object with the observed brightness on earth. We determined theoretical corrections, that will have to be applied to supernovae at certain redshifts. A problem encountered by evaluating the integrals was the insufficient coverage in some of the used spectra. All spectra taken after March 1981 ($t_o \geq 26^d$, adopting the maximum on March 9) do not cover the whole V filter, which stretches from 4700Å to 7300Å, but as can be seen in Table 8 the coverage is acceptable in all cases. The percentage given is the ratio of the transmission of the truncated and the full filter. The spectra of May 4 and May 10 were joined by linear interpolation in the gap without information (541-569 nm). To compute corrections for high redshifts ($z \geq 0.4$) needs ultraviolet data, which are available only for the maximum epoch (Benvenuti et al. 1982) and as we are interested in the shape of the light curve we did not include any UV spectra in this investigation. Table 9 gives the K-corrections in V for the different epoches. The corrections marked were calculated with a truncated filter to cope with the incompleteness of the spectra. The interesting feature at maximum is the increase in brightness for all redshifts up to $z=0.45$. This means that SNe Ia at these redshifts

seem to be brighter than "normal" local SNe Ia. The reason for this astonishing result is that SNe Ia are brighter in B than in V at maximum. Thus, when the radiation is transferred to longer wavelengths, the magnitude in V increases. After z=0.6 (Table 10) more and more ultraviolet radiation enter the V band and the K-corrections become positive. Due to the fast colour evolution in (B-V) the corrections are greater than 0 for the decline phase. They are strongest after ~20-30 days past maximum. In these epoches the K-corrections generally increase with z. The effect changes sign again at the very late phases ($t_o \geq 90^d$), which is also supported by the bluer colour at this stage of the evolution. Nevertheless we think that the evolution at these epoches is less a continuums effect but the shifting of the strong emission band at ~4600Å rest wavelength associated with Fe II (Branch et al. 1983) into the filter region and the deep absorption trough ($\lambda_{rest} \approx 5800$Å, Na I) out of it. This is supported by the decrease of the corrections at $z \geq 0.15$, when the emission passed the region of highest transparency of the filter. Figures 20 and 21 illustrate the effect for the two cases of $t_o=0^d$ and $t_o=22^d$, respectively. It is obvious from the pictures, that no simple dependence of the corrections on redshift can be found, as the different absorption and emission features pass through the filter band. A similar discussion for the B filter is possible only with low redshifts ($z \leq 0.1$). The general behaviour is similar to the evolution in V, but the corrections are very small ($\leq 0.^m02$). The calculated corrections can now be applied to the standard V light curve. This is done in Figure 22. The main effect is the steepening of the decline after maximum, which is due to the colour evolution (i.e. the gradient of the spectrum). With increasing redshift the radiation observed in B for unshifted SNe Ia is transferred to the V filter and at $z \approx 0.3$ the V curve should approach the B curve. An exact equivalence though, is not expected, because the spectrum is also stretched. In Figure 22 the resulting points are compared to the standard V curve of an unshifted SN Ia. No errorbars are drawn, but an estimated error is $\approx 0.^m05$ for all points and $\approx 0.^m1$ or even somewhat more for the corrections calculated with truncated filters ($t_o=26^d$, 33^d and 93^d). The trend to faster decline with increasing redshift is obvious. The bump at $t_o \approx 30^d$ could be artificial, because these points are less certain. The final exponential decay of the light curve is flattened with increasing z, but this effect might level off at even higher redshifts. We normalised the data so as to fit the curve at maximum ($t_o=0^d$) to compare the calculations in the V band with the standard B curve (Figure 23). The best fit of the peak ($t_o \leq 40^d$) is at $z \approx 0.2$ but for later phases the points for z=0.3 seem closer to the curve. Again the final decline is more shallow than in the unshifted B curve. Here one could argue that the redshift changes Pskovskii's β, producing the mimicry of different supernova types.

b) The effect of time dilation

There is yet another effect changing the shape of supernova light curves with redshift. If the cosmological redshifts are due to expansion (cf. Harrison 1981), then all time intervals are shifted by the factor (1+z). This means for a supernova light curve a broadening of the peak and a more shallow slope for the late times (Tammann 1978). The effect of time dilation is shown in Figure 24, where the observations with $t_o \geq 0^d$ were shifted in regard to the maximum. The new curves still show an evolution from the V to the B standard curve with redshift. Now the points for z=0.3 fit the decline of the B curve best. The trend stops at this redshift because the strong decrease past maximum originates mainly from the brightening of the supernova at maximum and only little from the lower flux after maximum. The supernova is relatively brightest at z=0.3 (Table 9) and for higher redshifts the strongly depressed UV flux enters the V filter and causes its fading. This "stretching" of the light curve counteracts the steepening of the decline due to the K-correction. It is now possible to add a new test (beside the surface brightness of galaxies) for the hypothesis that cosmological redshifts are due to an expansion of the universe (Sandage 1988). If the redshifts are due to expansion then the light curve of a distant SN Ia differs exactly in the manner described above. A clear distinction should soon be possible by observing a supernova at a moderate redshift ($z \approx 0.2$). Around $t_o = 20^d$ the two curves for z=0.2 differ by $0.^m5$ in the sense that a supernova in a non-expanding universe would be brighter. Therefore for an observed z and the decline rate after maximum of only one supernova this distinction should be possible, provided the phase of the observations are known. The later epoches show a very flat tail. Again a distinction should be possible, but as the supernova faded already by more than 3 magnitudes by then and the maximum brightness for a SN Ia at z=0.2 is expected to be $\approx 20.^m5$, it will be difficult to observe it at such late times. SN 1988U (Hansen et al. 1988a, 1988b) in the galaxy cluster AC118 (z=0.31) provides the possibility to check the predictions. The supernova was supposedly of type Ia, had at discovery (August 9, 1988) $m_V = 22.^m3$ and faded with a slope of $0.^m15$/day, which is a very fast decrease (compared to $0.^m06$/day for standard SNe Ia). It was observable for only one week before it disappeared. Because neither the maximum nor the bend were observed the phase (t_o) of the observations is unknown. Hence it is not possible to make the test with this event. The very fast decline nevertheless indicates, that the predictions are correct.

c) Maximum brightness of SNe Ia with increasing redshifts

The effect of the changing of the maximum brightness of SN Ia with redshift introduces a correction for observed apparent maximum magnitudes, when they are used to test the standard candle character. Table 10 lists the apparent magnitudes of a supernova with the absolute maximum brightness $M_V = -19.^m9$ in

an open, flat Friedmann universe ($q_o=\frac{1}{2}$) and an empty universe ($q_o=0$) and the respective corrected values. For this computation we joined the IUE spectrum of March 9 (LWR10100, Benvenuti et al. 1982) to the optical, thus allowing calculations of redshifted spectra up to z=2.41. Column 5 and 6 show that a supernova search at high redshifts has to go very faint and must have a high temporal coverage of the fields. A filter at long wavelengths is to be preferred due to the very low fluxes in U. This pattern of magnitudes reveals, that searches up to z=0.6 are favoured by the relative increase of maximum brightness, whereas at higher redshifts SNe Ia seem also intrinsically fainter. If the K-corrections were not applied to observed magnitudes SNe Ia at intermediate redshifts would seem to be absolutely brighter objects than locally, what easily could be misinterpreted as evolutionary effects. The whole discussion of course assumes that SNe Ia really are standard candles.

6. Supernovae Ib

a) Construction of templates

Because supernovae Ib are established as a subclass of SNe I (e.g. Porter and Filippenko 1987, Filippenko 1986, Panagia et al. 1986, Uomoto and Kirshner 1985), we decided to build up an own set of fiducial curves for this group of objects. Although SNe Ib show intrinsic differences, their behaviour is still quite uniform when considering the optical light curves. This is one reason, why this subclass was not found earlier. Nevertheless some deviations from the standard Ia templates are discovered, if the objects belonging to this class are sorted out (c.f. Ensman and Woosley 1988).

For the construction of the light curves we have chosen six supernovae known to be Ib by spectral observations and infrared light curves. Three of them were chosen because they have at least one well defined light curve in the optical (SNe 1962L, 1964L, 1976B) and the rest (SNe 1983I, 1983N, 1984L) because of the infrared observations available. Table 11 gives a short summary on some parameters of the parent galaxies and the SNe themselves. The inhomogeneity of the set of data is evident from Table 12, which lists the available data and the references used. Especially the data in U is so scarce, that it was not possible to construct a light curve. For all other filters the curves were established by the combination of two segments describing the peak and the final exponential decay phase. The optical (B and V) and infrared (H,J and K) observations were shifted in time and brightness to fall together optically and then a polynom was fitted to the peak phase, whereas a linear regression was adapted for the late epoches. Thus we were able to fit the data to a first template. The procedure was repeated once with the newly determined shifts to establish "standard curves" for SNe Ib. Figures 25 and 26 display the resulting templates, which are tabulated in Table 13. Table 14 gives the epoches where the segments were joined and the slopes of the final decline. A comparison with the corresponding numbers of SNe Ia already shows some differences. The discrepancy is best seen in the infrared, where the slopes differ more than could be attributed to photometrical or fitting errors. For a determination of the different maximum epoches in the optical filters the data is not sufficient, so that we adopted the values of SNe Ia. Figures 27 and 28 show the quality of the curves for the optical and the infrared regions, respectively. In B the scatter around the fiducial curve is remarkably bigger than for SNe Ia. This is supported by Table 15, which gives the calculated standard deviations for each supernova and both fits, one on the new Ib templates and the other on the standard Ia curves (ignoring the spectral differences betraying the supernovae as type Ib). The deviations in the optical improved only little with the newly found curves in agreement with the optical impression, that the points do not scatter much more around Ia curves than a badly observed SN Ia. The improvement

can be attributed to the fact, that the new curves were defined by the observations. The main improvement for SN 1962L is due to the long observed light curve which now can be fitted at late times, whereas it lay too high for the template of SNe Ia in B, making it a typical "slow" supernova (Barbon et al. 1973a). The same applies to SN 1964L but here the peak cannot be fitted equally well as for other SNe because the observations indicate a brighter maximum, although this supernova was classified as slow, too. In the infrared, however, the differences are immense (Elias et al. 1985), this being attributed to the distinguished shape (Figure 26), which does not exhibit the minimum typical for SNe Ia. The small scatter of these data is due to the fact, that the curves were defined by the few observations and only few overlapping data exist. Further observations will probably introduce larger deviations, especially as a standard behaviour is not expected (Wheeler and Levreault 1985, Porter and Filippenko 1987, Panagia et al. 1986, Uomoto and Kirshner 1985; for models Gaskell et al. 1986, Begelman and Sarazin 1986, Iben et al. 1987). So the good fits arise from the scarceness of the observations and probably not from a uniformity of the objects. Hence the curves do not represent a "standard" evolution, but describe an average behaviour of this subclass. Of course we do not imply a standard behaviour for these objects, as they are known to show individual differences.

b) The optical curves

The main distinction in the B curves in comparison to SNe Ia is the brightness difference at $t_o \geq 30^d$. Before that epoch the two curves are barely distinguishable. At $t_o \geq 30^d$ the Ib curve lies ~$0.^m45$ higher than the Ia template. The difference between the maximum and this epoch in brightness is $\Delta m(t_o=30^d)=2.^m07$ for SNe Ib and $\Delta m(t_o=30^d)=2.^m53$ for SNe Ia. Therefore, it should be possible in principle to distinguish well observed supernovae by the magnitude decrease after maximum to a fixed epoch. Unfortunately this effect is only noticeable, when the accuracy of the photometry is better than $0.^m1$, which is not the case for most supernovae and absorption bending the light curves, as shown for the case of SNe Ia, contaminates this effect easily. The final slopes compare quite well and considering that the Ib curve is determined by only one supernova, it is possible that they are equal. An illustration of the point made above is Figure 29, which shows the discrepancies between the two subclasses of SNe I in the B filter. It is not surprising, that this has gone undetected for so long, because the new picture evolves from a shift of the maximum epoches of each supernova. Fitting the observations to the standard Ia curve hides the separation visible in Figure 29. In Table 16 we list the Julian dates of the B maxima found by fits on the B light curves of the different subtypes. The strong changes of SNe 1964L and 1983I are due to the distribution of the observations. SN 1964L has a very well and long observed late phase, but only a few measurements in the peak. These points are not

fitted well and the main contribution originates at the long tail, so that the data shifted for several days. The same applies to SN 1983I observed at the transitional phase around $t_o \approx 30^d$ for SNe Ib curves ($t_o \approx 40^d$ for SNe Ia). Thus the new view is a combination of shifts in both variables, t_o and m_B.

In V a similar behaviour can be stated but the difference here is smaller and even less measurable. SNe Ib fade much faster after maximum than SNe Ia. The difference amounts to $0.^m3$ at $t_o \approx 20^d$, when the exponential decay phase starts in SNe Ib and the curve crosses the Ia template at $t_o \approx 30^d$. The slopes differ only marginally and the light curves after the bending $t_o \approx 20^d$ are powered probably by a similar mechanism as SNe Ia. The statements in this discussion are relative assuming a normalisation of the curves to have zero magnitude at $t_o = 0^d$. Taking the exponential decline (e.g. at $t_o = 50^d$) as a reference the differences would occur at maximum. Implying that supernovae of both subtypes produce an equal amount of radioactive Ni^{56}, i.e. the final decay emits the same energy, leads to a brightness difference at maximum of $0.^m7$, which is much lower than earlier measurements (Wheeler and Levreault 1985, Uomoto and Kirshner 1985, Panagia 1985, Filippenko 1986). This is only a rough estimate and the final answer will have have to be provided by the bolometric light curves. It will be difficult to determine the subtype of a SN I by optical photometry, but we think it is possible in principle.

Although there are suggestions, that the ultraviolet radiation does not diverge too strongly from the standard Ia curve, distinct differences are observed (Panagia 1984, 1985). No information at all exist for the late epoches ($t_o \geqq 30^d$).

c) Infrared curves and colours

The situation is much clearer in the infrared, where the shapes of the curves are so distinct. They exhibit a similar "simple" shape as the optical. A broad peak ends in an exponential decay with a smooth transition. Table 17 lists the epoches of the maximum in each filter. The dates are very insecure, because of the broad peak. The error limits are ±2 days. A trend can be noticed nevertheless, as the maxima occur later in filters at longer wavelengths. No internal structure of the curves can be distinguished, which indicates, that absorption troughs affect the filters only little. No strong changes can be found in either filter and the depression of the J band like in SNe Ia is not visible. This will be shown even clearer, when the colours will be discussed. Infrared curves provide one of the main tools, beside spectroscopy, to uncover SNe Ib.

Because SNe Ib are not objects following a close "standard" evolution, we do not expect the colours to have only small deviations from a mean curve. Nevertheless we give the colours and brightness of the six SNe Ib in our sample in Table 18. The expectation is confirmed, as in all colours a large scatter can be noticed. Some values are very uncertain, because they are determined by only one measurement in a filter. Even when

disregarding these determinations it is obvious, that each supernova has an individual colour and no significant average can be defined. The only exception, $(H-K)_o^o$, is probably due to the little temporal variations of this curve. The comparison with SNe Ia (Table 6) shows, that SNe Ib have redder colours (Wheeler and Levreault 1985, Uomoto and Kirshner 1985, Filippenko 1986, Porter and Filippenko 1987) by at least $0.^m5$ in $(B-V)_o^o$. The effect is even more stringent in $(B-H)_o^o$ and $(V-K)_o^o$, where the differences arise to more than one magnitude.

d) Colour temperatures of SN 1983N

Because no standard colours can be determined for SNe Ib we consider the special case of SN 1983N in M83 (NGC 5236), the best observed SN Ib so far, for further discussion. With the colours given in Table 18 it is possible to evaluate a 3-dimensional plot of all magnitudes as a function of t_o and the filter wavelengths. This is shown in Figure 30. As the curves are well defined in the premaximum phase, all bands exhibit the full investigated range in t_o. We excluded the U curve because the picture would be adulterated by adding a badly defined template. It is striking how smooth the transitions between all curves are. The steep decline after maximum in the optical changes into a shallow decrease, not showing any "bend" at any epoch in the infrared. Another remarkable difference to SNe Ia is, that all curves have a comparable level of intensity and no strongly absorbed filters are encountered. The J flux now equals all other bands. This suggests thermal radiation. To test this hypothesis it would be instructive to construct a two colour diagram with optical colours (U-B) and (B-V). Unfortunately no U curve could be established and no (U-B) curve is available. Hence we tried another test using the calculated colour temperatures of the different colours. The result in Figure 31 is not a single value. Nevertheless, the curves do not exhibit the violent changes as SNe Ia. The temperature range is much smaller and the temperatures are in general lower. Also no increase of temperature after $t_o \geq 20^d$ occurs with the exception of T(B-V). The evolution of this colour temperature is almost like in SNe Ia, but the temperature of SN 1983N lies ~1600K lower for all times after $t_o \approx 30^d$. This is a remarkable difference to all other colours, which also lead to smaller temperatures but have a distinct behaviour compared to SNe Ia. The temperature is almost stable after a cooling phase and a unique value is reached at $t_o \approx 105^d$ ($T \approx 5000K$). This coincidence is surprising considering the relative scarceness of data defining the decay phase in all filters. After the cooling the temperatures are ~4400K and ~5100K for (B-H) and (V-H), respectively. This is ~2500K lower than for SNe Ia. The picture given in Figure 31 shows, that SNe Ib are not "born old" (Panagia 1984), but exhibit a different evolution as there is no general resemblance of the two sets of curves. That the curves converge can be interpreted as a thermalisation of the atmosphere. If this is true, a break in the light curves should occur. Our light curves are not defined for later

epoches, but Figure 28 suggests, that in the infrared the slope might be to steep to fit the observations of SN 1983N after 200 days past maximum. The interpretation of pure coincidence seems unlikely, because all five colours converge to a single value.

e) The bolometric light curve of SN 1983N

Despite the fact, that no information is provided in the U we tried to construct a bolometric light curve for SN 1983N. Luckily the whole range in time is observed well enough to show the curve also at maximum (Figure 32), which is reached at $t_o=3^d$, i.e. 3 days after the B maximum. An earlier attempt to construct the bolometric light curve of this SN was made by Panagia (1984, 1985). In Figure 33 we compare our curve to his data. As the points were given in flux units we decided to convert the bolometric magnitudes into fluxes rather than vice versa. The time scales of the data sets had to be shifted to allow the comparison. Assuming that ~17 days elapsed between the explosion (June 29, 1983, JD 2445514, Panagia 1985) and the B maximum (July 16, JD 2445531) adopted here we moved the observations to fit our time scale t_o. The points do not fit the curve too well, which can be attributed to the different wavelength ranges of the integration. Our set is confined to the range between 4000Å (B) and 22000Å (K), whereas Panagia used the whole spectrum including IUE data down to 1200Å. If the points join the light curve after $t\approx30^d$ as could be suspected, it would mean that the flux contribution at short wavelengths is significant only during the peak, much like for SNe Ia. The contribution amounts to $\sim2.5\cdot10^{-10}$ erg cm^{-2} s^{-1} at maximum, which is 25% of the totally emitted energy.

A comparison of the shapes of the curves after $t_o=50^d$ reveals the common nature of the two subtypes of SNe I. The slopes are $0.^m0248$/day and $0.^m0238$/day for SNe Ia and SN 1983N, respectively, which is well within the uncertainties. Thus the gradient can be regarded as equal indicating that the light curves of SNe Ib are probably powered by the same process as SNe Ia. For a comparison of the absolute energies one needs distance measurements and knowledge on the absorption. As no information on the absorption of SN 1983N is available (no intrinsic colours of SNe Ib are known) it is not feasible to attempt this. Hence we decided to compare only the shapes of the bolometric light curves at the moment and will postpone the discussion of the absolute values to a later chapter. The curve of SN 1983N was shifted in brightness in order to match the bolometric light curve of SNe Ia as given in Figures 12 and 13 at $t_o=100^d$. This anticipates that the total flux indeed is identical at this phase. Figure 34 displays the resulting image. The late epoches are obviously identical, but the peaks differ considerably. At $t_o=5^d$, the first point for the Ia curve, the difference arises to $0.^m74$ in brightness and stays fairly stable until $t_o\approx20^d$, when it diminishes and the curves converge at $t_o\approx40^d$. The transition from the steep decline to the shallow end phase occurs at different epoches. For SNe Ia this is only 40 days

past maximum, whereas SN 1983N changes slopes at $t_o \approx 20^d$. Hence SN 1983N evolved quicker than SNe Ia. Regarding also the shorter time interval for SN 1983N between explosion and maximum ($\Delta t = 17^d$) this means, that the outburst is retained in the beginning and the photosphere never reached the expansion as in SNe Ia, thus being fainter. If much of the energy is converted into kinetic energy to push the surrounding material and the photosphere is heated less then the red colours could be explained as well. Another piece in the puzzle is the radio radiation, which is interpreted as interaction with the surrounding matter (Chevalier 1984). All this fits neatly into the picture of a massive star, which falls to the lot of a core explosion (Begelman and Sarazin 1986, Harkness et al. 1987, van den Bergh 1988b, Panagia and Laidler 1988). For the problems in reproducing such an explosion theoretically see Ensman and Woosley (1988). In this discussion we mainly treated SN 1983N, but we think that with the according modifications, this picture is correct for all SNe Ib.

7. Supernova 1986G in Cen A (NGC 5128)

a) Construction of the curves

At the beginning of 1986 it was clear that the simple picture of having one confined class of practically identical objects, i.e. SNe I before 1983, had to be modified by a distinction into the subclasses Ia and Ib. Thus the bright supernova in Centaurus A (Evans 1986) gave hope to provide an excellent possibility for an extensive investigation of one of these events. Although this supernova suffered heavy absorption within the peculiar S0 galaxy it offered a marvellous opportunity to observe a SN I, as it was one of the nearest supernovae ever observed and also because it was discovered during the rising phase (Phillips et al. 1987 and references therein). Instead of becoming a standard example of a SN Ia, the new and unexpected features which this supernova exhibited threatened the classification scheme once more (Phillips et al. 1987, Frogel et al. 1987). They are, as listed in Phillips et al.:

- a very high value of Pskovskii's β parameter ($\approx$12), i.e. a fast decline after maximum in the optical light curves B and V,

- several spectral differences compared to standard SNe Ia, mainly stronger absorptions in certain lines,

- distinct infrared light curves in J,H and K, not fitting either Ia or Ib templates.

Due to these arguments it has been claimed that even in the subclass of SNe Ia real discrepancies exist which renders their use as standard candles inappropriate (van den Bergh 1988c, Canal et al. 1988). Fits on standard curves indeed yield very large scatters, which cannot be explained by observational problems regarding the high standard of the observations and the brightness of the supernova. Table 19 lists the values of magnitudes and estimated standard deviations of the fits on templates of SNe Ia and SNe Ib, respectively. Any suspicion of being a type Ib supernova is ruled out by the large errors in these fits. This supports the spectral evidence showing a spectrum with typical features of SNe Ia. But also the discrepancies in the infrared in the case of the fit on SNe Ia templates are not conceivable with the quality of the observations. Another indication of the strange nature of this supernova are the colours, which are very unusual for a type Ia. All this led us to construct a special set of templates for SN 1986G. We were in the comfortable situation that extensive photometry was carried out on this event and is available in the literature (Phillips et al. 1987, Frogel et al. 1987) covering all photometric bands used in this study. The procedure to obtain the curves equalled the method for the other sets of curves. The resulting light curves are again a composite of a polynom of

10^{th} power for the peak phase and a linear regression for the late decline. In Table 20 we give a listing of the curves. The confrontation of the templates with the observations is shown in Figures 35 and 36 normalised to $B_o^o=0^m$ at $t_o=0^d$. The points are fitted exceedingly well (see also Table 19) and we think the curves provide a suitable tool for the further investigations of this special supernova. Only the U curve had too few observations to establish a unique light curve. Here the last observation might indicate the "bend" normally present in SNe Ia. To have a reasonable continuation beyond $t_o=20^d$, we assumed the slope to be equal as in SNe Ia. This also fixed the transitional time between peak and linear phase.

b) The curves

A summary of the parameters of the templates is given in Table 21. It is striking how similar the slopes are to the corresponding values of SNe Ia (Table 1). It seems likely that SN 1986G had the same declining curves as other SNe Ia several weeks past maximum, another correspondance with normal SNe Ia although its light curves do not exhibit exactly the same form of the peak. The main difference in B is the very fast decline just after maximum, which is faster than for almost all SNe Ia observed before (Phillips et al. 1987). But this phase ends at $t_o\approx30^d$, when the curve enters the final exponential decay. If one compares the brightness difference of SN 1986G and SNe Ia between maximum ($t_o=0^d$) and $t_o=50^d$, another surprising result is found. The two values differ only by $0.^m03$. Thus the decrease ends at the same level as in SNe Ia. The V curve, however, does not show such a similarity. Although the slope is almost equal to normal SNe Ia, its brightness level is lower by $0.^m43$, which is a considerable difference. The comparison in U is hindered quite a bit by the lack of data. The only remark here is that the last observed point would again lie on a normal SNe Ia curve yielding a similar picture as in the B filter.

The clear dip in SNe Ia infrared curves has almost vanished in SN 1986G. It is only slightly visible in H and K and somewhat clearer in J and the second maxima do not show up so prominently, as they resemble more plateaus. It is probable, that the first maxima have been observed in this supernova because the curves indicate a rise at $t_o\leq-3^d$. This remark is based on two observations, however.

We determined the B maximum to JD 2446560.6 with an insecurity of $0.^d5$, which is in good agreement with the directly observed date of Phillips et al. The relative epoches of the occurrence of the maxima in the other filters is another parameter for a comparison with standard SNe Ia. Table 22 gives the values for SN 1986G, which have to be compared to the figures in Table 5. The uncertainty of the numbers prevent clear distinctions, but again the optical exhibits less changes than the infrared. The minima in two bands (J and K) occur at the same epoches as in SNe Ia, they are in both cases so shallow and broad that no decisive conclusions can be drawn. The H band

displays its minimum considerably earlier. The evolution then drives the curves in about a week to their second maxima, which is about half the time of a normal SN Ia. Due to the different shapes of the templates this confrontation is only weak and cannot yield decisive results. The transition to the late phase seems in general to occur earlier in SN 1986G.

c) Colours

The colours of this supernova are very red (Table 23) and make it one of the reddest supernovae ever observed and let it rival Kepler's SN 1604 in its reddening. This is mainly due to internal absorption in Cen A. The position of SN 1986G in the middle of the dust lane of the peculiar galaxy endorses the conjecture of absorption. The foreground reddening in the Galaxy is $E_{B-V}\approx 0.^m123$ (Burstein and Heiles 1982) because of the small elevation above the galactic plain ($b\approx 19°$). The estimates of the total reddening of SN 1986G is based on measurements of the strength of diffuse interstellar bands in spectra range from $E_{B-V}=0.^m63\pm 0.^m11$ (di Serego Alighieri and Ponz 1987) up to $E_{B-V}=0.^m90\pm 0.^m10$ (Phillips et al. 1987, Rich 1987). A SN Ia showing the observed (B-V) of SN 1986G would have a reddening of $E_{B-V}=1.^m23$ assuming an intrinsic colour of $(B-V)_o^o=-0.^m27$. This large number cannot be reconciled with the reddening measurements above and speaks strongly against the identification as a SN Ia for this object. But these estimates assume a similar reddening law in Cen A and the solar neighbourhood (Rich 1987, di Serego Alighieri and Ponz 1987). Nevertheless also the infrared colours differ significantly from the ones found in SNe Ia. Especially $(J-H)_o^o$ is much redder, which could be explained with a smaller absorption in J (Frogel et al. 1987), whereas $(H-K)_o^o$ is less stringent, but this colour is not very sensitive as mentioned previously. Furthermore a comparison of the infrared colours depends on the evolution of the curves and as the infrared templates differ so strongly from SNe Ia curves it is obvious that also the colours exhibit this discrepancy.

d) Absorption and SN 1971I

As explained in a previous chapter absorption changes the shape of SN light curves. It was also pointed out, that β correlates with absorption. Hence we checked the possibility that the steep decline in B and V could be explained by this effect. The standard deviations increased when we fitted the data to reddened SNe Ia templates, whereas it decreased in the case of V. Nevertheless no satisfying fit could be achieved. Thus we conclude that the shape of optical light curves of SN 1986G cannot solely be attributed to the heavy absorption through which it was seen, but that there indeed are qualitative differences. Any other explanation would have to introduce different reddening processes for the dust in Cen A, which seems to be unlikely (Rich 1987, di Serego Alighieri and Ponz 1987). It has been proposed that SN 1971I in NGC 5055 was comparable to

SN 1986G (Phillips et al. 1987, Frogel et al. 1987). Therefore we tested this hypothesis by fitting the observations of this supernova on our templates. The data in B and V (for references see Cadonau 1986) scatter very strongly and no curve is defined. The standard deviations are very high (~$0.^m2$ in B and ~$0.^m4$ in V) for a fit on the SNe Ia standard set. The value in K (~$0.^m2$) indicates that the curve does not fit the observations. So we tried the special set of curves we determined for SN 1986G for a fit of the observations of SN 1971I. The curves of SN 1986G do not fit any better and even in the K band no acceptable fit can be found, although absorption which distorts the optical curves should be minor in this filter. Also the large errors quoted for the measurements (Elias et al. 1985) cannot explain the discrepancies found. This means that the observations of SN 1971I as a β=12 supernova do not follow the curves defined by the β=12 SN 1986G better than the templates of the standard ($\beta \approx 9$) SNe Ia.

The 3-dimensional plot (Figure 37) reveals the complex nature of SN 1986G. The absorption in J is present, but not as strong as in SNe Ia. Also the plateau (or second maxima) in the infrared can easily be seen. Like in SNe Ia the J band exhibits the strongest fluctuations. But the epoches of the maxima are not the same as in SNe Ia nor is their occurrence. Here the H band has its maximum and minimum before the corresponding extrema of J and K (Table 22). This underlines the fact that the J band is influenced by an absorption trough, but with a different evolution than in SNe Ia, because the curve peaks much earlier. Another interesting feature is the decrease of the decay rates after maximum from shorter to longer wavelengths in the optical, which is broken in the infrared, where the curves reach the final decay phase very quickly. The overall picture emerging is a very flat spectrum with very intensive infrared and strongly depressed optical radiation. This is due to the strong absorption affecting mainly the optical part of the spectrum. No calculations on the colour temperatures were carried out, because of the heavy reddening which renders such investigations useless. Also a comparison with black bodies is only feasible with dereddened magnitudes. This needs knowledge of the absorption law in Cen A which is somewhat in dispute (di Serego Alighieri and Ponz 1987, Rich 1987, Phillips et al. 1987). Thus we pass this study over because we think that the data are not reliable enough.

e) Bolometric light curve

The bolometric light curve for the received flux, i.e. the uncorrected light curves, is given in Figure 38. This curve clearly displays a "bump" between 5 and 30 days past maximum. This is due to absorption and the hence relative high infrared fluxes compared to the optical filters, which gives the infrared curves with the late second maxima more weight. The slope after t_o=40^d is $0.^m031$ per day, which is higher than for SNe Ia and SNe Ib. The influence of the U is minor for the shape as it

does not differ strongly from the assumed curve. For a comparison of the bolometric light curves with the according curves of the other type I SNe, it was necessary to correct the measured curves for absorption. This was done using the corrections given by Schmidt-Kaler (1982) for the U,B and V filters and Elias et al. (1985) for J,H and K. Thus we assume equal absorbing properties of the dust in Cen A and locally, which is the best possible approximation, (Rich 1987, Phillips et al. 1987). An $E_{B-V}=0.^m9$ and the corrections applied yield the magnitudes and colours in Table 24. The B value lies slightly higher than the one quoted by Phillips et al., but regarding the uncertainties in the corrections we think that the given values compare well with theirs. The colours still differ significantly from those of normal SNe Ia, but surprisingly $(B-H)_o^o$ and $(V-K)_o^o$ are even bluer, although the optical colours are redder. $(J-H)_o^o$ displays the small absorption in J, whereas $(H-K)_o^o$ is somewhat bluer than in SNe Ia. Hence either SN 1986G was a SN Ia and the corrections applied are wrong or the corrections are right and the supernova was intrinsically different. If one uses a curve with corrected magnitudes (Figure 39) the excess radiation in the beginning decay disappears as the optical bands now carry much more energy than the infrared. The final slope is now $0.^m027$ closer to the value of the other SNe I, suggesting that this phase again is driven by the Ni^{56}-Co^{56}-Fe^{56} decay chain. Thus we have another hint that the absorption corrections applied are not too far off.

f) Comparison to other SNe I

It is now possible to compare again the shape of the bolometric curves of SNe I. This is done in Figure 40. There we shifted the curves to match at the arbitrary chosen phase $t_o=100^d$. As pointed out above the slopes do not differ much after $t_o=40^d$ but the peak in SN 1986G exhibits a steeper decline as was already seen in the individual optical bands. How much of this can be attributed to absorption is not clear, but surprisingly the magnitude difference between the maximum and the late epoches seem to be bigger in SN 1986G than in SNe Ia. If the same amount of Ni^{56} was produced in SN 1986G and in SNe Ia, so that the late phases emit a comparable energy flux, this would imply that the supernova in Cen A was brighter than normal SNe Ia. If on the other hand the maxima were equal, then less Ni^{56} would have been produced in the explosion of SN 1986G. It is also possible that the radiation somehow was blocked and we saw less radiation at late times. Again we are forced to introduce distances to compare the absolute emitted fluxes of the supernovae. The comparison with the bolometric light curve of SN 1983N reveals a steeper decline after maximum and hence a bigger difference in brightness for SN 1986G. The values are $\Delta m_{Bol}=2.^m1$ for the time interval between $t_o=2^d$ (maximum of the curve) and $t_o=30^d$. The according number in SN 1983N in M83 is $1.^m22$. The exponential decay phase sets in much earlier in SN 1983N ($t_o\approx20^d$) than in SN 1986G ($t_o\approx35^d$), whereas it is even

later in SNe Ia ($t_o \approx 40^d$; Figure 40). The picture emerging from the discussion above is a supernova Ia with some modifications. The origin and the nature of these modifications are unknown. It is not clear to what extent the distinct nature of SN 1986G is due to the very strong absorption in Cen A. The shapes of the infrared curves are not explained by absorption effects at all (unless one invokes variable absorption), nor are the colours of SN 1986G. Nevertheless it exhibited an equality to a normal SN Ia in many aspects:

- the slopes of the final decay phase in the light curves are very similar.

- the equal magnitude differences of the supernova in B between $t_o=0^d$ and $t_o=50^d$.

- the absorption in J is present, less strong though.

- the bolometric light curve (corrected assuming the same absorption law in Cen A and the Galaxy) follows closely the one determined for SNe Ia.

Thus SN 1986G is another puzzling event in the history of supernovae. It poses the severe question of the uniformity of SNe Ia once more. Perhaps the environmental effects distorted the picture we received, perhaps an object of a new subclass was seen. We think an unanimous answer cannot be found the time being. Supernova theory may sometime explain what occurred in Cen A.

8. Differences of subtypes of SNe I

a) The two-colour diagrams

As described in the previous chapters, significant differences between individual SNe I can be found in the shapes of light curves in almost all filter bands, leading to the distinction of three subclasses. The additional effects of absorption and redshift were exemplified for the special case of SNe Ia, which exhibit a close standard behaviour and are the only subgroup suited for such an investigation. The class of SNe Ib is not homogeneous enough, although the internal differences still admit their confinement into a separate class. The outstanding SN 1986G is still not understood adequately to classify it as a new, special subtype of SNe Ia. Any attempt to solve this problem will have to treat absorption correctly. The main differences in the optical light curves are the fast decline of SN 1986G compared to SNe Ia and the different slopes of SNe Ib for the late decaying light curve ($t_o \geq 40^d$). In the infrared the characteristic bumps of SNe Ia are suppressed and shifted in SN 1986G and not observed in SNe Ib. Again the decline is different for SNe Ib after 40 days past maximum. In this chapter we will discuss further distinguishing features of subtypes of SNe I. The distinctive differences of SNe Ib (spectral variations, radio sources, special infrared light curves, different slopes, red colours) call for a further investigation of this subclass. The red colours noticed very early (Wheeler and Levreault 1985, Uomoto and Kirshner 1985, Panagia 1985) are a practical tool for the separation of such events from SNe Ia. Also the new templates of chapter 6 provided these colours. Table 18 lists the values, which have to be compared to those given in Table 6 for SNe Ia. It is not possible to determine an absorption for SNe Ib as the intrinsic colours are not known. In spite of this obstacle it should be possible qualitatively to collate the two subclasses. The strongly absorbed SN 1986G will be given in the same context. We confined the discussion to the colours at maximum ($t_o = 0^d$), because we assumed that the colour evolution follows equal tracks for each subtype. This assumption is valid for the standard Ia's, but for SNe Ib a looser definition of the behaviour must be accepted, whereas the evolution of SN 1986G is fixed by the observations of this single event. Thus a direct connection can be made to any epoch given the maximum data and the light curves. In Figure 41 the two-colour diagram of all standard SNe with available UBV data are shown. The different colours of SNe Ia are due to reddening. Also given is the adopted intrinsic colour of SNe Ia (filled dots) at $(B-V)_o^o = -0.^m27$ and $(U-B)_o^o = -0.^m4$. Its definition is very insecure, especially in (U-B), where an error limit of $0.^m1$ seems to be appropriate (cf. chapter 3). The arrow shows the reddening line for foreground absorption in this diagram. Again, as mentioned, above SN 1986G - if a type Ia supernova - would imply a different reddening law for Cen A. SNe Ib are significantly redder in both colours than SNe Ia, the bluest SN Ib being SN 1984L, which lies more

than $0.^m2$ to the red in (B-V) and (U-B). A clear separation of all subtypes is visible not only in (B-V) but also in (U-B). Strangely enough SNe Ib look like heavily reddened SNe Ia. Whether this has some physical reason is not known yet, but it can hint towards a possible connection of the two subtypes. The scatter around the reddening line is considerable in the case of SNe Ia. The procedure to determine the individual maximum magnitudes in each filter and to subtract them to get the colours is not very accurate so that an error of $0.^m1$ has to be accepted. An investigation of many more SNe I will improve this diagram notably, but will have to cope with bad observations. To amend the knowledge on the absorption we plotted colours which carry big absorption effects (like B-H) against a colour almost not influenced (e.g. H-K). The infrared colour is very insensitive to changes at low temperatures and is almost equal for SNe Ia and SNe Ib, a further hint to the common nature of these objects. Thus we chose (B-V) as the "unabsorbed" colour because the distinction of the subtypes is clearer (Figure 42). The reason for this choice is the supposition that both magnitudes are absorbed comparably. Interestingly the SNe Ia do not follow the reddening line in this diagram. The scatter in the diagram with the optical colours is too big to be narrative but here a clear trend is visible. The reddening line was defined using the absorption corrections given in Elias et al. (1985). The line described by the supernovae (Ia and Ib) would suggest a more shallow correlation implying smaller absorption corrections for the H band. The point of SN 1984L is very insecure because the (B-V) value relies on only one measurement in B. Again SN 1986G cannot be accommodated with the other SNe. The dot gives the value used in the computation of the bolometric light curve of SNe Ia. A $(B-H)\leqq-1^m$ would suit the data better but we argued above why $(B-H)_o{}^o=-0.^m85$ was chosen. The difference in (B-H) is obvious, but it has to be commented. All maximum values in H are extrapolated, because no SN Ia has been observed earlier than 5 days past maximum in the infrared. The extrapolation is a steep decline, which might be wrong as the first maximum of these SNe may occur during that time, so that all estimates in H are too high and hence $(B-H)_o{}^o$ too big. This would move all points by an equal amount down. To remedy this we calculated the same diagram at the epoch of $t_o=10^d$. The picture (Figure 43) does not change drastically, but again a tentative connection between SNe Ia and SNe Ib via reddening is detected. The slope defined by SNe Ia alone deviates from the reddening line, which is not understood at all. The position of SN 1986G does not lie far away of the reddening line in this depiction. These diagrams are not conclusive and will have to await further (high quality) data to clarify the nature of the connections or relations between the different subtypes.

b) Relative luminosities of SNe I

Another often discussed feature of SNe Ib is their relative lower radiation at maximum compared to SNe Ia (Panagia 1985,

Wheeler and Levreault 1985, Uomoto and Kirshner 1985, Filippenko 1986, Porter and Filippenko 1987, van den Bergh 1988c). The maximum brightness of SN 1986G is not well known either (Phillips et al. 1987, Frogel et al. 1987). Rather than determining the absolute magnitudes of SNe with the inherent problems of distances and internal scatter in the subtypes (though mainly observational) we advocate here two cases where the luminosities of SNe of distinct subtypes can be compared directly.

The first example is SN 1976B which occurred in the edge on galaxy NGC 4402. This galaxy is a member of the Virgo cluster (Binggeli et al. 1985, Kraan-Korteweg 1986) and hence its apparent brightness is directly comparable to SNe Ia in this cluster. A list of such SNe Ia is given in Tammann (1988, Table 1). His sample includes also SN 1981B in NGC 4536, one of the standard SNe Ia. The case of the parent galaxy of this supernova is ambiguous; Binggeli et al. (1985) do not include it as a member of the Virgo cluster and Kraan-Korteweg (1986) finds a solution in the Virgo Infall model which places the galaxy in the background of the cluster. The position though (~10° from the cluster centre) and its velocity (v_o=1680 km s^{-1}, Kraan-Korteweg 1986) do not completely exclude a membership. The Tully Fisher relation as defined by Kraan-Korteweg et al. (1988) puts the galaxy slightly behind Virgo (Kraan-Korteweg 1988). Another argument is based on the absolute magnitudes of SNe Ia. Taking the solution of the infall model would yield an absolute magnitude of $M_B \approx -21.^m0$ which is too high for SNe Ia, whereas this supernova at the Virgo distance would have had $M_B \approx -19.^m7$ which is closer to the generally accepted value of $-19.^m7$ (Tammann 1988) and $-20.^m0$ (van den Bergh 1988d). The direct comparison of the maximum magnitudes shows that SN 1976B was ~3^m fainter in B than SN 1981B if they were at the same distance. The difference in V is $1.^m4$. The magnitudes are corrected for foreground but not for internal absorption. SN 1976B was supposedly reddened substantially which causes the red colour. This is supported by its position in the dust lane of the galaxy. The $(B-V)_o^o$ of SN 1976B is $0.^m9$ redder than for SN 1983N. Hence the colour excess is at least this big (assuming that SN 1983N was not absorbed). If a normal absorption law ($A_B \approx 4 \cdot E_{B-V}$) would be applied this supernova would have been brighter than a SN Ia. So either SNe Ib do not exhibit a single colour value at maximum or the absorption overestimates the corrections. A third possibility is that the range of maximum luminosities of SNe Ib extends up to above SNe Ia brightness (Ensman and Woosley 1988).

A second check is provided by the coincidence of three supernovae type I in a small group of galaxies nearby (B6 in Kraan-Korteweg and Tammann 1979, Tammann and Kraan-Korteweg 1978, Sandage and Tammann 1975). The group embodies NGC 5128 (Cen A, SN 1986G) as its biggest member and NGC 5236 (M83, SN 1983N) and probably NGC 5253 (SN 1972E), which means that we have all subtypes of SNe I in a sample at supposedly the same distance. It is still questionable if NGC 5253 really is a member of the group due to its low recession velocity. Luckily the sample contains the best observed examples of each subtype, al-

lowing to compare the SNe in all filters. Again no corrections for internal absorption were applied to SN 1983N and for SN 1986G we adopted the corrections of chapter 7. Table 25 lists the differences in the six investigated filters. The gap in B between the Ia and the Ib supernovae are similar to those derived above in the case of supernovae in Virgo. In V the difference is a magnitude bigger, whereas the U has a value of ~3.^{m}9. The fact that SN 1972E was less reddened than SN 1981B and no reddening is known for SN 1983N suggests that SNe Ib exhibit a wide range of absolute magnitudes (Ensman and Woosley 1988). The infrared magnitudes show the subluminosity of SN 1983N, because only small corrections would be applied to this spectral region. Here intrinsic differences are directly visible. Again the caveat of the extrapolated Ia curves has to be placed here, but also the differences at $t_o \approx 10^{d}$ are incompatible. The differences between SN 1986G and SN 1972E are surprisingly small. The absorption corrections are probably not very accurate as described in the previous chapter, nevertheless a good agreement is achieved in all filters but the J band. The strong absorption in SNe Ia which is much smaller in SN 1986G (Frogel et al. 1987) may cause the difference in this filter. Also the other infrared differences are influenced by the extrapolation of the SNe Ia templates. The check at $t_o = 10^{d}$ reveals this, as all magnitude differences in the infrared filters are less than 0.^{m}2. The big variations in the optical could be due to insufficient reddening corrections. The emerging picture is thus a real difference between SNe Ia and SNe Ib, which are probably ~3.^{m}0 less luminous in B and ~2.^{m}0 in V. In the infrared the difference at maximum is around 1^{m} in all bands. SN 1986G on the other hand exhibits similar brightness as SN 1972E, if one corrects for absorption, and if these corrections are alright.

c) Bolometric light curves

A last test is provided by the comparison of the bolometric light curves of the three supernovae. The result is Figure 44, where the fluxes measured on earth are compared. The curve of SN 1983N is clearly subluminous by 2.^{m}5 at $t_o = 5^{d}$. This trend is maintained and in the final decay phase ($t_o = 50^{d}$) SN 1983N is 1.^{m}9 fainter than SN 1972E. Once more we have to point out that we do not know to what extent this result is influenced by absorption. But it is clear that SN 1983N emitted less energy than SN 1972E. For all epoches with $t_o \geq 50^{d}$ this means that either less Ni^{56} was produced in the explosion or the transformation of the γ energies into optical and infrared radiation was less efficient in this supernova than in SNe Ia. The conclusion for SNe Ib is that they are indeed subluminous by ~2.^{m}5 at maximum and ~2^{m} for later epoches. Similar values can be obtained for the optical filters and in the infrared. The bolometric light curve of SN 1986G follows the curve of SN 1972E reasonably well, although the faster decline after maximum is obvious. At maximum the two supernovae were comparable in the

emitted flux (Δm_{Bol}=0.^{m}4 at t_o=50^d). As indicated above the curve of SN 1986G carries a considerable degree of uncertainties due to the absorption corrections so that a complete equality of the curves of SN 1986G and SN 1972E cannot be excluded. Thus at least at maximum it is reasonable to assume that the two supernovae emitted a similar amount of energy. If SN 1986G really was an example of a SN Ia explosion of its own kind then it will be interesting to observe a similar event with less absorption. It is of tantalising interest to explain why this supernova exhibited such strange (infrared) light curves when it resembled a normal SN Ia so closely in many other aspects. To provide further clues to the nature of the subtypes of SNe I we now have to turn to absolute magnitudes, widen the sample and include all reasonably well observed SNe in galaxies with known distances. Hence we confirm the picture that SNe Ib are much redder ($(B-V)_o^o \geq 0.^m5$) and less luminous ($\Delta m_{Bol} \approx 2.^m5$) at maximum. These are higher values than considered so far (Panagia 1985, van den Bergh 1988c, Uomoto and Kirshner 1985, Filippenko 1986). SN 1986G resembled normal SNe Ia much more than was expected and the assumption of comparable maximum luminosities seems to be acceptable (Phillips et al. 1987).

9. Absolute magnitudes of SNe I

a) Introduction

The determination of absolute magnitudes of SNe at maximum has been a long-standing and intriguing problem. It is interwoven with the implication that SNe I represent standard candles and are a good tool to measure distances in the universe, hence the parameters of expansion H_o and deccelaration q_o. Much work has been done in this field (Tammann 1982, 1976, Branch and Bettis 1978, Branch 1978, 1982, 1985, Elias et al. 1985, reviews: Bartel 1985, Tammann 1987, van den Bergh 1988d). The properties of SNe Ia as standard candles have often been doubted (Branch et al. 1988, Canal et al. 1988). Since the subgroup of SNe Ib was detected this argument has proven to be partially right. The discussion now centres on SNe Ia for which the hope that they represent probes to determine cosmological distances remains. Out of the different approaches to determine the absolute magnitudes of SNe I we will use the direct measurement involving the distances to the parent galaxies. The calculations were carried out for all SNe I in the hope to find a clear separation of SNe Ia and SNe Ib in maximum brightness. In another attempt the calculation of an absolute bolometric light curve of SNe Ia will be ventured.

The main problem in the absolute calibration of SNe lies in the distances as independent measurements are often not available. Contaminating effects like our motion towards Virgo, peculiar velocities in groups and clusters or in the field, and a possible motion against a great attractor have to be accounted for and corrected. The catalogues of Kraan-Korteweg (1986), Kraan-Korteweg and Tammann (1979) and Binggeli et al. (1985) provide a good data basis for distances relative to Virgo in the infall model (Kraan-Korteweg 1986, Schechter 1980), group members (Kraan-Korteweg and Tammann 1979) and membership to Virgo (Binggeli et al. 1985). All distances are taken from one of these sources. Some distances will be discussed specially. For the Virgo cluster distance we adopted r_v=21 Mpc for simplicity, which is slightly higher than the recent determination by Kraan-Korteweg et al. (1988) using the Tully Fisher method and by ~1 Mpc less than found by Tammann (1988) reviewing different methods. The assumption of a Virgo distance of 21 Mpc implies a Hubble constant of H_o=57 km s^{-1} Mpc^{-1}, if v_o(Virgo)=1196 km s^{-1} (Binggeli et al. 1987). To reduce our absolute magnitudes to any other distance scale one has to use the formula

$$M_i = M_i^0(r_V = 21 Mpc) - 5 \log \left(\frac{r_V}{21 Mpc} \right)$$

b) The standard SNe Ia

The four standard SNe Ia and SN 1983G have distances in the range of up to twice the Virgo distance. The only unambiguous case in the sample is the galaxy Fornax A (NGC 1316, SNe 1980N

and 1981D). NGC 5253 (SN 1972E) is an amorphous galaxy with a low velocity (v_o=147 km s^{-1}) but is possibly a member of the Centaurus A group (Kraan-Korteweg and Tammann 1979) and hence at a relative Virgo distance of d_v=0.23 (Kraan-Korteweg 1988). This must be opposed to the distance computed in the infall model of d_v=0.13. The case of NGC 4536 (SN 1981B) is discussed in the previous chapter. The conclusion that this galaxy is a member of Virgo is tentative and we will also present absolute magnitudes for the case placing it in the background. Unfortunately NGC 4753 (SN 1983G) has no clear solution either. Its proximity to Virgo led to ambiguities. Tammann (1988) ranks it as a member but its distance from the cluster centre (~13°) seems to be too large to allow this conclusion. Again two solutions will be presented. A best bet may represent the choice of distances given in Table 26. The individual magnitudes are the corresponding brightness at $t_o=0^d$ and not at the individual filter maxima and were determined without correction for internal absorption so that they still carry a certain contamination. Nevertheless the mean value is defined exceedingly well. The infrared data is problematic because they rest on the extrapolated maxima. The absolute value in these filters may be in error regarding the real value at $t_o=0^d$. This becomes relevant only when a SN Ia will be observed at such an early epoch. To give values that are directly comparable and do not rest on extrapolation the absolute magnitudes at $t_o=10^d$ are added for the infrared filters. It is remarkable how small the scatter in all filter determinations is. In U one expected the biggest deviations because this filter normally is not very well observed and the template is the worst determined (cf. discussion in chapter 3 on the individual light curves). The scatter in B and V is small, although no corrections for internal absorption has been applied. The standard deviation in V is almost as small as the one in the infrared bands H and K. These filters are less affected by absorption and should provide more reliable absolute magnitudes. For the J filter the deviations are bigger probably due to the absorption trough that falls into the wavelength range of this filter. Again the light curve of this filter is not defined so well as the other infrared templates. It has been argued that $A_B=E_{B-V}$ for SNe Ia (Tammann 1987) which would also explain the slopes in Figures 42 and 43 within SNe Ia. If this is true then almost no absorption should be present in V and hence the scatter of this optical filter comparable to that in the infrared and smaller than the one in the absorbed B filter. This astonishing result throws doubt on the simple application of the local absorption law in other galaxies. If the chosen distances are right then SNe Ia indeed are very good standard candles and could provide us with deep probes of the universe. The reasons for the special choices of the distances are pointed out above, they could be wrong, however. Thus we calculated absolute magnitudes for the case that NGC 5253 is not a member of the Cen A group, NGC 4536 is a distant galaxy behind Virgo but NGC 4753 is a member of this cluster, despite its big angular distance from the cluster centre. This choice yields the

numbers given in Table 27. The calculations are based on the same assumptions like in Table 26. The averages do not differ much from the former. They are in general a tenth of a magnitude fainter, but the deviations are bigger and for all filters almost the same size. This is interpreted that an overlaying effect, i.e. the inappropriate choice of distances, hides the real scatter in the sample. Nevertheless it is not possible to exclude these results entirely on the basis of the five supernovae. This is especially tantalising because the small scatter of the first solution (Table 26) would make SNe Ia marvellous standard candles, whereas in the second case we would have no better tool than other distance indicators (like e.g. the Tully-Fisher relation or brightest galaxies in clusters).

c) A sample of SNe Ia in Virgo

It is necessary to enlarge the sample by adding other SNe Ia in galaxies either in clusters, when their membership is beyond doubt, or in galaxies with individually well observed distances. No information on the infrared is available for others than the five standard SNe Ia presented, so the further discussion will focus entirely on optical filters and is confronted with the severe problem of internal absorption. The best example for the first case is the Virgo cluster. A compilation of SNe Ia in Virgo is given by Tammann (1988). In his list is one SN Ib (SN 1976B) which has to be excluded. He enclosed also SNe 1981B and 1983G, whos cases have been discussed extensively above. Because of the uncertainties of their membership to the cluster we omitted all SNe in these galaxies (i.e. also SN 1965I in NGC 4753). If only SNe Ia with B observations are considered three SNe are left over. They are SN 1960R in NGC 4382, SN 1961H in NGC 4564 and SN 1984A in NGC 4419. All these galaxies are believed to be members of the cluster (Binggeli et al. 1985). Additionally included is SN 1960F in NGC 4496. This galaxy is not listed in the Virgo catalogue (Binggeli et al. 1985) because of its outlying position (~8° from the centre), but its velocity of v_o=1570 km s^{-1} puts it into the cluster. Unfortunately the older three supernovae in Virgo have only a few B observations and each has one V measurement. SN 1984A has a better defined V curve and even provides infrared measurements (Graham et al. 1988, Meikle et al. 1984, Meikle 1984). Some properties of the selected supernovae are given in Table 28. The scatter around the B template is the smallest for SN 1960R which follows the standard curve exceptionally well. The other SNe have bigger deviations but they are still within the expected errors. The mean is well defined and corresponds to an absolute magnitude of M_B^o=-19.^{m}60±0.^{m}22 (r_V=21 Mpc). This value is close to those calculated previously. Especially the comparison with SN 1981B is interesting, because its brightness puts this supernova into the Virgo distance. The difference between the B value of this supernova and the average of the Virgo SNe is 0.^{m}04. Thus if one puts these five SNe into one sample a mean apparent B magni-

tude in Virgo is $12.^m02 \pm 0.^m19$, which corresponds to an absolute brightness of $M_B^0 = -19.^m59$ (r_V=21 Mpc) or $M_B^0 = -19.^m84$ (r_V=23.9 Mpc, H_0=50 km s^{-1} Mpc^{-1}). Nevertheless there arises in all other filters a severe problem with SN 1984A. The direct comparison with SN 1981B reveals that SN 1984A is $0.^m3$ fainter in all filters but B than the standard supernova. It also had a very blue colour $(B-V)_0^0 = -0.^m27$ at maximum, which implies that this supernova was not absorbed and yet it is fainter in the infrared than the standard SNe Ia. SN 1984A has been discussed recently in the literature (Graham et al. 1988, Graham 1988a, Pearce et al. 1988, Branch 1987, Branch et al. 1988) and it is possible that this supernova may represent another special case of SNe Ia (Graham 1988) as it displayed an unusually high expansion velocity (Branch 1987, Branch et al. 1988) and an uncommon J curve (Graham 1988). Graham et al. (1988) however claim that this brightness difference is not present due to the different distance estimates of SN 1981B, which has been **brighter** than SN 1984A. Their infrared data fit reasonably well on the templates but the discrepancies vanish if their corrections for the galaxy background are too large. Omitting this supernova in the determination of the average B maximum magnitude of SNe Ia in Virgo would lower that value by $0.^m04$ but does not affect the standard deviations.

d) A bigger sample

The other route to the absolute magnitudes of SNe Ia is their determination in galaxies the distances of which are known. This approach is inflicted with the obstacle of poor observations of certain SNe. From the compilation of SNe Ia of Cadonau (1986) we selected the SNe I best observed in B. Table 29 contains the list of these SNe with the references of the data. All observations were corrected for foreground absorption. The determination of the maxima and the magnitudes are in good agreement with Cadonau. The velocities are given corrected to the centroid of the local group as defined in Kraan-Korteweg (1986). The distance relative to Virgo is taken from the same source. All distances marked were calculated by Kraan-Korteweg (1988) with the heliocentric velocities of the references cited. For these supernovae we determined the maximum brightness in all filters where observations were available. Table 30 lists the apparent and the absolute magnitudes of the 20 SNe. It is evident that a certain scatter had to be expected due to the fact that no internal absorption was treated in the data. The very red SN 1984I could well have been a SN Ib. There is unfortunately no spectrum available for this supernova but the very red $(B-V)_0^0$ puts it close to the region of SNe Ib. If it was a SN Ia it was heavily absorbed and thus we excluded this supernova from the calculation of the average values. For two SNe (1975G and 1978E) no distances could be found. The distance to NGC 7343 (SN 1974J) is ambiguous, because three redshift observations in the range from 5600 km s^{-1} to 7400 km s^{-1} are reported in Huchtmeier and Richter (1987), which impedes an un-

equivocal distance determination. SN 1974G definitely was a SN Ia as it exhibited the betraying absorption trough at 6150Å in an early spectrum (Ciatti and Rosino 1977). The fit on the standard Ia curves is reasonably good. Its colours are quite red and an $E_{B-V}\approx 0.^m45$ is observed. Its proximity also enlarges the effect of a possible peculiar velocity masking the real distance. Because of these doubts we exclude this SN. Two intriguing cases are SNe 1971G and 1971I. SN 1971I was proposed to be a similar event like SN 1986G (Frogel et al. 1987, Phillips et al. 1987) due to its steep decline after maximum. It has been discussed already in chapter 7, where we showed that this supernova does not fit onto either sets of curves. Spectra of early epoches clearly show the absorption at 6150Å (Barbon et al. 1973b) and leave no doubt about its identification as a SN Ia. The scatter at maximum is not too big in B, but the data in V disperse widely around the standard curve and allow no satisfying fit. The nature of this supernova is not clear and due to the large deviations in V no reddening can be measured. Nevertheless even a strong absorption, which seems unlikely considering the outlying position of the supernova in the galaxy, would not brighten the SN sufficiently to make it comparable to other SNe Ia. The distance is again very small and thus the effect of peculiar velocity introduces an uncertainty of 15% at the 1σ level. The data of SN 1971G is ambiguous at maximum and do not allow an accurate determination of the maximum magnitude. Because of these reasons we did not include these two SNe. Hence we stay with 13 SNe for the determination of the absolute magnitudes. From the standard deviations given for the fit on the B curve in Table 30 it is clear that any determination will be approximate and the number of observations is very small for certain SNe which introduces further incertitudes. The unweighted average of the SNe 1959C, 1966J, 1967C, 1969C, 1970J, 1971L, 1972J, 1973N, 1975N, 1975O, 1976J, 1979B and 1982B are $M_B^o=-19.^m55\pm0.^m38$, $M_V^o=-19.^m55\pm0.^m40$ (12 SNe) and $M_U^o=-19.^m89\pm0.^m50$ (7 SNe). These values compare well with the determinations using only the five standard SNe Ia. The B and V values are slightly fainter here but this is attributed to contamination of the data by internal absorption. It is surprising though, how little the deviations are, considering the fact that the inhomogeneity of the sample and the insecuritiy of some magnitude determinations. Taking into account all available absolute maximum brightness (including SNe 1971G, 1971I, 1974G and 1984I) yields $M_B^o=-19.^m20\pm0.^m75$, $M_V^o=-19.^m23\pm0.^m69$ and $M_U^o=-19.^m56\pm0.^m82$. It is clear that these figures are too faint and the scatter is increased because some very strongly absorbed SNe (e.g. 1984I, if type Ia at all) and badly defined maximum values are included.

All determinations (best observed standard SNe Ia, SNe Ia in Virgo and the sample of reasonably measured SNe) lie within $0.^m1$ in B and $0.^m2$ in V which we think is very encouraging. Therefore we adopt an overall mean absolute brightness of $M_{B0}=-19.^m6\pm0.^m3$, $M_V^o=-19.^m6\pm0.^m3$ and $M_U^o=-19.^m8\pm0.^m4$ for a Virgo distance of $r_V=21$ Mpc ($H_o=57$ km s^{-1} Mpc^{-1}), giving the standard

SNe Ia a higher weight. M_B^o is in good agreement with van den Bergh (1988d) and Kowal (1968) but $0.^m2$ or brighter than several earlier findings (Cadonau et al. 1985, Tammann 1982, Branch and Bettis 1985, Branch 1985, Arnett et al. 1985). No estimates for other filters were found in the literature. Probably because of absorption the intrinsic colours are not reproduced in the absolute magnitudes. A better understanding of absorption in external galaxies will certainly tighten the absolute values of SNe Ia. It is remarkable, however, that a few odd SNe are observed (like SNe 1971I, 1974G, 1984A), which threaten the status as standard candles.

e) SNe Ib

That SNe Ib are fainter at maximum than SNe Ia has been stated several times. This is endorsed by the three galaxies in which both types of SNe I were observed. SN 1976B in the Virgo galaxy NGC 4402 and SN 1983N in NGC 5236 (M83) were discussed extensively in the previous chapter. A new possibility to test the subluminosity of SNe Ib is provided by SN 1979B and SN 1963J which both occurred in NGC 3913. All available observations of SN 1963J are in the photographic band and not directly comparable to B measurements. Using $m_B=m_{pg}+0.^m29$ (Cadonau 1986) we determined a maximum B magnitude of $B_o^o=13.^m48$ for SN 1963J, which contrasts with $B_o^o=12.^m79$ of SN 1979B. This supernova had a $E_{B-V}\approx0.^m51$ indicating the strong absorption. The difference here is at least $0.^m6$, probably higher. The absolute magnitudes of all SNe Ib in this work are listed in Table 31. The distances were taken from Table 11 and the apparent magnitudes from Table 18. It is evident that this subtype of SNe I is subluminous by 2-3 magnitudes compared to SNe Ia. As no correction for internal absorption was applied a comparable scatter should be expected, if SNe Ib have a similar confined evolution as SNe Ia. The biggest differences within the sample appear in the infrared, where absorption plays a minor role, which clearly displays the non uniformity of this set of SNe. The difference in absolute infrared brightness is more than 2^m between SN 1983I and SN 1984L, a clear sign of the internal differences. Strangely SN 1984L was as bright in the infrared as a typical SN Ia. The scatter around the mean values are $\geq0.^m7$ in the optical and $>1^m$ in the infrared. It is surprising that the scatter in the optical is smaller than in the infrared. This implies that SNe Ib events differ considerably from each other but some unknown process dampens the infrared differences so that they appear suppressed in the optical.

f) The two-colour diagram

As a by-product of this investigation we got new colour data for 8 SNe Ia ($(B-V)_o^o$ and $(U-B)_o^o$). The two-colour diagram (Figure 41) of the maximum colours of SNe I is shown again in Figure 45 with the new data. The spread of the points is increased for SNe Ia. Nevertheless the data generally follow the

reddening line. The error bars indicate estimated errors of the colours. The U magnitude of SN 1976J is determined by only 3 observations and is very insecure. The transitional position of SN 1984I between SNe Ia and SNe Ib complicates the situation. Judging by its faintness it is probably a type Ib event but its colours could as well be interpreted as a strongly absorbed SN Ia. Further SNe I will clear the point if two separate groups exist in this diagram or an overlapping region, i.e. a smooth transition from SNe Ia to SNe Ib.

g) The bolometric light curve of SNe Ia in absolute units

With the absolute magnitudes we are now able to compute the bolometric light curves in absolute units. We used the estimates for the maximum brightness given above and transformed the magnitudes into fluxes. The value depends of course on the choice of the distance to the Virgo cluster, as all magnitudes are tied to this distance. The figures can easily be transformed by

$$F = F^{\star}(21Mpc) \cdot \left(\frac{r_V}{21Mpc}\right)^2$$

We determined the absolute bolometric flux at $t_0=0^d$ (the B maximum) to $F^{\star}_{Bol}=2.2\cdot10^{43}$ erg s^{-1} ($\approx5.7\cdot10^9 L_\odot$), i.e. the total energy radiated by a SN Ia in all directions in the wavelength range between ~3400Å and ~23000Å. This value is an extrapolation because of the lacking observations in the infrared at $t_0\leqq5^d$. Therefore we give the corresponding energy output 10 days past maximum: $F^{\star}_{Bol}(t_0=10^d)=1.5\cdot10^{43}$ erg s^{-1} ($3.9\cdot10^9 L_\odot$). The curve (Figure 46) drops steadily until the transition at $t_0\approx40^d$ takes place. Here the flux diminished considerably to $F^{\star}_{Bol}(t_0=40^d)=3.0\cdot10^{42}$ erg s^{-1}. The slope is approximately $4.4\cdot10^{41}$ erg s^{-1} day^{-1} and lowers to $3.2\cdot10^{40}$ erg s^{-1} day^{-1} after the transitional phase. A direct comparison to the theoretical bolometric light curve of Graham (1987) is not possible because of the different distance scales. His models produce only half the fluxes we derived for our sample but he assumed a lower distance to SN 1972E (NGC 5253). The absolute fluxes agree with the theoretical predictions of a carbon-oxygen white dwarf detonation with the production of ~0.7 $M_\odot$ Ni^{56} (Wheeler and Sutherland 1985, Arnett et al. 1985). The flux of SN 1986G in Cen A was presumably comparable (see chapter 7 and the discussion there), if absorption was treated adequately and NGC 5253 indeed belongs to the Centaurus group, but SNe Ib are subluminous and their bolometric light curves do not coincide because they exhibit very non uniform behaviour (cf. Table 31). Hence we omitted the calculation of their bolometric curves.

The determinations of the maximum magnitudes in the different filters has shown that SNe Ia might still yield good standard candles, in spite of the fact of internal discrepancies (e.g. 1984A; Branch 1987, Branch et al. 1988), which may be observable in the future. The three subsets of SNe Ia (the standard SNe, a sample of Virgo SNe and SNe observed mainly in B) led to

very similar mean values and scatter little, although the SNe were not corrected for internal absorption. Better and more frequent observations of SNe in the infrared will hopefully confine the scatter of SNe Ia brightness in this spectral region to the uncertainties due to peculiar velocities of the galaxies and provide a convenient tool to determine subtypes of SNe I. The absolute bolometric light curves might be improved by better coverage of the electromagnetic radiation. SNe Ib possibly will be detected by their colours and their relative faintness, provided good distances are known.

10. Conclusions

a) Supernovae type Ia

Supernova phenomenology always suffered of sparse and inaccurate data. This makes it difficult to sort out real, intrinsic differences between individual events from observational uncertainties and errors. The concept of templates proved to be very useful allowing to calculate continuous evolutions and bolometric light curves rather than single points, hence providing a better picture of the changes in SNe. With the fiducial curves it was also possible to reduce the individual differences between distinct events to a single epoch (here often the time of the B maximum), thus providing a direct measure for the comparison. This of course relies on the uniformity of the physical event, which seems to be proven for SNe Ia. The assumption of a unique shape of the curves also allowed the calculations of the expected changes due to external effects like extinction or redshift on the optical light curves of SNe Ia. The complication by distorting effects will have to be treated in future, when more precise observations will be possible.

It is, however, encouraging to see, that the sample of the four best observed SNe Ia (SNe 1972E, 1980N, 1981B, 1981D) exhibit so little scatter around a set of templates in six photometric filters. It was possible for the first time to set up fiducial curves for the infrared bands connecting the time scale to the optical. It would have been better in principle to proceed vice versa, because the infrared presumably is less affected by absorption than the optical and some shift in the epoches of the B maximum due to the reddening, though probably small, cannot be excluded entirely. The four supernovae used were fortunately little obscured and they show only small colour excesses. The derived infrared curves should hold for SNe Ia. The long-standing assumption of a black body approximation of the continuum radiation is shown to be wrong by two tests. The extraordinary evolution in the two-colour diagrams, where the black body line is approached only for a short phase ($t_o \approx 40^d$), and the strongly different colour temperatures for individual colours at the same epoch show the strong deviations of the emitted radiation from a thermal energy distribution. The deviations from the black body radiation can only partially be explained by strong depressions in the spectrum, like in U, which is affected by heavy blocking due to Fe lines, and the J band, which suffers a strong absorption. The fluxes in H and K are too small to be explained only be absorption.

The curves presented for distinct reddenings assumed the same colour dependence for extinction as a function of the colour excess in external galaxies and locally. Regarding the small reddenings of SNe Ia measured so far and the smallness of the effect caused by absorption no direct verification of the reality of these changes could be presented. The size of the changes is comparable to the photometric errors of the observations. The only discussed example was Kepler's SN 1604, for which

the observations are too disputed to derive a clear result. Redshift affects the shapes of optical SNe Ia curves much stronger. The K-corrections are big at maximum in V, which seems to be an ideal filter for supernova searches up to z=0.6, because here the corrections are negative making a SN Ia apparently brighter at maximum. A search would have to attempt a high temporal coverage due to the rapid fading of SNe Ia at intermediate redshifts. SN 1988U was the first event discovered at such a distance and exhibited a very fast decline confirming the predictions. For redshifts with $z \geq 0.6$ filter bands at longer wavelengths are more suited. Increasing redshift causes a slimming of the peak in the V curve for intermediate redshifts ($z \leq 0.3$). An interesting side effect is the possibility of testing, whether cosmological redshifts really are caused by the expansion of the universe. A scaling by a factor (1+z) of the time in the light curve is expected due to time dilation. If it is absent we will have to find a new explanation for the redshifts. This test works already at redshifts $z \approx 0.3$ and adds to the surface brightness test (Sandage 1988).

Absolute magnitudes of SNe Ia were determined with several samples. The standard SNe Ia exhibit a very small scatter if we choose the most probable distances of the parent galaxies. Unfortunately these distances are not beyond doubt. A very strange case is NGC 4536 (SN 1981B) for which solutions behind (Kraan-Korteweg 1986, infall model), in (Kraan-Korteweg 1988, Tully-Fisher method) and in front (Graham 1988, Graham et al. 1988, apparent magnitude of SN 1981B and infall model Aaronson et al. 1982) of the Virgo cluster seem possible. The sample of SNe Ia in Virgo yielded very small deviations from a mean value, because no contamination due to distance uncertainties introduced by peculiar velocities of galaxies is present and the scatter can be attributed entirely to photometry. This sample probably provides the best determination of absolute magnitudes of SNe Ia. The optical brightness of SN 1981B compares exceedingly well with the Virgo sample, so that this supernova most probably lay in Virgo, too. A third sample of 13 SNe I gave again similar results compared to the other sets. All SNe I (Tables 26, 28 and 13 SNe from Table 30) yield means of $M_B^o = -19.^m55 \pm 0.^m32$ (22 SNe), $M_V^o = -19.^m57 \pm 0.^m34$ (18 SNe) and $M_U^o = -19.^m82 \pm 0.^m42$ (12 SNe). The small scattering is very encouraging considering that the data were not corrected for internal absorption and partially are influenced by uncertain distance estimates due to peculiar velocities. Not included in this calculation are SNe 1971G, 1971I, and 1974G, which have been discussed extensively. Out of the sample of 25 SNe with known distances these three were the only really disaccording supernovae (SN 1984I is very red, so that extinction has to be treated). They have partially bad photometry (SNe 1971G and 1971I) and occurred in nearby galaxies, so that the effect of peculiar velocities are largest (SNe 1974G and 1971I). Despite these few exceptions the average absolute magnitudes are defined very well. The small scatter also implies small absorption corrections, because the colours of the SNe extend from $(B-V)_o^o = -0.^m31$ to $+0.^m44$. This is a range of $0.^m7$ and

would imply corrections of up to ~2.^{m}8, which would destroy the correspondence of the absolute magnitudes completely. The scatter of the absolute magnitudes is less by a factor 7. A mere coincidence can be excluded, because of the low probability, so that we are faced with the new problem that extinction in galaxies might differ considerably from the known rules as long as we maintain the assumption of an intrinsic colour of SNe Ia. If internal absorption in galaxies does not follow the local extinction laws, SNe Ia as standard candles and hence a singled valued intrinsic colour will be tools for such measurements.

The good correspondance of the bolometric light curve with theoretical predictions (Graham 1987, Nomoto et al. 1984) endorses the model of an exploding white dwarf. The emission at maximum assuming a Virgo distance of r_{Vir}=21 Mpc is close to the predicted energy output (Wheeler and Sutherland 1985, Arnett et al. 1985) The total emitted flux as computed by the bolometric light curve during the period of defined light curves ($-5^{d} \leq t_{o} \leq 110^{d}$) is $5 \cdot 10^{49}$ erg. This is a tenth of the theoretical estimate (Nomoto et al. 1984), but not the complete electromagnetic spectrum is covered and considerable flux during the rising phase is not included.

b) SNe Ib

The sample of SNe Ib exhibits large internal differences and no uniform scenario seems to be appropriate to describe such events. The light curves are defined well in the optical, where SNe Ib follow closely the templates of SNe Ia. The discrepancies appear at the final decay, where the slopes differ from those of SNe Ia curves (Ensman and Woosley 1988). The infrared shows completely distinct curves (Elias et al. 1985). The main differences will probably be observable in this range in future. The colours differ considerably, but no intrinsic colour can be derived because the extinction is unknown. The comparison of the (B-V) of SN 1976B with the other SNe Ib indicates, that no single value for an intrinsic colour may be expected, because the difference is too large to be explained solely by extinction. The temperatures of the SNe Ib seem to be lower as inferred from the red colours, but the radiation is thermalised more than in SNe Ib. The differences in magnitudes are exemplified with three cases of SNe I of the different subtypes at presumably the same distance. The subluminosity of SNe Ib is 2-3 magnitudes in B and V, but varies possibly considerably due to internal differences of SNe Ib. This is underlined by the absolute magnitudes, which exhibit strong variations, they display a wide range of absolute brightness of ~1.^{m}5 in B and in the infrared, a further manifestation of the non uniformity of this subclass. The magnitudes are in general 1^{m}-2^{m} fainter but SN 1984L was as bright in the infrared as SNe Ia. The shapes of the bolometric light curves differ only during the peak, which is less pronounced in time and brightness in SNe Ib. The final declines correspond very well in slope. The quicker evolution of SNe Ib is also supported by the shorter time interval between explo-

sion and the B maximum (~17^{d}, in SNe Ia ~20^{d}). The comparison of bolometric light curves of SN 1983N and SN 1972E reveals the subluminosity of the SN Ib. At maximum the brightness difference is ~3^{m} and also during the final decays, when the slopes are almost equal, SNe 1983N was fainter by ~2^{m}. Thus SNe Ib probably produce less Ni^{56}.

c) SN 1986G

The unique supernova 1986G in Cen A was studied extensively. The differences to normal SNe Ia are mainly in the infrared light curves and the colour excess. Extinction hindered a detailed investigation, but it has been shown that it might explain part of the fast declines of this supernova in the optical. Further conclusions have to be drawn after absorption corrections have been applied, hence introducing strong uncertainties. It has been argued, that the corrections could be in error considerably, but lacking more information we corrected SN 1986G assuming the local extinction law for the internal absorption in Cen A. Some features of SNe Ia were reproduced (apparent peak brightness in the optical) others still differed (magnitudes in the infrared). The bolometric light curve for the corrected magnitudes followed the curve of SNe Ia quite well, however.

d) Colours

Colours separate the subclasses well as long as the epoches of the observations are known. The construction of templates allowed to compare SNe I at a determined epoch. Hence SNe Ib can be detected by photometry not only by their distinct difference in brightness between maximum and the late times, but also by the red colours at maximum. In the two-colour diagram the separation is obvious, although it is still open, if a connection between these two subclasses exists. SN 1986G again lies isolated from both groups, but a normal reddening line cannot explain its position. As pointed out, we have to apply either a different extinction law or it was intrinsically different from SNe Ia in colours.

Extinction first as a problem in SN 1986G hinders all investigations of SNe due to the incomplete understanding of the absorbing processes in other galaxies. Supernovae Ia may become backlights for measuring the intervening material (as in the case of SN 1987A). The standard behaviour of this subtype of SNe I will place it on the top level of probes of the universe.

References

Aaronson,M.,Huchra,J.,Mould,J.,Schechter,P.L.,Tully,R.B.: 1982, Astrophys.J. **258**,64

Arnett,W.D.,Branch,D.,Wheeler,J.C.: 1985, Nature **314**,337

Axelrod,T.S.: 1980, *Texas Workshop on Type I Supernovae*, ed. J.C. Wheeler,Austin:University of Texas,p.80

Baade,W.,Zwicky F.: 1934a, Proc. Natl. Acad. Sci. USA **20**,254

Baade,W.,Zwicky F.: 1934b, Proc. Natl. Acad. Sci. USA **20**,259

Baade,W.: 1943, Astrophys.J. **97**,119

Barbon,R.: 1980, *Texas Workshop on Type I Supernovae*, ed. J.C. Wheeler,Austin:University of Texas,p.16

Barbon,R.,Ciatti,F.,Rosino,L.: 1973a, Astron. Astrophys. **25**,241

Barbon,R.,Ciatti,F.,Rosino,L.: 1973b, Mem. Soc. Astron. Ital. **44**,65 (=Contr. Asiago No. 284)

Barbon,R.,Ciatti,F.,Rosino,L.: 1979, Astron. Astrophys. **72**,287

Barbon,R.,Capaccioli,M.,West,R.M.,Barbier,R.: 1982, Astron. Astrophys. Supp. **49**,73

Barbon,R.,Cappellaro,E.,Ciatti,F.,Turatto,M.,Kowal,C.T.: 1984, Astron. Astrophys. Suppl. **58**,735

Barbon,R.,Cappellaro,E.,Turatto,M.: 1988, *The Asiago Supernova Catalogue 1988*, preliminary version

Bartel,N.,(ed.): 1985, *Supernovae as Distance Indicator*,Berlin:Springer

Begelmann,M.C.,Sarazin,C.L.: 1986, Astrophys.J. **302**,L59

Benvenuti,P.,Sanz Fernandez de Cordoba,L.,Wamsteker,W.,Macchetto,F., Palumbo,G.C.,Panagia,N.: 1982, *An Atlas of UV Spectra of Supernovae*, ESA SP-1046

Bertola,F.: 1964, Ann. Astrophys. **27**,319 (= Cont. Asiago No. 159)

Bertola,F.,Mammano,A.,Perinotto,M.: 1965, Contr. Asiago Obs. No. 174

Binggeli,B.,Sandage,A.,Tammann,G.A.: 1985, Astron.J. **90**,1681

Binggeli,B.,Tammann,G.A.,Sandage,A.: 1987, Astron.J. **94**,251

Branch,D.: 1982, Astrophys.J. **258**,35

Branch,D.: 1985, *Supernovae as Distance Indicators*,ed. N.Bartel,Berlin:Springer,p.138

Branch,D.: 1986, Astrophys.J. **300**,L51

Branch,D.: 1987, Astrophys.J. **316**,L81

Branch,D.,Bettis,C.: 1978, Astron.J. **83**,224

Branch,D.,Lacy,C.H.,McCall,M.L.,Sutherland,P.G.,Uomoto,A.,Wheeler,J.C., Wills,B.J.: 1983, Astrophys.J. **270**,123

Branch,D.,Doggett,J.B.,Nomoto,K.,Thielemann,F.-K.,1985, Astrophys.J. **294**,619

Branch,D.,Nomoto,K.: 1986, Astron. Astrophys. **164**,L13

Branch,D.,Venkatakrishna,K.L.: 1986, Astrophys.J. **306**,L21

Branch,D.,Drucker,W.,Jeffery,D.J.: 1988, Astrophys.J. **330**,L117

Burstein,D.,Heiles,C.: 1982, Astron.J. **87**,1165

Buser,R.: 1978, Astron. Astrophys. **62**,411

Cadonau,R.: 1986, Ph.D. Thesis, University of Basel

Cadonau,R.,Sandage,A.,Tammann,G.A.: 1985, *Supernovae as Distance Indicators*,ed. N.Bartel,Berlin:Springer,p.151

Canal,R.,Isern,J.,Lopez,R.: 1988, Astrophys.J. **330**,L113

Cappellaro,E.,Turatto,M.: 1988, Astron.Astrophys. **190**,10

Chevalier,R.A.: 1984, Astrophys.J. **285**,L63

Ciatti,F.,Rosino,L.: 1977, Astron. Astrophys 57,73
Clark,D.H.,Stephenson,F.R.: 1977, *The Historical Supernovae*, New York/London:Pergamon
D'Odorico,S.,Bandiera,R.,Danziger,J.,Focardi,P.: 1986, Astron.J. 91,1382
Danziger,I.J.,(ed.): 1987, *ESO Workshop on SN 1987A*, Garching:ESO Proceedings No.26
Danziger,I.J.,Goss,W.M.: 1980, Monthly Notices Roy. Astron. Soc. **190**,47P
di Serego Alighieri,S.,Ponz,J.D.: 1987, *Supernova 1987A*, ed. J.Danziger, Garching: ESO Proceedings
Doggett,J.B.,Branch,D.: 1985, Astron.J. **90**,2303
Elias,J.H.,Frogel,J.A.,Hackwell,J.A.,Persson,S.E.: 1981, Astrophys.J. **251**,L13
Elias,J.H.,Matthews,K.,Neugebauer,G.,Persson,S.E.: 1985, Astrophys.J. **296**,379
Ensman,L.M.,Woosley,S.E.: 1988, Astrophys.J. 333,754
Evans,R.: 1986, IAU Circ. 4208
Fairall,A.P.,Jones,A.: 1988, Publ. Dept. Astr. University of Cape Town No. 10
Filippenko,A.V.,Sargent,W.L.W.: 1985, Nature **316**,407
Filippenko,A.V.,Sargent,W.L.W.: 1986, Astron.J. **91**,691
Filippenko,A.V.: 1986, *Highlights of Astronomy*, ed. J.-P.Swings, p.589
Filippenko,A.V.,Shields,J.C.: 1986, IAU Circ. 4288
Filippenko,A.V.: 1987, IAU Circ. 4459
Filippenko,A.V.: 1988a, IAU Circ. 4587
Filippenko,A.V.: 1988b, IAU Circ. 4597
Filippenko,A.V.,Porter,A.C.,Sargent,W.L.W.,Schneider,D.P.: 1986, Astron.J. **92**,1341
Frogel,J.A.,Gregory,B.,Kawara,K.,Laney,D.,Phillips,M.M.,Terndrup,D.,Vrba,F.,Whitford,A.E.: 1987, Astrophys.J. **315**,L129
Frogel,J.A.,Persson,S.E.,Aaronson,M.,Mattews,K.: 1978, Astrophys.J. 220,75
Fu,A.J.,Arnett,W.D.: 1986, Astrophys.J. **307**,726
Gaskell,C.M.,Cappellaro,E.,Dinerstein,H.L.,Garnett,D.R.,Harkness,R.P.,Wheeler,J.C.: 1986, Astrophys.J. **306**,L77
Gezari,D.Y.,Schmitz,M.,Mead,J.M.: 1984, *Catalog of Infrared Observations*, Nasa Reference Publ. 1118
Graham,J.R.: 1987, Astrophys.J. **315**,588
Graham,J.R.: 1988a, Astrophys.J. **326**,L51
Graham,J.R.: 1988b, IAU Circ. 4597
Graham,J.R.,Meikle,W.P.S.,Allen,D.A.,Longmore,A.J.,Williams,P.M.: 1986, Monthly Notices Roy. Astron. Soc. **218**,93
Graham,J.R.,Meikle,W.P.S.,Longmore,A.J.,Williams,P.M.: 1988, Astrophys.J. 333,743
Hansen,L.,Norgaard-Nielsen,H.U.,Jorgensen,H.E.: 1987, The Messenger **47**,46
Hansen,L.,Norgaard-Nielsen,H.U.,Jorgensen,H.E.: 1988a, IAU Circ. 4641
Hansen,L.,Jorgensen,H.E.,Norgaard-Nielsen,H.U.: 1988b, IAU Circ. 4656
Harkness,R.P.,Wheeler,J.C.,Margon,B.,Downes,R.A.,Kirshner,R.P.,Uomoto,A.,Barker,E.S.,Cochran,A.L.,Dinerstein,H.L.,Garnett,D.R.,Levreault,R.M.: 1987, Astrophys.J. **317**,355
Harris,G.L.H.,Hesser,J.E.,Massey,P.,Peterson,C.J.,Yamanaka,J.M.: 1983, Publ. Astron. Soc. Pacific 95,607

Harrison,E.R.: 1981, *Cosmology* Cambridge University Press, Cambridge
Huang,Y.-L.: 1987, Publ. Astron. Soc. Pacific **99**,461
Hubble,E.: 1925a, Pop. Astr. **33**,252
Hubble,E.: 1925b, Observatory **48**,140
Huchtmeier,W.K.,Richter,O.-G.: 1987, HI-Observations of External Galaxies, private communication
Hughes,J.P.,Helfand,D.J.: 1985, Astrophys.J. **291**,544
Iben,I.,Tutukov,A.V.: 1985, Astrophys.J. Suppl. **58**,661
Iben,I.,Nomoto,K.,Tornambé,A.,Tutukov,A.: 1987, Astrophys.J. **317**,717
Kirshner,R.,Oke,J.B.,Penston,M.V.,Searle,L.: 1973a, Astrophys.J. **185**,303
Kirshner,R.P.,Willner,S.P.,Becklin,E.E.,Neugebauer,G.,Oke,J.B.: 1973b, Astrophys.J. **180**,L97
Kowal,C.T.,Sargent,W.L.W.: 1971, Astron.J. **76**,756
Kowal,C.T.: 1968, Astron.J. **73**,1021
Kraan-Korteweg,R.C.,Tammann,G.A.: 1979, Astron. Nachr. **300**,181
Kraan-Korteweg,R.C.: 1986, Astron. Astrophys. Suppl. Series **66**,255
Kraan-Korteweg,R.C.: 1988, private communication
Kraan-Korteweg,R.C.,Cameron,L.M.,Tammann,G.A.: 1988, Astrophys.J. **331**,620
Lee,T.A.,Wamsteker,W.,Wisniewski,W.Z.,Wdowiak,T.J.: 1972, Astrophys.J. **177**,L59
Lopez,R.,Isern,J.,Canal,R.,Labay,J.: 1986a, Astron. Astrophys. **155**,1
Lopez,R.,Isern,J.,Labay,J.,Canal,R.: 1986b, Rev. Mexicana Astr. Ap. **13**,41
Lundmark,K.: 1920, Sven. Vetekapsakad. Handlingar. 60, No. 8.
Matthews,T.A.,Sandage A.R.: 1963, Astrophys.J. **138**,30
Maza,J.,van den Bergh,S.: 1976, Astrophys.J. **204**,519
McClure,R.D.,van den Bergh,S.,Evans,R.: 1987, Publ. Dominian Astrophys. Obs., Vol.XVI, No. 16, Victoria B.C.
Meikle,W.P.S.,Graham,J.R.,Bode,M.F.: 1984, IAU Circ. 3918
Meikle,W.P.S.: 1984, IAU Circ. 3924
Minkowski,R.: 1939, Astrophys.J. **89**,156
Minkowski,R.: 1941, Publ. Astron. Soc. Pacific **53**,224
Minkowski,R.: 1964, *Ann. Rev. Astron. Astrophys. 2*,247
Nicolet,B.: 1978, Astron. Astrophy. Suppl. **34**,1
Nomoto,K.,Thielemann,F.-K.,Yokoi,K.: 1984, Astrophys.J. **286**,644
Oemler,A.,Tinsley,B.M.: 1979, Astron.J. **84**,985
Oke,J.B.,Sandage,A.: 1968, Astrophys.J. **154**,21
Oke,J.B.,Searle,L.: 1974, *Ann. Rev. Astron. Astrophys. 12*,315
Palumbo,G.G.C.,Tanzanella-Nitti,G.,Vettolani,G.: 1983, Catalogue of Radial Velocities of Galaxies, New York:Gordon and Breach
Panagia,N.,Laidler,V.G.: 1988, preprint, to appear in *Supernova Shells and their Birth Rates*, ed. W.Kundt, Berlin:Springer
Panagia,N.: 1982, Proc. *3rd European IUE Conference,ESA-SP176*, p.31
Panagia,N.: 1984, Proc. *4th European IUE Conference,ESA-SP218*, p.21
Panagia,N.: 1985, *Supernovae as Distance Indicators*,ed. N.Bartel,Berlin:Springer,p.14

Panagia,N.: 1987, *High Energy Phenomena Around Collapsed Stars*, ed. F.Pacini, NATO Advanced Study Institute, Dordrecht:Reidel
Panagia,N.,Sramek,R.A.,Weiler,K.W.: 1986, Astrophys.J. **300**,L55
Pearce,E.C.,Colgate,S.A.,Petschek,A.G.: 1988, Astrophys.J. **325**,L33
Phillips,M.M. et al.: 1987, Publ. Astron. Soc. Pacific **99**,592
Porter,A.C.,Filippenko,A.V.: 1987, Astron.J. **93**,1372
Porter,A.C.: 1987, IAU Circ. 4470
Pskovskii,Y.P.: 1967, Sov. Astron. **11**,63
Pskovskii,Y.P.: 1968, Sov. Astron. **11**,570
Pskovskii,Y.P.: 1971, Sov. Astron. **14**,798
Pskovskii,Y.P.: 1977, Sov. Astron. **21**,675
Pskovskii,Y.P.: 1978, Sov. Astron. **22**,420
Pskovskii,Y.P.: 1984, Sov. Astron. **28**,658
Rees,M.J.,Stoneham,R.J.,(eds.): 1982, *Supernovae: A Survey of Current Research*, Dordrecht:Reidel
Rich,R.M.: 1987, Astron.J. **94**,651
Richter,O.-G.,Rosa,M.: 1984, Astron. Astrophys. **140**,L1
Richtler,T.,Sadler,E.M.: 1983, Astron. Astrophys. **128**,L3
Sandage,A.: 1973, Astrophys.J. **183**,711
Sandage,A.: 1988, *Ann. Rev. Astron. Astrophys.* **26**,561
Sandage,A.,Tammann,G.A.: 1975, Astrophys.J. **196**,313
Sandage,A.,Tammann,G.A.: 1982, Astrophys.J. **256**,339
Schechter,P.L.: 1980, Astron.J. **85**,801
Schmidt-Kaler,T.: 1982, *Landolt-Börnstein* Vol. 2b, eds. K.Schaifer, H.H. Voigt, Berlin:Springer
Schneider,D.P.,Mould,J.R.,Porter,A.C.,Schmidt,M.,Bothun,G.D.,Gunn,J.E.: 1987, Publ. Astron. Soc. Pacific **99**,1167
Sramek,R.A.,Panagia,N.,Weiler,K.W.: 1984, Astrophys.J. **285**,L59
Strom,R.G.: 1988, Monthly Notices Roy. Astron. Soc. **230**,331
Tammann,G.A.: 1976, *Supernovae*, ed. D.Schramm, Dordrecht:Reidel
Tammann,G.A.: 1978, *Astronomical Uses of the Space Telescope*, eds. Macchetto,F.,Pacini,F.,Tarenghi,M., Garching:ESO Proceedings, p.329
Tammann,G.A.: 1982, *Supernovae: A Survey of Current Research*, ed. by M.J. Rees,R.J. Stoneham, Dordrecht:Reidel,p.371
Tammann,G.A.: 1987, *Observational Cosmology*, IAU Symp. 124, eds. Hewitt et al., Dordrecht:Reidel,p.151
Tammann,G.A.: 1988, preprint
Tammann,G.A.,Kraan-Korteweg,R.C.: 1978, *The Large Scale Structure of the Universe*, eds. M.S. Longair,J. Einasto, Dordrecht:Reidel
Tinsley,B.M.,Oemler,A.: 1980,, *Texas Workshop on Type I Supernovae*, ed. J.C. Wheeler, Austin:University of Texas,p.9
Tornambé,A.,Matteucci,F.: 1987, Astrophys.J. **318**,L25
Trimble,V.: 1982, Rev. Mod. Phys. **54**,1183.
Tsvetkov,D.Y.: 1986, Variable Stars **22**,279
Uomoto,A.,Kirshner,R.P.: 1985, Astron. Astrophys. **149**,L7
Uomoto,A.: 1986, Astrophys.J. **310**,L35
van den Bergh,S.: 1983, Mem. Soc. Astron. Italiana **54**,309
van den Bergh,S.: 1987, *ESO Workshop on SN 1987A*, ed. J.Danziger, Garching:ESO Proceedings No.26,p.557

van den Bergh,S.: 1988a, Astrophys.J. **327**,156
van den Bergh,S.: 1988b, preprint to appear *Supernova Shells and Their Birth Rates*, ed. W.Kundt, Berlin:Springer
van den Bergh,S.: 1988c, Publ. Astron. Soc. Pacific **100**,8
van den Bergh,S.: 1988d, preprint, to be published in A.S.P. Symp. Ser. Vol. 2
Wheeler,J.C.,(ed.): 1980, *Texas Workshop on Type I Supernovae*, Austin:University of Texas
Wheeler,J.C.: 1985, *Supernovae as Distance Indicators*, ed. N.Bartel, Berlin:Springer,p.34
Wheeler,J.C.,Levreault,R.: 1985, Astrophys.J. **294**,L17
Wheeler,J.C.,Sutherland,P.G.: 1985, *Supernovae as Distance Indicators*, ed. N.Bartel,Berlin:Springer,p.200
Wheeler,J.C.,Harkness,R.P.,Barkat,Z.,Swartz,D.: 1986, Publ. Astr. Soc. Pac. **98**,1018
Woosely,S.E.,Weaver,T.A.: 1986, *Ann. Rev. Astron. Astrophys.* **24**,205
Woosley,S.E.,Taam,R.E.,Weaver,T.A.: 1986, Astrophys.J. **301**,601
Xi Ze-zong,Po Shu-jen: 1966, Science **154**,597
Younger,P.F.,van den Bergh,S.: 1985, Astron. Astrophys. Suppl. **61**,365
Zwicky,F.: 1963, *Problems of Extragalactic Research*,IAU Symp. 15, ed. McVittie, New York:MacMillan,p.347
Zwicky,F.: 1938, Phys. Rev. **53**,1019
Zwicky,F.,Berger,J.,Gates,H.S.,Rudnicki,K.: 1963, Publ. Astron. Soc.Pacific **75**,236
Zwicky,F.: 1964, "List of Supernovae Discovered Since 1885",Pasadena:Caltech

Tables and Figures

Filter	t_1 (days past B maximum)	t_2	α_1 (mag/day)	α_2 (mag/day)
B	-11	44	-0.332	0.017
V	-15	41	-0.313	0.026
U	- 8	31	-0.332	0.025
H	6	45	0.040	0.040
J	9	60	0.270	0.043
K	7	35	0.080	0.040

Table 1: Epoches of the connections of the various segments of the light curves in the different filters. t_1 is the transition from the rise to the peak and t_2 the connection of peak and the late decay. α_1 is the slope of the rise, α_2 of the final decay.

t_0(days)	B	V	U	H	J	K	B-V	U-B	B-H	J-H	H-K
-5.0	0.15	0.26	-0.05	-0.20	-1.35	-0.40	-0.10	-0.20	0.35	-1.15	0.20
-4.0	0.10	0.18	-0.07	-0.16	-1.08	-0.32	-0.08	-0.17	0.26	-0.92	0.16
-3.0	0.05	0.11	-0.08	-0.12	-0.81	-0.24	-0.06	-0.13	0.17	-0.69	0.12
-2.0	0.02	0.06	-0.07	-0.08	-0.54	-0.16	-0.04	-0.09	0.10	-0.46	0.08
-1.0	0.01	0.03	-0.04	-0.04	-0.27	-0.08	-0.02	-0.05	0.05	-0.23	0.04
0.0	0.00	0.00	0.00	0.00	0.00	0.00	0.00	0.00	0.00	0.00	0.00
1.0	0.01	-0.02	0.06	0.04	0.27	0.08	0.02	0.05	-0.03	0.23	-0.04
2.0	0.02	-0.02	0.12	0.08	0.54	0.16	0.04	0.10	-0.06	0.46	-0.08
3.0	0.05	-0.02	0.20	0.12	0.81	0.24	0.07	0.15	-0.07	0.69	-0.12
4.0	0.09	0.00	0.29	0.16	1.08	0.32	0.09	0.20	-0.07	0.92	-0.16
5.0	0.14	0.02	0.38	0.20	1.36	0.38	0.12	0.24	-0.06	1.16	-0.18
6.0	0.21	0.05	0.48	0.23	1.63	0.46	0.16	0.28	-0.02	1.40	-0.23
7.0	0.28	0.08	0.59	0.27	1.91	0.53	0.19	0.31	0.01	1.64	-0.26
8.0	0.36	0.13	0.69	0.31	2.18	0.61	0.23	0.33	0.05	1.87	-0.30
9.0	0.45	0.17	0.80	0.33	2.45	0.60	0.28	0.35	0.12	2.12	-0.27
10.0	0.55	0.22	0.91	0.31	2.55	0.54	0.32	0.36	0.24	2.24	-0.23
11.0	0.65	0.28	1.02	0.27	2.60	0.47	0.37	0.37	0.38	2.33	-0.20
12.0	0.76	0.33	1.13	0.21	2.65	0.44	0.42	0.38	0.55	2.44	-0.23
13.0	0.87	0.39	1.25	0.17	2.63	0.39	0.48	0.39	0.70	2.46	-0.22
14.0	0.98	0.45	1.37	0.13	2.57	0.35	0.53	0.39	0.85	2.44	-0.22
15.0	1.10	0.51	1.48	0.09	2.53	0.30	0.58	0.38	1.01	2.44	-0.21
16.0	1.22	0.58	1.60	0.05	2.49	0.26	0.64	0.38	1.16	2.44	-0.21
17.0	1.33	0.64	1.71	0.01	2.44	0.24	0.69	0.38	1.32	2.43	-0.23
18.0	1.45	0.70	1.83	-0.04	2.39	0.21	0.75	0.38	1.49	2.43	-0.25
19.0	1.56	0.76	1.94	-0.08	2.34	0.19	0.80	0.38	1.64	2.42	-0.27
20.0	1.67	0.82	2.05	-0.12	2.28	0.18	0.84	0.39	1.79	2.40	-0.30
21.0	1.77	0.88	2.17	-0.16	2.20	0.18	0.89	0.39	1.93	2.36	-0.34
22.0	1.88	0.95	2.28	-0.20	2.15	0.18	0.93	0.41	2.08	2.35	-0.38
23.0	1.97	1.00	2.39	-0.24	2.10	0.19	0.97	0.42	2.21	2.34	-0.43
24.0	2.07	1.07	2.51	-0.25	2.05	0.21	1.00	0.44	2.32	2.30	-0.46
25.0	2.16	1.13	2.62	-0.26	1.99	0.24	1.03	0.47	2.42	2.25	-0.50
26.0	2.24	1.18	2.74	-0.24	1.97	0.27	1.06	0.50	2.48	2.21	-0.51
27.0	2.32	1.24	2.85	-0.21	1.95	0.30	1.08	0.53	2.53	2.16	-0.51
28.0	2.39	1.30	3.04	-0.17	1.93	0.36	1.09	0.65	2.57	2.10	-0.53
29.0	2.46	1.36	3.07	-0.13	1.93	0.40	1.11	0.60	2.60	2.06	-0.53
30.0	2.53	1.42	3.10	-0.06	1.95	0.46	1.11	0.56	2.59	2.01	-0.52
31.0	2.59	1.47	3.12	0.01	1.98	0.51	1.12	0.53	2.58	1.97	-0.50
32.0	2.65	1.53	3.14	0.08	2.03	0.57	1.12	0.50	2.57	1.95	-0.49
33.0	2.70	1.58	3.17	0.16	2.11	0.65	1.12	0.47	2.54	1.95	-0.49
34.0	2.75	1.63	3.19	0.20	2.20	0.73	1.11	0.45	2.55	2.00	-0.53
35.0	2.79	1.68	3.22	0.27	2.32	0.83	1.11	0.43	2.52	2.05	-0.56
36.0	2.83	1.73	3.25	0.35	2.42	0.85	1.10	0.41	2.48	2.07	-0.50
37.0	2.87	1.78	3.27	0.40	2.52	0.89	1.09	0.40	2.47	2.12	-0.49
38.0	2.90	1.82	3.30	0.47	2.60	0.93	1.08	0.39	2.43	2.13	-0.46
39.0	2.93	1.86	3.32	0.55	2.71	0.97	1.08	0.39	2.38	2.16	-0.42

Table 2: The standard light curves of SNe Ia, normalised to $t_0 = 0^d$ (B maximum)

t_0(days)	B	V	U	H	J	K	B-V	U-B	B-H	J-H	H-K
40.0	2.96	1.89	3.35	0.63	2.81	1.01	1.07	0.38	2.33	2.18	-0.38
41.0	2.99	1.93	3.37	0.69	2.90	1.05	1.06	0.38	2.30	2.21	-0.36
42.0	3.02	1.96	3.40	0.75	3.00	1.09	1.06	0.38	2.27	2.25	-0.34
43.0	3.04	1.98	3.42	0.82	3.09	1.13	1.06	0.38	2.22	2.27	-0.31
44.0	3.07	2.01	3.45	0.89	3.19	1.17	1.05	0.38	2.17	2.30	-0.28
45.0	3.09	2.03	3.47	0.92	3.28	1.21	1.06	0.38	2.17	2.36	-0.29
46.0	3.09	2.06	3.50	0.95	3.37	1.25	1.03	0.41	2.14	2.42	-0.30
47.0	3.12	2.09	3.52	0.99	3.45	1.29	1.02	0.41	2.13	2.46	-0.30
48.0	3.13	2.12	3.55	1.03	3.53	1.33	1.02	0.42	2.10	2.50	-0.30
49.0	3.15	2.14	3.57	1.07	3.61	1.37	1.01	0.43	2.08	2.54	-0.30
50.0	3.16	2.17	3.60	1.11	3.69	1.41	1.00	0.43	2.06	2.58	-0.30
55.0	3.25	2.29	3.72	1.31	4.04	1.61	0.95	0.48	1.94	2.73	-0.30
60.0	3.33	2.42	3.85	1.51	4.32	1.81	0.91	0.52	1.82	2.81	-0.30
65.0	3.41	2.55	3.98	1.71	4.55	2.01	0.87	0.56	1.71	2.85	-0.30
70.0	3.50	2.68	4.10	1.91	4.77	2.21	0.82	0.60	1.59	2.86	-0.30
75.0	3.58	2.81	4.23	2.11	4.99	2.41	0.78	0.65	1.47	2.88	-0.30
80.0	3.67	2.93	4.36	2.31	5.20	2.61	0.73	0.69	1.36	2.89	-0.30
85.0	3.75	3.06	4.48	2.51	5.41	2.81	0.69	0.73	1.24	2.90	-0.30
90.0	3.83	3.19	4.61	2.71	5.63	3.01	0.64	0.77	1.12	2.92	-0.30
95.0	3.92	3.32	4.73	2.91	5.84	3.21	0.60	0.82	1.01	2.93	-0.30
100.0	4.00	3.45	4.86	3.11	6.06	3.41	0.55	0.86	0.89	2.95	-0.30
105.0	4.08	3.57	4.99	3.31	6.28	3.61	0.51	0.90	0.77	2.96	-0.30
110.0	4.17	3.70	5.11	3.51	6.49	3.81	0.46	0.94	0.66	2.98	-0.30

Table 2: (continued)

SNe	Galaxy	type	v_o (km s^{-1})	d_{Vir}	A_B (mag)	t^{Bmax} (JD)
1972E	NGC 5253	I0	147	0.23,(0.13)	0.13	2441449
1980N	NGC 1316	Sa_{pec}	1712	1.22	0.00	2444585
1981B	NGC 4536	Sc	1647	1.00,(1.78)	0.00	2444672
1981D	NGC 1316	Sa_{pec}	1712	1.22	0.00	2444630
1983G	NGC 4753	$S0_{pec}$	1126	1.38,(1.00)	0.00	2445431

Table 3: Parameters of the standard SNe Ia. Galaxy type, the velocity corrected to the centroid of the Local Group and the distance relative to the Virgo cluster were taken from Kraan-Korteweg (1986). The distances to NGC 5253, NGC 4536 and NGC 4753 are discussed in the text. Foreground absorption were determined according to Sandage (1973). For the determination of the date of the B maximum see text.

SNe	N_B	N_V	N_U	N_H	N_J	N_K	σ_B	σ_V	σ_U	σ_H	σ_J	σ_K
1972E	47	55	47	9	5	19	0.08	0.09	0.12	0.06	0.24	0.26
1980N	44	45	32	14	13	10	0.06	0.07	0.18	0.08	0.20	0.11
1981B	82	85	31	15	15	14	0.09	0.11	0.19	0.05	0.10	0.13
1981D	9	9	9	7	7	7	0.13	0.08	0.19	0.04	0.10	0.03
All Standard SNe	182	194	119	45	40	50	0.08	0.10	0.16	0.06	0.16	0.18
1983G	21	23	11	5	5	5	0.10	0.11	0.10	0.13	0.32	0.08

Table 4: Number of observations of the standard SNe Ia in each filter (N_i) and the standard deviations of the points around the templates (σ_i)

Filter	t_o^{max} (days)	t_o^{min} (days)
U	-2	-
B	0	-
V	3	-
H	29	12
J	25	9
K	21	8

Table 5: Epoches of the maxima relative to the B maximum. For the infrared the data of the second maxima are given.

SNe	B_o^o	V_o^o	U_o^o	H_o^o	J_o^o	K_o^o	$(B-V)_o^o$	$(U-B)_o^o$	$(B-H)_o^o$	$(V-K)_o^o$	$(J-H)_o^o$	$(H-K)_o^o$
1972E	8.42	8.50	8.12	9.29	7.93	9.02	-0.08	-0.30	-0.87	-0.52	-1.36	0.27
1980N	12.53	12.49	12.44	13.23	11.81	12.92	0.04	-0.09	-0.70	-0.43	-1.42	0.31
1981B	12.05	12.04	11.89	12.83	11.62	12.54	0.01	-0.16	-0.78	-0.50	-1.21	0.29
1981D	12.51	12.24	12.31	13.22	12.09	12.98	0.27	-0.20	-0.71	-0.74	-1.13	0.24
1983G	13.02	12.76	12.99	13.49	12.05	13.26	0.26	-0.03	-0.47	-0.50	-1.44	0.23

Table 6: Apparent magnitudes and colours at $t_o=0^d$ (B maximum) of the standard SNe Ia. The magnitudes are corrected for foreground absorption.

E_{B-V}	t_o^{Bend} (days)	Δm_B^{Bend}	β	Δm_B^{40}
0	31	2.86	9.2	2.96
0.5	31	3.00	9.7	3.11
1.0	30	3.17	10.6	3.26
1.5	30	3.36	11.2	3.41
2.0	29	3.48	12.0	3.56

Table 7: Variation of various parameters with extinction. β is Pskovskii's parameter of the decline past maximum. Δm_B^{40} the magnitude difference between maximum and t_o=40^d.

Date in 1981	JD 2444000+	t_o (days)	λ (nm)	coverage of V filter at z=0
March 6.-9.	669-672	0	310-834	100%
March 24.	687	15	367-858	100%
March 27.	690	18	358-867	100%
March 31.	694	22	338-878	100%
April 4.-5.	698	26	380-653	98%
April 11.	705	33	388-633	97%
May 4.-10.	728-734	56-62	340-720	100%
June 10.	765	93	354-625	95%
July 1.	786	114	418-713	100%

Table 8: Spectra used for the calculation of K-corrections. The coverage is the ratio of the transmitted flux in the truncated and the complete filter.

t_o	$\Delta m_v(0.05)$	$\Delta m_v(0.1)$	$\Delta m_v(0.15)$	$\Delta m_v(0.2)$	$\Delta m_v(0.25)$	$\Delta m_v(0.3)$	$\Delta m_v(0.35)$	$\Delta m_v(0.4)$	$\Delta m_v(0.45)$
0	−0.12	−0.29	−0.38	−0.49	−0.62	−0.67	−0.62	−0.57	−0.48
15	0.05	0.04	0.07	0.16	0.24	–	–	–	–
18	0.14	0.22	0.30	0.40	0.45	0.46	–	–	–
22	0.22	0.39	0.51	0.65	0.75	0.79	0.84	–	–
26	0.18*	0.32*	0.43*	0.53*	–	–	–	–	–
33	0.19*	0.36*	0.50*	0.60*	–	–	–	–	–
59	0.06	0.04	0.07	0.15	0.21	0.25	0.34	–	–
93	−0.05*	−0.29*	−0.35*	−0.32*	−0.27*	−0.18*	–	–	–
114	−0.13	−0.39	–	–	–	–	–	–	–

Table 9: Magnitude shifts (K-corrections) of spectra at different epoches. See text for details.

z	$m_v(q_o=0)$	$m_v(q_o=\frac{1}{2})$	$\Delta m_v(z)$	$m_v^c(q_o=0)$	$m_v^c(q_o=\frac{1}{2})$
0.1	19.1	19.0	−0.29	18.8	18.7
0.2	20.7	20.6	−0.49	20.2	20.1
0.3	21.7	21.5	−0.67	21.0	20.8
0.4	22.4	22.2	−0.57	21.8	21.6
0.5	23.0	22.7	−0.33	22.7	22.4
0.6	23.5	23.1	−0.01	23.5	23.1
0.7	23.9	23.5	0.26	24.2	23.8
0.8	24.2	23.8	0.45	24.7	24.3
0.9	24.6	24.1	0.78	25.4	24.9
1.0	24.9	24.3	1.25	26.2	25.6

Table 10: Expected apparent maximum magnitudes of SNe Ia in Friedmann universes without K-corrections and corrected for the brightness shift $\Delta m(z)$. The absolute magnitude assumed is $M_v^{max}=-19.^m9$ ($H_o=50$ km s^{-1} Mpc^{-1}).

SNe	Galaxy	type	v_o (km s^{-1})	d_{Virr}	A_B (mags)	t_o^{Bmax} (JD)
1962L	NGC 1073	SBc	1317	1.06	0	2438004
1964L	NGC 3938	Sc	845	0.89	0	2438739
1976B	NGC 4402	Sc	71	1.00	0	2442875
1983I	NGC 4051	Sbc	747	0.74	0	2445459
1983N	NGC 5236	SBc	275	0.25	0.12	2445531
1984L	NGC 991	Sc	1606	1.29	0	2445936

Table 11: Same as Table 3, for SNe Ib

SNe	B	N_B	V	N_V	U	N_U	H	N_H	J	N_J	K	N_K
1962L	1	31	1	11	1	11	–	–	–	–	–	–
1964L	2	34	–	–	–	–	–	–	–	–	–	–
1976B	3,4,5	40	3,4	17	–	–	–	–	–	–	–	–
1983I	6,7	22	6	18	–	–	8	5	8	5	8	5
1983N	9	10	9	15	9	5	8	18	8	18	8	18
1984L	10	1	10,11,12	7	10	1	8	5	8	5	8	5

1. Bertola,F.: 1964, Ann. Astrophys. 27,319
2. Bertola,F.,Mammano,A.,Perinotto,M.: 1965, Contr. Asiago Obs. No.174
3. de Vaucouleurs,G.,de Vaucouleurs,A.,Odewahn,S.: 1980, Publ. Astron. Soc. Pacific 93,181
4. Ciatti,F.,Rosino,L.: 1978, Astron. Astrophys. Suppl. Ser. 34,387
5. Tsvetkov,Y.P.: 1983, Perem. Zvezdy 5,176
6. Tsvetkov,Y.P.: 1985, Sov. Astron. 29,211
7. Kielkopf,J.: 1987, Publ. Astron. Soc. Pacific 99,374
8. Elias,J.H.,Matthews,K.,Neugebauer,G.,Persson,S.E.: 1985, Astrophys.J. 296,379
9. Cadonau,R.: 1986, Ph.D. Thesis, Universitiy of Basel
10. Buta,R.: 1984, IAU Circ. 3981
11. Waagen,E.,Evans,R.: 1984, IAU Circ. 3979
12. McNaught,R.: 1984, IAU Circ. 4001

Table 12: Photometry used und number of observations in each filter

t_{rf}(days)	B	V	U	H	J	K	B-V	U-B	B-H	J-H	H-K
-5.0	0.27	0.24	0.04	0.41	0.35	0.33	0.04	-0.24	-0.14	-0.06	0.08
-4.0	0.18	0.17	-0.01	0.31	0.26	0.25	0.00	-0.18	-0.14	-0.06	0.06
-3.0	0.10	0.12	-0.03	0.22	0.18	0.18	-0.01	-0.13	-0.12	-0.05	0.04
-2.0	0.05	0.07	-0.04	0.14	0.11	0.12	-0.02	-0.09	-0.09	-0.03	0.03
-1.0	0.02	0.03	-0.03	0.07	0.05	0.05	-0.01	-0.04	-0.05	-0.02	0.01
0.0	0.00	0.00	0.00	0.00	0.00	0.00	0.00	0.00	0.00	0.00	0.00
1.0	0.00	-0.02	0.04	-0.06	-0.04	-0.05	0.02	0.04	0.06	0.02	-0.01
2.0	0.02	-0.02	0.10	-0.12	-0.07	-0.09	0.04	0.08	0.13	0.04	-0.02
3.0	0.05	-0.02	0.17	-0.16	-0.10	-0.13	0.07	0.12	0.21	0.06	-0.03
4.0	0.09	0.00	0.24	-0.20	-0.12	-0.16	0.09	0.15	0.29	0.09	-0.04
5.0	0.15	0.04	0.33	-0.24	-0.13	-0.19	0.11	0.19	0.39	0.11	-0.05
6.0	0.21	0.08	0.43	-0.27	-0.14	-0.21	0.13	0.22	0.48	0.13	-0.06
7.0	0.28	0.14	0.52	-0.29	-0.14	-0.23	0.14	0.24	0.57	0.15	-0.06
8.0	0.36	0.20	0.63	-0.31	-0.14	-0.25	0.16	0.27	0.67	0.17	-0.06
9.0	0.44	0.28	0.73	-0.33	-0.13	-0.26	0.17	0.29	0.77	0.19	-0.07
10.0	0.53	0.36	0.84	-0.34	-0.12	-0.26	0.18	0.31	0.87	0.22	-0.07
11.0	0.63	0.44	0.95	-0.34	-0.11	-0.27	0.19	0.33	0.97	0.23	-0.08
12.0	0.72	0.52	1.06	-0.34	-0.09	-0.27	0.19	0.34	1.06	0.25	-0.08
13.0	0.81	0.61	1.17	-0.34	-0.07	-0.26	0.20	0.36	1.16	0.27	-0.08
14.0	0.91	0.69	1.30	-0.34	-0.05	-0.26	0.22	0.39	1.25	0.29	-0.08
15.0	1.00	0.77	1.41	-0.33	-0.03	-0.25	0.23	0.41	1.34	0.30	-0.08
16.0	1.10	0.85	1.52	-0.32	0.00	-0.24	0.25	0.43	1.42	0.32	-0.08
17.0	1.19	0.92	1.64	-0.31	0.02	-0.23	0.27	0.45	1.50	0.33	-0.08
18.0	1.28	0.99	1.75	-0.29	0.05	-0.21	0.29	0.47	1.57	0.34	-0.08
19.0	1.37	1.04	1.87	-0.28	0.08	-0.20	0.32	0.50	1.64	0.35	-0.08
20.0	1.45	1.10	1.98	-0.26	0.11	-0.18	0.35	0.53	1.71	0.37	-0.08
21.0	1.53	1.14	2.10	-0.24	0.13	-0.16	0.39	0.56	1.77	0.38	-0.08
22.0	1.61	1.18	2.21	-0.22	0.16	-0.14	0.42	0.60	1.83	0.38	-0.08
23.0	1.68	1.22	2.32	-0.20	0.19	-0.11	0.46	0.64	1.88	0.39	-0.09
24.0	1.75	1.25	2.44	-0.18	0.22	-0.09	0.50	0.69	1.93	0.40	-0.09
25.0	1.81	1.28	2.55	-0.16	0.25	-0.06	0.53	0.74	1.97	0.41	-0.10
26.0	1.87	1.30	2.66	-0.14	0.28	-0.04	0.57	0.79	2.01	0.41	-0.10
27.0	1.93	1.33	2.78	-0.11	0.31	-0.01	0.60	0.85	2.04	0.42	-0.10
28.0	1.98	1.35	2.89	-0.09	0.34	0.01	0.63	0.91	2.07	0.43	-0.10
29.0	2.03	1.38	3.09	-0.07	0.33	0.04	0.65	1.06	2.10	0.40	-0.11
30.0	2.07	1.40	3.11	-0.04	0.39	0.07	0.67	1.04	2.12	0.44	-0.11
31.0	2.11	1.44	3.14	-0.02	0.42	0.09	0.67	1.02	2.13	0.44	-0.11
32.0	2.15	1.47	3.16	0.00	0.45	0.12	0.69	1.01	2.15	0.45	-0.12
33.0	2.18	1.49	3.19	0.02	0.47	0.14	0.70	1.00	2.16	0.45	-0.12
34.0	2.22	1.51	3.21	0.04	0.50	0.17	0.70	1.00	2.17	0.46	-0.12
35.0	2.24	1.54	3.24	0.06	0.52	0.19	0.71	0.99	2.18	0.46	-0.13
36.0	2.27	1.56	3.26	0.09	0.55	0.22	0.71	0.99	2.19	0.46	-0.13
37.0	2.30	1.58	3.29	0.10	0.57	0.24	0.71	0.99	2.19	0.47	-0.14
38.0	2.32	1.61	3.31	0.13	0.60	0.27	0.71	1.00	2.19	0.47	-0.15
39.0	2.34	1.63	3.34	0.14	0.62	0.30	0.71	1.00	2.19	0.48	-0.15

Table 13: Normalised light curves of SNe Ib

t_0(days)	B	V	U	H	J	K	B-V	U-B	B-H	J-H	H-K
40.0	2.36	1.66	3.36	0.16	0.65	0.32	0.70	1.01	2.19	0.49	-0.16
41.0	2.37	1.68	3.39	0.18	0.68	0.35	0.69	1.01	2.19	0.50	-0.16
42.0	2.39	1.70	3.41	0.20	0.71	0.37	0.68	1.02	2.19	0.51	-0.17
43.0	2.40	1.73	3.44	0.21	0.74	0.40	0.68	1.03	2.19	0.53	-0.19
44.0	2.42	1.75	3.46	0.23	0.77	0.42	0.67	1.05	2.18	0.54	-0.19
45.0	2.43	1.78	3.49	0.26	0.80	0.45	0.66	1.06	2.17	0.54	-0.19
46.0	2.44	1.80	3.51	0.28	0.83	0.47	0.65	1.07	2.16	0.55	-0.19
47.0	2.46	1.82	3.54	0.30	0.86	0.50	0.63	1.08	2.15	0.56	-0.20
48.0	2.47	1.85	3.57	0.33	0.89	0.53	0.62	1.09	2.14	0.56	-0.20
49.0	2.48	1.87	3.59	0.35	0.92	0.55	0.61	1.11	2.13	0.57	-0.20
50.0	2.50	1.90	3.62	0.37	0.95	0.58	0.60	1.12	2.13	0.58	-0.20
55.0	2.57	2.02	3.74	0.49	1.10	0.70	0.55	1.17	2.08	0.61	-0.22
60.0	2.65	2.13	3.87	0.61	1.25	0.83	0.51	1.22	2.04	0.64	-0.23
65.0	2.70	2.26	3.99	0.72	1.40	0.96	0.45	1.29	1.98	0.67	-0.24
70.0	2.76	2.37	4.12	0.84	1.54	1.09	0.39	1.36	1.92	0.71	-0.25
75.0	2.82	2.49	4.24	0.95	1.69	1.22	0.32	1.43	1.87	0.74	-0.26
80.0	2.88	2.61	4.37	1.07	1.84	1.34	0.26	1.49	1.81	0.77	-0.27
85.0	2.93	2.73	4.50	1.19	1.99	1.47	0.20	1.56	1.75	0.80	-0.29
90.0	2.99	2.85	4.62	1.30	2.14	1.60	0.14	1.63	1.69	0.84	-0.30
95.0	3.05	2.97	4.75	1.42	2.29	1.73	0.08	1.70	1.63	0.87	-0.31
100.0	3.11	3.09	4.88	1.53	2.44	1.86	0.01	1.77	1.57	0.90	-0.32
105.0	3.16	3.21	5.00	1.65	2.59	1.98	-0.05	1.84	1.51	0.94	-0.33
110.0	3.22	3.33	5.13	1.77	2.73	2.11	-0.11	1.90	1.46	0.97	-0.35

Table 13: (continued)

Filter	t_2 (days past B maximum)	α_2 (mag/day)
B	60	0.012
V	34	0.024
H	42	0.023
J	40	0.030
K	22	0.026

Table 14: Epoches of the transitions between peak and late phases of SNe Ib curves and slopes after the transition

SNe	N_B	N_V	N_U	N_H	N_J	N_K	Fit on Ib curve σ_B	σ_V	σ_U	σ_H	σ_J	σ_K	Fit on Ia curve σ_B	σ_V	σ_U	σ_H	σ_J	σ_K
1962L	31	11	11	–	–	–	0.12	0.08	–	–	–	–	0.32	0.11	0.12	–	–	–
1964L	34	–	–	–	–	–	0.16	–	–	–	–	–	0.17	–	–	–	–	–
1976B	40	17	–	–	–	–	0.20	0.12	–	–	–	–	0.32	0.27	0.51	–	–	–
1983I	22	18	–	5	5	5	0.14	0.10	–	0.10	0.11	0.04	0.13	0.12	–	0.32	0.47	0.29
1983B	10	15	5	18	18	18	0.05	0.03	–	0.06	0.08	0.08	0.05	0.10	0.09	0.50	1.57	0.61
1984L	–	7	–	6	6	5	–	0.13	–	0.09	0.13	0.08	–	0.13	–	0.52	0.65	0.38
ALL	137	68	16	29	29	28	0.17	0.10		0.08	0.10	0.07	0.25	0.17	0.29	0.47	1.20	0.81

Table 15: Number of observations and standard deviations for fits of SNe Ib on templates of SNe Ia and SNe Ib, respectively

SNe	Ib t_o^{Bmax} (JD)	Ib B_o^o	Ia t_o^{Bmax} (JD)	Ia B_o^o
1962L	2438004	13.95	2438005	13.77
1964L	2438739	13.86	2438732	12.97
1976B	2442875	15.04	2442877	14.95
1983I	2445459	14.76	2445452	13.80
1983N	2445531	11.75	2445531	11.80

Table 16: Julian dates and corresponding magnitudes of the B maximum for fits on Ib templates and Ia curves

Filter	t_o^{max} (days)
U	(-2)
B	0
V	2
J	7
H	12
K	12

Table 17: Epoches of the maxima

SNe	B_o^o	V_o^o	U_o^o	H_o^o	J_o^o	K_o^o	$(B-V)_o^o$	$(U-B)_o^o$	$(B-H)_o^o$	$(V-K)_o^o$	$(J-H)_o^o$	$(H-K)_o^o$
1962L	13.89	13.08	14.03	-	-	-	0.81	0.14	-	-	-	-
1964L	13.86	(13.62)	-	-	-	-	(0.24)	-	-	-	-	-
1976B	15.04	13.37	-	-	-	-	1.67	-	-	-	-	-
1983I	14.76	14.16	-	14.03	14.05	13.82	0.60	-	0.73	0.34	0.02	0.21
1983N	11.75	10.93	12.00	10.66	10.57	10.46	0.82	0.25	1.09	0.47	-0.11	0.20
1984L	(14.28)	13.71	(14.37)	13.11	12.86	12.85	(0.57)	(0.09)	(1.17)	0.86	-0.25	0.26

Table 18: Apparent maximum magnitudes and colours of SNe Ib

SN type	t_o (JD 2446000+)	B_o^o	V_o^o	U_o^o	H_o^o	J_o^o	K_o^o	σ_B	σ_V	σ_U	σ_H	σ_J	σ_K
Ia	559	12.62	11.74	13.42	10.20	9.04	9.94	0.13	0.20	0.20	0.42	0.67	0.41
Ib	559	12.85	11.78	13.46	10.54	11.06	10.48	0.33	0.35	0.21	0.51	0.60	0.57
Special curves	560.6	12.50	11.54	13.26	10.00	10.05	9.88	0.04	0.03	0.03	0.07	0.12	0.07

Table 19: Maximum dates, magnitudes and standard deviations of SN 1986G for fits on the different templates

t_0(days)	B	V	U	H	J	K	B-V	U-B	B-H	J-H	H-K
-5.0	0.52	0.45	0.47	0.45	0.12	0.11	0.07	-0.05	0.07	-0.33	0.34
-4.0	0.34	0.33	0.25	-0.02	0.04	0.01	0.01	-0.09	0.36	0.06	-0.03
-3.0	0.20	0.23	0.11	-0.17	-0.01	-0.03	-0.03	-0.09	0.37	0.17	-0.14
-2.0	0.10	0.13	0.02	-0.16	-0.03	-0.04	-0.04	-0.08	0.26	0.13	-0.12
-1.0	0.03	0.06	-0.01	-0.08	-0.03	-0.03	-0.03	-0.04	0.12	0.06	-0.06
0.0	0.00	0.00	0.00	0.00	0.00	0.00	0.00	0.00	0.00	0.00	0.00
1.0	0.00	-0.04	0.05	0.06	0.05	0.03	0.04	0.05	-0.06	-0.01	0.03
2.0	0.03	-0.06	0.14	0.10	0.13	0.06	0.09	0.11	-0.07	0.03	0.03
3.0	0.08	-0.06	0.25	0.10	0.23	0.09	0.15	0.16	-0.02	0.13	0.01
4.0	0.16	-0.05	0.38	0.09	0.34	0.12	0.21	0.22	0.07	0.25	-0.03
5.0	0.26	-0.02	0.53	0.06	0.46	0.13	0.28	0.28	0.20	0.40	-0.07
6.0	0.37	0.02	0.69	0.03	0.58	0.14	0.35	0.33	0.34	0.56	-0.11
7.0	0.49	0.07	0.86	0.00	0.70	0.15	0.41	0.38	0.49	0.70	-0.15
8.0	0.62	0.14	1.04	-0.02	0.81	0.14	0.48	0.42	0.64	0.83	-0.17
9.0	0.75	0.21	1.21	-0.03	0.89	0.14	0.55	0.46	0.79	0.93	-0.17
10.0	0.89	0.29	1.38	-0.03	0.96	0.13	0.61	0.49	0.93	1.00	-0.16
11.0	1.03	0.37	1.55	-0.03	1.01	0.11	0.67	0.51	1.06	1.04	-0.14
12.0	1.18	0.46	1.70	-0.01	1.03	0.10	0.72	0.53	1.19	1.05	-0.12
13.0	1.32	0.54	1.85	0.00	1.04	0.10	0.77	0.54	1.31	1.04	-0.09
14.0	1.45	0.63	1.99	0.02	1.03	0.09	0.82	0.54	1.43	1.01	-0.07
15.0	1.58	0.73	2.14	0.04	1.00	0.10	0.85	0.56	1.54	0.96	-0.06
16.0	1.71	0.82	2.29	0.06	0.97	0.11	0.89	0.58	1.65	0.91	-0.05
17.0	1.83	0.91	2.44	0.08	0.95	0.14	0.92	0.61	1.75	0.87	-0.06
18.0	1.94	0.99	2.59	0.10	0.93	0.17	0.94	0.65	1.84	0.82	-0.07
19.0	2.05	1.08	2.74	0.13	0.93	0.22	0.97	0.69	1.91	0.79	-0.09
20.0	2.15	1.16	2.87	0.17	0.94	0.28	0.98	0.72	1.98	0.77	-0.11
21.0	2.24	1.24	2.90	0.22	0.99	0.36	1.00	0.66	2.02	0.77	-0.14
22.0	2.33	1.32	2.92	0.29	1.07	0.45	1.01	0.59	2.04	0.78	-0.16
23.0	2.41	1.40	2.95	0.37	1.18	0.55	1.01	0.54	2.04	0.80	-0.17
24.0	2.49	1.47	2.97	0.48	1.32	0.66	1.02	0.48	2.01	0.84	-0.18
25.0	2.56	1.54	3.00	0.61	1.48	0.77	1.02	0.44	1.95	0.88	-0.17
26.0	2.63	1.61	3.02	0.75	1.67	0.89	1.02	0.39	1.88	0.92	-0.14
27.0	2.69	1.67	3.05	0.96	1.87	1.01	1.02	0.36	1.73	0.91	-0.05
28.0	2.77	1.73	3.07	1.00	2.08	1.13	1.03	0.31	1.76	1.08	-0.13
29.0	2.79	1.79	3.10	1.03	2.20	1.23	0.99	0.32	1.74	1.16	-0.20
30.0	2.81	1.85	3.12	1.07	2.23	1.28	0.95	0.33	1.72	1.16	-0.21
31.0	2.83	1.90	3.15	1.11	2.27	1.32	0.91	0.34	1.70	1.16	-0.21
32.0	2.85	1.95	3.17	1.15	2.31	1.36	0.88	0.35	1.68	1.16	-0.22
33.0	2.87	2.00	3.20	1.18	2.35	1.41	0.84	0.35	1.66	1.16	-0.23
34.0	2.89	2.05	3.22	1.22	2.38	1.45	0.81	0.36	1.64	1.16	-0.23
35.0	2.91	2.10	3.25	1.26	2.42	1.50	0.78	0.37	1.62	1.16	-0.24
36.0	2.92	2.14	3.27	1.29	2.46	1.54	0.76	0.38	1.60	1.16	-0.24
37.0	2.94	2.18	3.30	1.33	2.49	1.58	0.73	0.39	1.58	1.16	-0.25
38.0	2.96	2.22	3.33	1.37	2.53	1.63	0.71	0.40	1.56	1.16	-0.26
39.0	2.98	2.26	3.35	1.41	2.57	1.67	0.69	0.41	1.54	1.16	-0.26

Table 20: Normalised light curves of SN 1986G

t_{tr}(days)	B	V	U	H	J	K	B-V	U-B	B-H	J-H	H-K
40.0	3.00	2.30	3.38	1.44	2.61	1.71	0.67	0.41	1.52	1.16	-0.27
41.0	3.02	2.33	3.40	1.48	2.64	1.76	0.65	0.42	1.50	1.16	-0.28
42.0	3.04	2.36	3.43	1.52	2.68	1.80	0.63	0.43	1.48	1.16	-0.28
43.0	3.06	2.39	3.45	1.55	2.72	1.85	0.62	0.44	1.46	1.16	-0.29
44.0	3.08	2.42	3.48	1.59	2.76	1.89	0.61	0.45	1.44	1.16	-0.30
45.0	3.09	2.45	3.50	1.63	2.79	1.93	0.59	0.46	1.41	1.16	-0.30
46.0	3.11	2.48	3.53	1.67	2.83	1.98	0.58	0.47	1.39	1.17	-0.31
47.0	3.13	2.51	3.55	1.70	2.87	2.02	0.57	0.47	1.37	1.17	-0.32
48.0	3.15	2.54	3.58	1.74	2.91	2.06	0.56	0.48	1.35	1.17	-0.32
49.0	3.17	2.57	3.60	1.78	2.94	2.11	0.54	0.49	1.33	1.17	-0.33
50.0	3.19	2.60	3.63	1.82	2.98	2.15	0.53	0.50	1.31	1.17	-0.34
55.0	3.28	2.74	3.75	2.00	3.17	2.37	0.47	0.54	1.21	1.17	-0.37
60.0	3.38	2.89	3.88	2.19	3.36	2.59	0.41	0.59	1.11	1.17	-0.40
65.0	3.47	3.03	4.01	2.37	3.54	2.81	0.35	0.63	1.00	1.17	-0.44
70.0	3.56	3.18	4.13	2.56	3.73	3.03	0.28	0.67	0.90	1.17	-0.47
75.0	3.66	3.32	4.26	2.74	3.92	3.25	0.22	0.72	0.80	1.17	-0.50
80.0	3.75	3.47	4.39	2.93	4.10	3.46	0.16	0.76	0.70	1.17	-0.53
85.0	3.85	3.61	4.51	3.12	4.29	3.68	0.10	0.80	0.59	1.17	-0.57
90.0	3.94	3.76	4.64	3.30	4.48	3.90	0.04	0.84	0.49	1.17	-0.60
95.0	4.03	3.90	4.76	3.49	4.66	4.12	-0.03	0.89	0.39	1.17	-0.63
100.0	4.13	4.05	4.89	3.67	4.85	4.34	-0.09	0.93	0.29	1.18	-0.67
105.0	4.22	4.19	5.02	3.86	5.04	4.56	-0.15	0.97	0.18	1.18	-0.70
110.0	4.32	4.34	5.14	4.05	5.22	4.78	-0.21	1.02	0.08	1.18	-0.73

Table 20: (continued)

Filter	t_2 (days past B maximum)	α_2 (mags/day)
B	28	0.019
V	41	0.029
U	(20)	(0.025)
H	26	0.037
J	28	0.037
K	28	0.044

Table 21: Same as Table 1 for the curves of SN 1986G

Filter	t_o^{max}	t_o^{min}
B	0	-
V	3	-
U	-1	-
H	10	3
J	19	13
K	14	8

Table 22: Same as Table 5 for SN 1986G

	B_o^o	V_o^o	U_o^o	H_o^o	J_o^o	K_o^o	$(B-V)_o^o$	$(U-B)_o^o$	$(B-H)_o^o$	$(V-K)_o^o$	$(J-H)_o^o$	$(H-K)_o^o$
SN 1986G	12.50	11.54	13.26	10.00	10.05	9.88	0.96	0.76	2.50	1.66	0.05	0.12

Table 23: Maximum magnitudes and colours of SN 1986

A_B	A_V	A_U	A_H	A_J	A_K
3.9	3.0	4.6	0.4	0.8	0.3
$B^o_{o,corr}$	$V^o_{o,corr}$	$U^o_{o,corr}$	$H^o_{o,corr}$	$J^o_{o,corr}$	$K^o_{o,corr}$
8.6	8.5	8.7	9.6	9.3	9.6
$(B-V)^o_{o,corr}$	$(U-B)^o_{o,corr}$	$(B-H)^o_{o,corr}$	$(V-K)^o_{o,corr}$	$(J-H)^o_{o,corr}$	$(H-K)^o_{o,corr}$
0.1	0.1	-1.0	-1.1	-0.3	0.0

Table 24: Absorption corrections, corrected magnitudes and colours of SN 1986G (see text for details)

	Δm_B	Δm_V	Δm_U	Δm_H	Δm_J	Δm_K
1983N - 1972E	3.3	2.4	3.9	1.4	2.6	1.4
$1986G^{corr}$-1972E	0.2	0.0	0.6	0.3	1.4	0.6
	Δm_B^{10}	Δm_V^{10}	Δm_U^{10}	Δm_H^{10}	Δm_J^{10}	Δm_K^{10}
1983N - 1972E	2.3	1.6	3.8	0.7	0.0	0.6
$1986G^{corr}$-1972E	-0.5	0.1	1.1	0.0	-0.2	0.1

Table 25: Brightness differences of SNe I in the Cen A group of galaxies at maximum and $t_o=10^d$

SNe	Galaxy	d_{vir}	M_U^o	M_B^o	M_V^o	M_J^o	M_H^o	M_K^o	M_J^{10}	M_H^{10}	M_K^{10}
1972E	NGC 5253	.23	-20.30	-20.00	-19.92	-20.49	-19.13	-19.40	-17.94	-18.82	-18.86
1980N	NGC 1316	1.22	-19.60	-19.51	-19.55	-20.23	-18.81	-19.12	-17.68	-18.50	-18.58
1981B	NGC 4536	1.00	-19.72	-19.56	-19.57	-19.99	-18.78	-19.07	-17.44	-18.47	-18.53
1981D	NGC 1316	1.22	-19.73	-19.53	-19.80	-19.95	-18.82	-19.06	-17.40	-18.51	-18.52
1983G	NGC 4753	1.38	-19.32	-19.29	-19.55	-20.26	-18.82	-19.05	-17.71	-18.51	-18.51
MEAN			-19.73	-19.58	-19.68	-20.18	-18.87	-19.14	-17.63	-18.56	-18.60
σ			± 0.36	± 0.26	± 0.17	± 0.22	± 0.15	± 0.15	± 0.22	± 0.15	± 0.15

Table 26: Absolute magnitudes of the standard SNe Ia for the most probable distances of the parent galaxies at the B maximum (all filters) and $t_o=10^a$ (infrared filters)

SNe	Galaxy	d_{vir}	M_U^o	M_B^o	M_V^o	M_J^o	M_H^o	M_K^o	M_J^{10}	M_H^{10}	M_K^{10}
1972E	NGC 5253	.13	-19.06	-18.76	-18.68	-19.25	-17.89	-18.16	-16.70	-17.58	-17.62
1980N	NGC 1316	1.22	-19.60	-19.51	-19.55	-20.23	-18.81	-19.12	-17.68	-18.50	-18.58
1981B	NGC 4536	1.78	-20.97	-20.81	-20.82	-21.24	-20.03	-20.32	-18.69	-19.72	-19.78
1981D	NGC 1316	1.22	-19.73	-19.53	-19.80	-19.95	-18.82	-19.06	-17.40	-18.51	-18.52
1983G	NGC 4753	1.00	-18.62	-18.59	-18.85	-19.56	-18.12	-18.35	-17.01	-17.71	-17.81
MEAN			-19.60	-19.44	-19.54	-20.05	-18.73	-19.00	-17.50	-18.42	-18.46
σ			± 0.89	± 0.88	± 0.85	± 0.76	± 0.83	± 0.85	± 0.76	± 0.83	± 0.85

Table 27: Same as Table 26 with possible distances of the parent galaxies

SNe	Galaxy	t_o^{Bmax} (JD)	B_o^o	V_o^o	H_o^o	J_o^o	K_o^o	Source of observations
1960F	NGC 4496	2437045	11.75	-	-	-	-	1
1960R	NGC 4382	2437287	11.90	(11.72)	-	-	-	1,2
1961H	NGC 4564	2437430	12.20	(10.78)	-	-	-	1,3
1984A	NGC 4419	2445719	12.18	12.45	13.27	11.94	12.92	4,5,6,7,8

1. Tvestkov,P.Y.: 1983, Perem. Zvedzy 5,176
2. Gates,H.S.: 1961, Harvard Coll. Announc. Card No. 1521
3. van den Bergh,S.,Henry,R.C.: 1961, Journ. Royal Astr. Soc. Canada 55,173
4. Cadonau,R.: 1986, Ph.D. Thesis, University of Basel
5. Rosino,L.: 1984, IAU Circ. 3910
6. Meikle,W.P.S.,Graham,J.R.,Bode,M.F.: 1984, IAU Circ. 3918
7. Meikle,W.P.S.: 1984, IAU Circ. 3924
8. Graham,J.R.,Meikle,W.P.S.,Longmore,A.J.,Williams,P.M.: 1988, Astrophys.J. 333,743

Table 28: SNe I in Virgo. Julian dates of B maximum and apparent magnitudes at maximum. Also given are the references of the used observations.

SNe	t^{Bmax} (JD)	Galaxy	d_{vir}	v_o (km s^{-1})	source of v_o	source of photometry
1959C	2436750	A 1308+03	2.74	~2900	b,c,d	1
1966J	2439457	NGC 3198	0.73	704	a	2
1967C	2439549	NGC 3389	1.29	1128	a	3,4,5
1969C	2440256	NGC 3811	2.91	3159	a	6
1970J	2440868	NGC 7619	3.27	4019	a	7,8
1971G	2441055	NGC 4195	1.83	3747	a	7,9,10
1971I	2441097	NGC 5055	0.48	551	a	7,11,12,13
1971L	2441135	NGC 6384	1.62	1736	a	7,14
1972J	2441551	NGC 7634	2.74	3374	a	15
1973N	2441921	NGC 7495	4.20	~5126	b,c,d	15
1974G	2442170	NGC 4414	0.56	704	a	15
1974J	2442367	NGC 7343	see text		d	15
1975G	2442572	A 1359+55	-	-	-	16
1975N	2442723	NGC 7723	1.57	1975	a	9,16,17
1975O	2442743	NGC 2487	4.19	~4818	b,c,d	16
1976J	2443129	NGC 977	3.76	~4607	e	16,18
1978E	2443815	A 2233+37	-	-	-	19
1979B	2443952	NGC 3913	1.13	~1051	d	19
1982B	2445011	NGC 2268	2.20	~2228	b,c,d	20,21
1984I	2445843	ESO 323-G99	2.66	~2922	f	22

a. Kraan-Korteweg, 1986
b. Palumbo et al., 1983
c. Barbon et al., 1988
d. Huchtmeier and Richter, 1987
e. Barbon et al., 1982
f. Fairall and Jones, 1988

Table 29: SNe I with reasonably well observed B curves. All relative distances and the velocity relative to centroid of the local group marked were computed from the heliocentric velocities in the referred sources by Kraan-Korteweg (1988), else they are from Kraan-Korteweg (1986). The last column gives the sources of the photometry used. For details see text.

1. Mihalas,D.M.: 1962, Publ. Astron. Soc.Pacific 74,116
2. Chincarini,G.,Perinotto,M.: 1968, Mem. Soc. Astron. Ital. 39,188 (=Contr.Asiago No. 205)
3. de Vaucouleurs,G.,Solheim,J.E.,Brown,R.: 1967, Contr.McDonald Obs. No.425 (=Astrofizika 3,365)
4. Chuadze,A.D.,Barblishvili,T.I.: 1969, Bull. Abastumani Obs. 37,9
5. Borzov,G.G.,Dibai,E.A.,Episov,V.F.,Pronik,V.I.: 1969, Sov. Astr. 13,423
6. Bertola,F.,Ciatti,F.: 1971, Mem. Soc. Astron. Ital. 42,67 (=Contr.Asiago No. 253)
7. Barbon,R.,Ciatti,F.,Rosino,L.: 1973, Mem. Soc. Astron. Ital. 44,65 (=Contr.Asiago No. 284)
8. Dubjago,I.,Tokhtsev,S.S.: 1975, IBVS No. 1062
9. Tsvetkov,P.Y.: 1983, Perem. Zvedzy 5,176
10. de Vaucouleurs,G.,de Vaucouleurs,A.,Brown,G.S.: 1971, Astrophys. Letters 9,77
11. Various Observers: 1971, IAU Circ. 2330,2332,2333,2334,2338,2341,2347
12. Locher,K.: 1971, Orion 125, private communication
13. Deming,D.,Rust,B.,Olson,E.: 1973, Publ. Astron. Soc. Pac. 85,321
14. Lyuty,V.M.: 1976, Astr. Circ. No. 906
15. Ciatti,F.,Rosino,L.: 1977, Astron. Astrophys. 57,73
16. Ciatti,F.,Rosino,L.: 1978, Astron. Astrophys. Suppl. Series 34,387
17. Wegner,G.: 1977, Monthly Notices Roy. Astron. Soc. 181,677
18. Wegner,G.: 1979, Astron.J. 84,502
19. Barbon,R.,Ciatti,F.,Rosino,L.,Ortolani,S.,Rafanelli,P.1982, Astron. Astrophys. 116,43
20. Cadonau,R.,Trefzger,C.F.: 1983, IBVS No. 2382
21. Tsvetkov,P.Y.: 1983, Astr. Circ. No. 1274
22. Binggeli,B.,Leibundgut,B., unpublished

Table 29: (continued)

SNe	B_o^o	N_B	σ_B	V_o^o	N_V	U_o^o	N_U	M_B^o	M_V^o	M_U^o	remarks
1959C	13.89	20	0.19	14.04	9	13.50	5	-19.91	-19.76	-20.30	
1966J	11.23	14	0.10	-	-	-	-	-19.70	-	-	
1967C	13.17	32	0.26	13.26	17	12.80	14	-18.99	-18.90	-19.36	
1969C	14.14	20	0.29	14.07	9	13.94	3	-19.79	-19.86	-19.99	
1970J	14.24	30	0.30	14.49	19	14.10	6	-19.94	-19.69	-20.08	
1971G	14.11	32	0.19	14.13	18	14.01	5	-18.81	-18.79	-18.91	ambiguous data, see text
1971I	12.04	39	0.23	11.92	78	-	-	-17.98	-18.10	-	Ia, large scatter, see text
1971L	13.14	13	0.23	12.73	13	12.52	2	-19.52	-19.93	-20.14	
1972J	14.30	16	0.21	14.61	14	-	-	-19.50	-19.19	-	
1973N	15.22	22	0.32	14.85	21	-	-	-19.51	-19.88	-	
1974G	12.57	11	0.14	12.40	11	-	-	-17.78	-17.95	-	Ia, see text
1974J	15.71	20	0.17	16.01	14	-	-	-	-	-	distance unclear
1975G	14.71	9	0.07	14.75	3	-	-	-	-	-	no distance available
1975N	13.69	26	0.16	13.51	20	13.57	10	-18.90	-19.08	-19.02	
1975O	15.19	9	0.05	15.46	4	-	-	-19.53	-19.26	-	
1976J	14.90	11	0.12	15.05	7	14.18	3	-19.59	-19.44	-20.31	
1978E	15.30	13	0.16	15.22	11	-	-	-	-	-	no distance available
1979B	12.79	18	0.28	12.45	11	-	-	-19.09	-19.43	-	
1982B	13.15	19	0.12	13.12	22	-	-	-20.17	-20.20	-	
1984I	16.00	8	0.17	15.56	7	15.82	6	-17.74	-18.18	-17.92	Ib?, red

Table 30: Apparent and absolute magnitudes of the sample of 20 SNe I. N_x is the number of observations, σ_B the standard deviation in B.

SNe	M_B^o	M_V^o	M_U^o	M_H^o	M_J^o	M_K^o
1962L	-17.85	-18.66	-17.71	-	-	-
1964L	-17.50	-	-	-	-	-
1976B	-16.57	-18.24	-	-	-	-
1983I	-16.20	-16.80	-	-16.93	-16.91	-17.14
1983N	-16.67	-17.49	-16.42	-17.76	-17.85	-17.96
1984L	(-17.88)	-18.45	(-17.79)	-19.05	-19.30	-19.31

Table 31: Absolute magnitudes of SNe Ib

Figure Captions

Figure 1: The normalised standard light curves of SNe Ia for the UBV filters as taken from Cadonau (1986)

Figure 2: The infrared (HJK) standard curves for SNe Ia, normalised to the B maximum ($t_o=0^d$)

Figure 3: Fit of the observations of the four standard SNe Ia (SNe 1972E, 1980N, 1981B, 1981D) on the standard B curve. The observations were shifted in brightness by the magnitudes given in Table 6.

Figure 4: Fit of the four standard SNe Ia on the H template. No observations fo² $t_o \leq 0^d$ are available.

Figure 5: Same as Figure 3 for the U and V filters.

Figure 6: Same as Figure 4 for the infrared J and K bands.

Figure 7: Fits of SN 1983G on the set of standard curves.

Figure 8: Comparison of the light curves. The curves were shifted to display the intrinsic colours. The connection of the infrared and the optical templates is described in the text. The whole range from $t_o=-5^d$ to $t_o=110^d$ is shown for the optical curves, the defined part ($-5^d \leq t_o \leq 110^d$) for the infrared.

Figure 9: The evolution of a SN Ia in the two-colour diagram (B-V,U-B). The line of black bodies with the corresponding temperatures is given (Matthews and Sandage 1963). The line of reddening is indicated.

Figure 10: The evolution of the colour temperatures of SNe Ia. The temperatures were computed according to Fu and Arnett (1987) with the zero-points given in the text.

Figure 11: Comparison of the radiation of SNe Ia with black body energy distributions. The black bodies were not normalised for this comparison.

Figure 12: Comparison of the integrated bolometric light curve with the one calculated with bolometric corrections.

Figure 13: Comparison of the bolometric light curve with calculations for SNe 1972E and 1981B (Graham 1987). The points were shifted in brightness to fit the curve. The time interval between explosion and B maximum is assumed to be 20 days.

Figure 14: Comparison of the bolometric light curve with a theoretical prediction (Graham 1987). The curves were shifted to achieve the fit. the time difference between explosion and the B maximum is 20 days.

Figure 15: The effect of absorption on the standard B curve of SNe Ia.

Figure 16: Same as Figure 15 for the V template.

Figure 17: Fit of SN 1983G ($E_{B-V} \approx 0.^m5$) on the B curves. The observations were shifted by to days (B maximum at JD 2445429) and $\Delta m_B = 0.^m23$ to obtain this fit.

Figure 18: Best fit of all observations of Kepler's SN 1604 on the V tamplates of SNe Ia. Also shown is the rising slope (Cadonau 1986).

Figure 19: Fit of Kepler's SN 1604 omitting all observations from comparison with Venus. The points were fitted to accord with the curve for a reddening of $E_{B-V} = 1.^m0$.

Figure 20: K-corrections in V for a SN Ia at maximum.

Figure 21: K-corrections in V for a SN Ia at $t_o = 22^d$.

Figure 22: The V light curve for SNe Ia at small redshifts.

Figure 23: Comparison of the V templates of redshifted SNe Ia and the B standard curve. The points were normalised to the maximum to compare the shapes of the curves.

Figure 24: The effect of time dilation. Comparison of the normalised points with the V and B curves. An evolution from the V to the B curve is visible. The strtching of the curves due to time dilation is obvious.

Figure 25: Mean light curves of SNe Ib normalised to the B maximum.

Figure 26: Normalised fiducial curves for the infrared filters for SNe Ib.

Figure 27: Comparison of the observations of six SNe Ib (SNe 1962L, 1964L, 1976B, 1983I, 1983N, 1984L) and the optical light curves.

Figure 28: Same as Figure 27 for the infrared. Only three SNe were used (SNe 1983I, 1983N, 1984L).

Figure 29: Comparison of the observations of SNe Ia and SNe Ib in B. The deviation of the SNe Ib from the standard SNe Ia is evident.

Figure 30: The continuum radiation of SNe Ib. The smooth transitions are clearly visible. No U curve was included. The whole range in all filters is shown.

Figure 31: Colour temperatures of SNe Ib.

Figure 32: The bolometric light curve of SN 1983N from integration over all filters.

Figure 33: Comparison of the bolometric light curve with observations (Panagia 1984, 1985) in flux units. The discrepancy is attributed to integration over different spectral ranges. The time interval between explosion and B maximum assumed is 17 days.

Figure 34: Comparison of the bolometric light curves of SN 1983N and SNe Ia. The cures were shifted to coincide at t_o=100^d.

Figure 35: The optical light curves of SN 1986G in Cen A. (Observations from Phillips et al. 1987)

Figure 36: The infrared light curves SN 1986G. (Observations from Frogel et al. 1987)

Figure 37: The continuum of SN 1986G. The second maxima in the infrared are less prominent than in normal SNe Ia. The colours were not corrected for internal absorption.

Figure 38: The bolometric light curve of SN 1986G integrated over the uncorrected filter curves. The bump between 5 and 30 days stems from the excessive infrared radiarion.

Figure 39: The bolometric light curve of SN 1986G for an integration over corrected curves.

Figure 40: Comparison of the shapes of the bolometric light curves of SN 1986G (corrected) and SNe Ia. The curves were shifted to match at t_o=100^d. A good correspondence is achieved.

Figure 41: The optical two-colour diagram for the colours at the B maximum of SNe I. The clear separation of the different subgroups can be seen. SNe Ib (filled squares) lie allong the reddening line from SNe Ia (open squares), whereas SN 1986G (cross) seems to hve been too red in U-B. The dot indicates the adopted intrinsic colours of SNe Ia.

Figure 42: Same as Figure 41 for the colours B-V and B-H. The reddening line was determined by absorption laws given by Schmidt-Kaler (1982) and Elias et al. (1985). The dot gives the adopted intrinsic colours for SNe Ia.

Figure 43: Same as Figure 42 at t_o=10^d.

Figure 44: Comparison of the bolometric light curves of SNe 1972E, 1983N and 1986G, which presumably occurred at the same distance (Centaurus A group). The subluminosity of SN 1983N is obvious. The correspondance between SN 1972E and SN 1983N is surprisingly good, considering the large corrections applied to the data of SN 1986G.

Figure 45: Same as Figure 41 for a bigger sample. The error bars indicate estimated errors.

Figure 46: The bolometric light curve of SNe Ia in absolute units. The curve gives the totally emitted radiation of such an event.

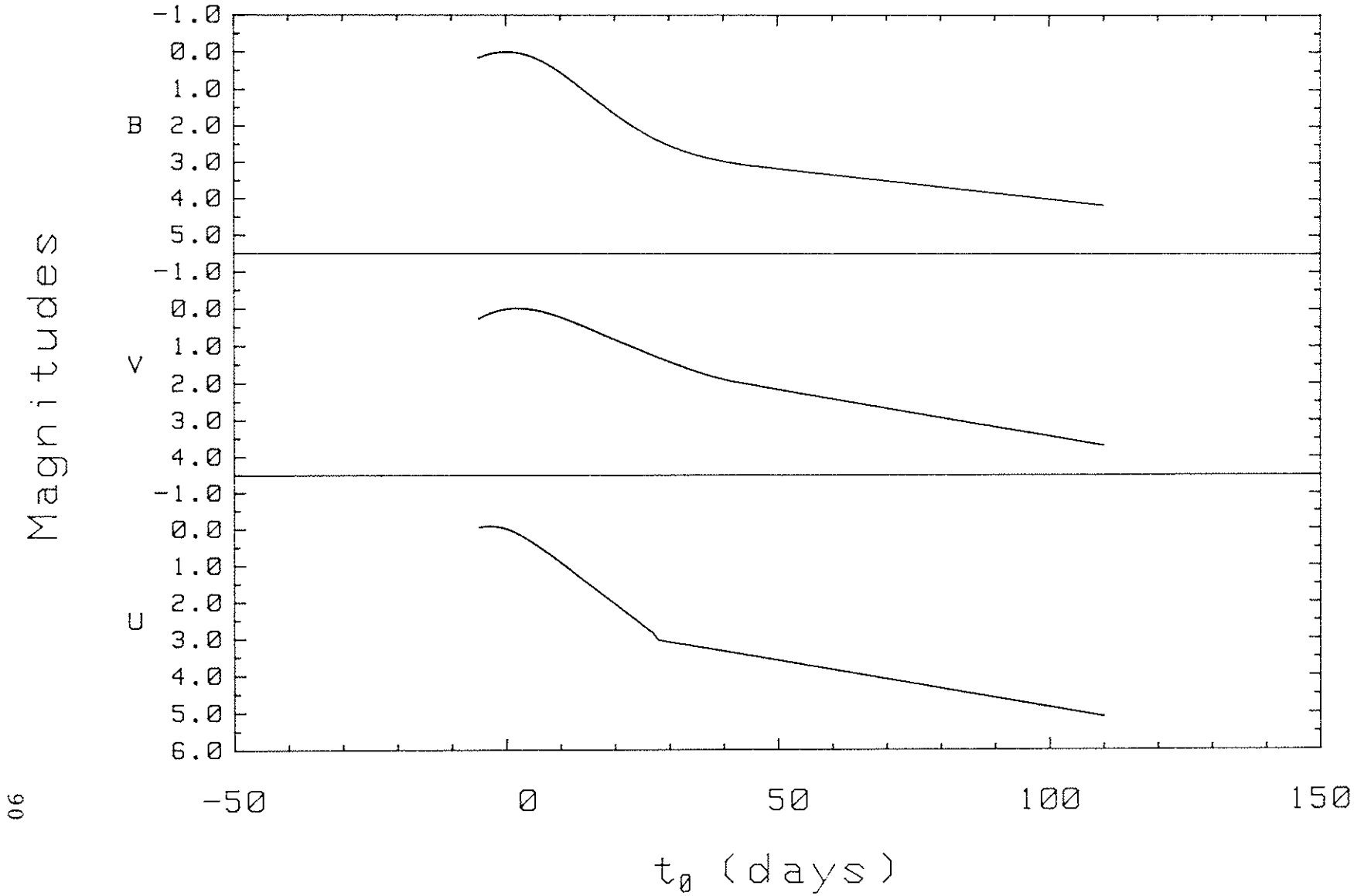

Figure 1

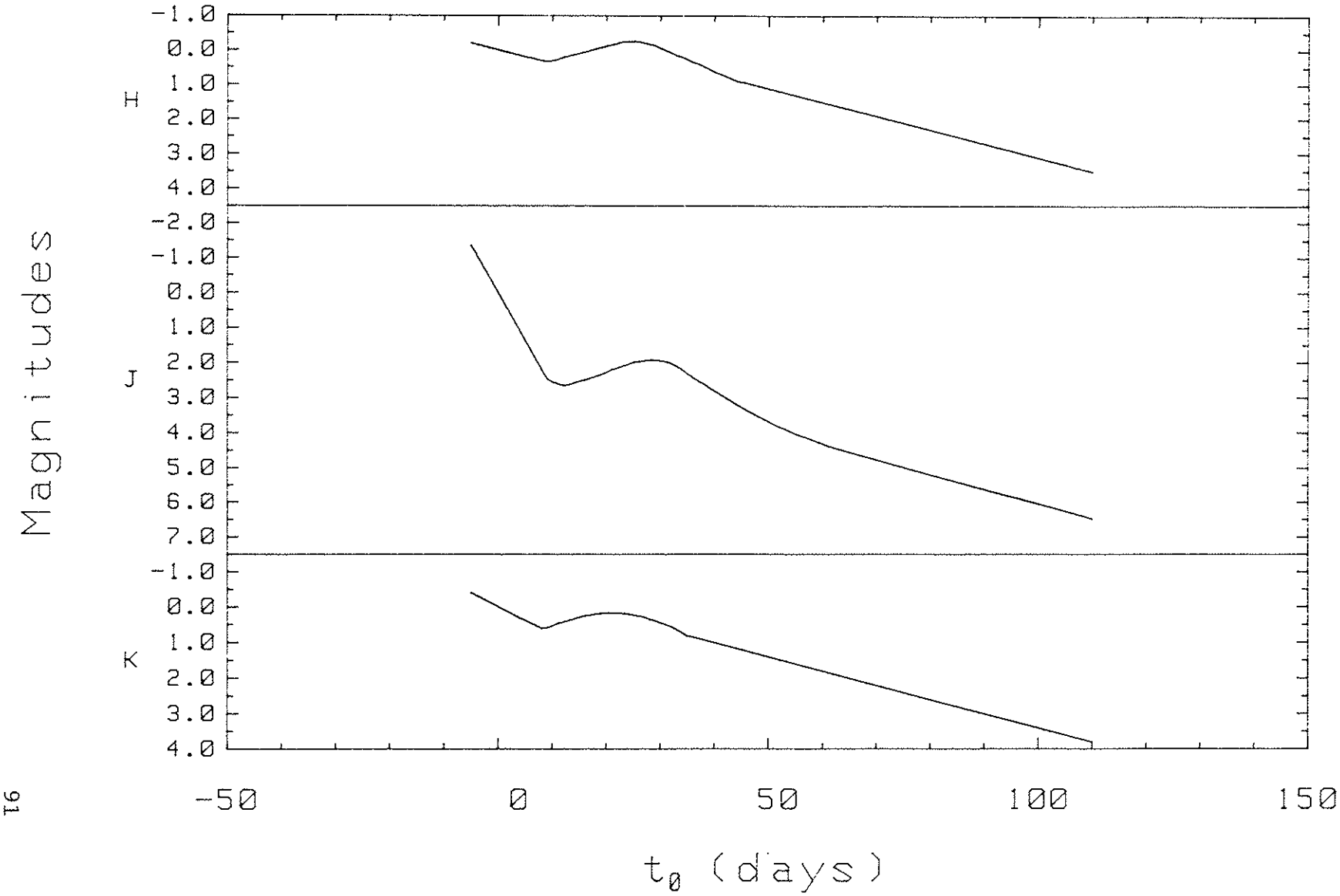
Magnitudes
H
J
K
-1.0
0.0
1.0
2.0
3.0
4.0
-2.0
-1.0
0.0
1.0
2.0
3.0
4.0
5.0
6.0
7.0
-1.0
0.0
1.0
2.0
3.0
4.0
-50
0
50
100
150
t0 (days)

Figure 2

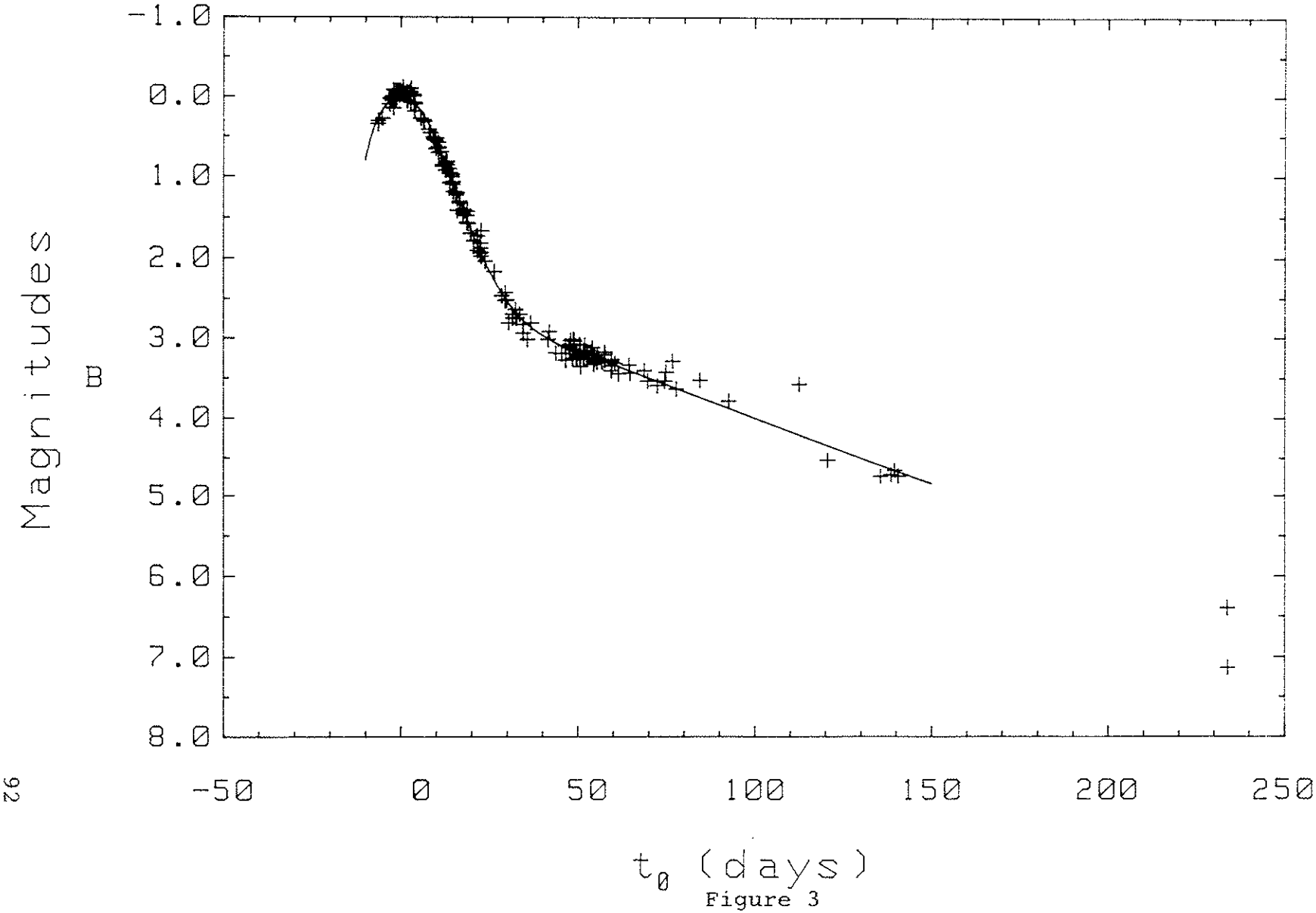
Magnitudes
B
-1.0
0.0
1.0
2.0
3.0
4.0
5.0
6.0
7.0
8.0
-50
0
50
100
150
200
250
t_0 (days)

Figure 3

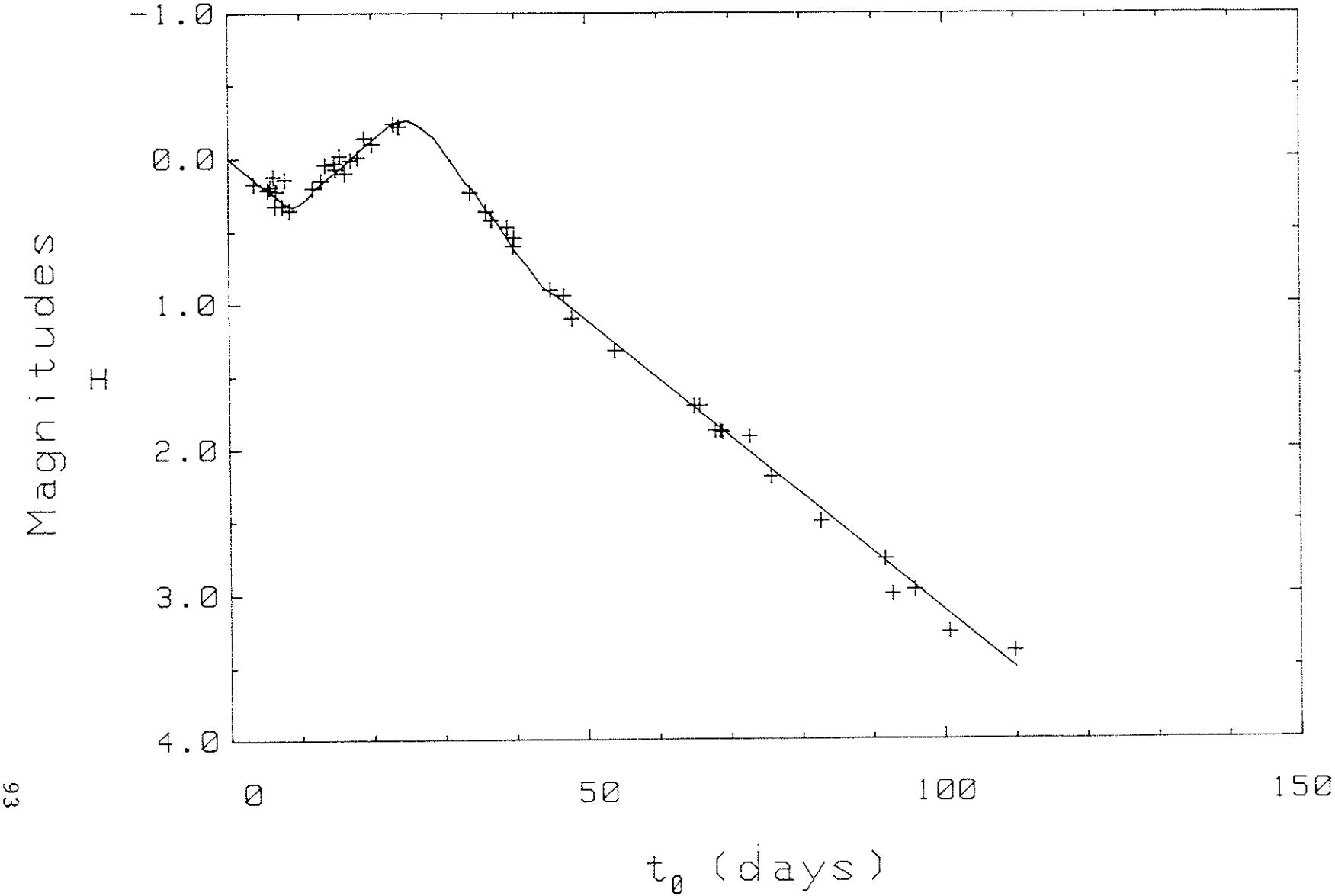

Figure 4

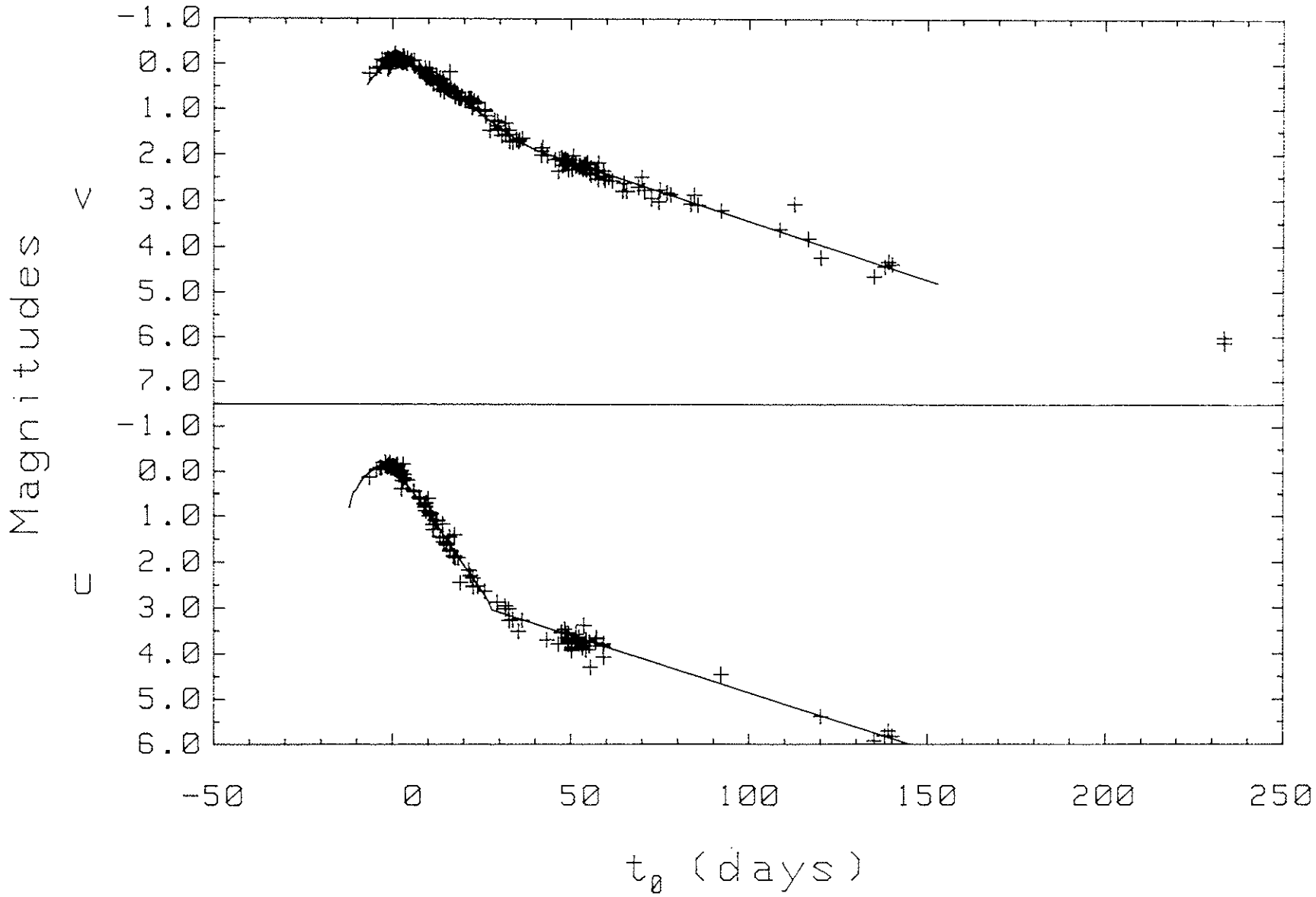
Magnitudes
V
U
-1.0
0.0
1.0
2.0
3.0
4.0
5.0
6.0
7.0
-50
0
50
100
150
200
250
t_0 (days)

Figure 5

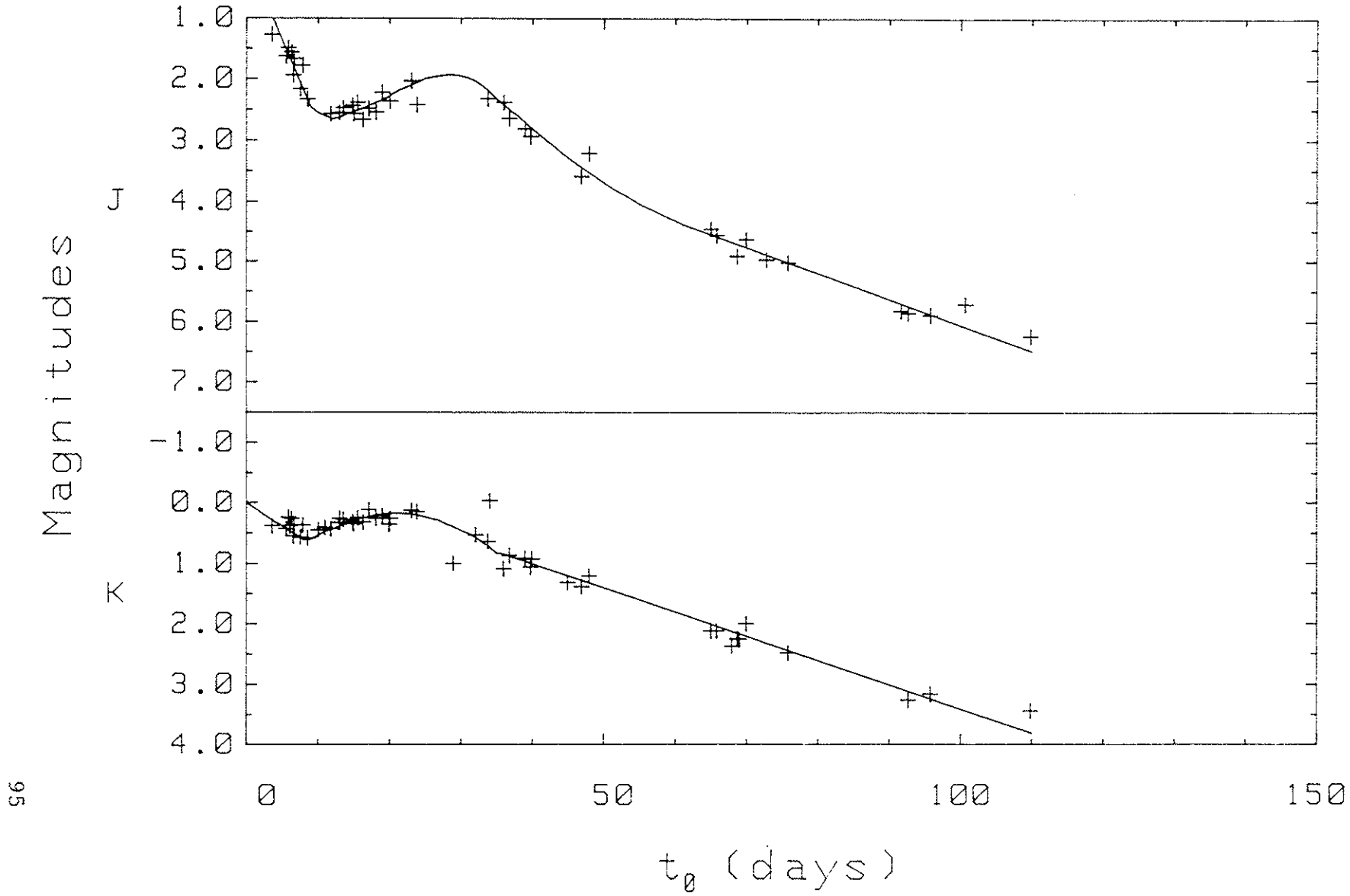
Magnitudes
J
K
1.0
2.0
3.0
4.0
5.0
6.0
7.0
-1.0
0.0
1.0
2.0
3.0
4.0
0
50
100
150
t_0 (days)

Figure 6

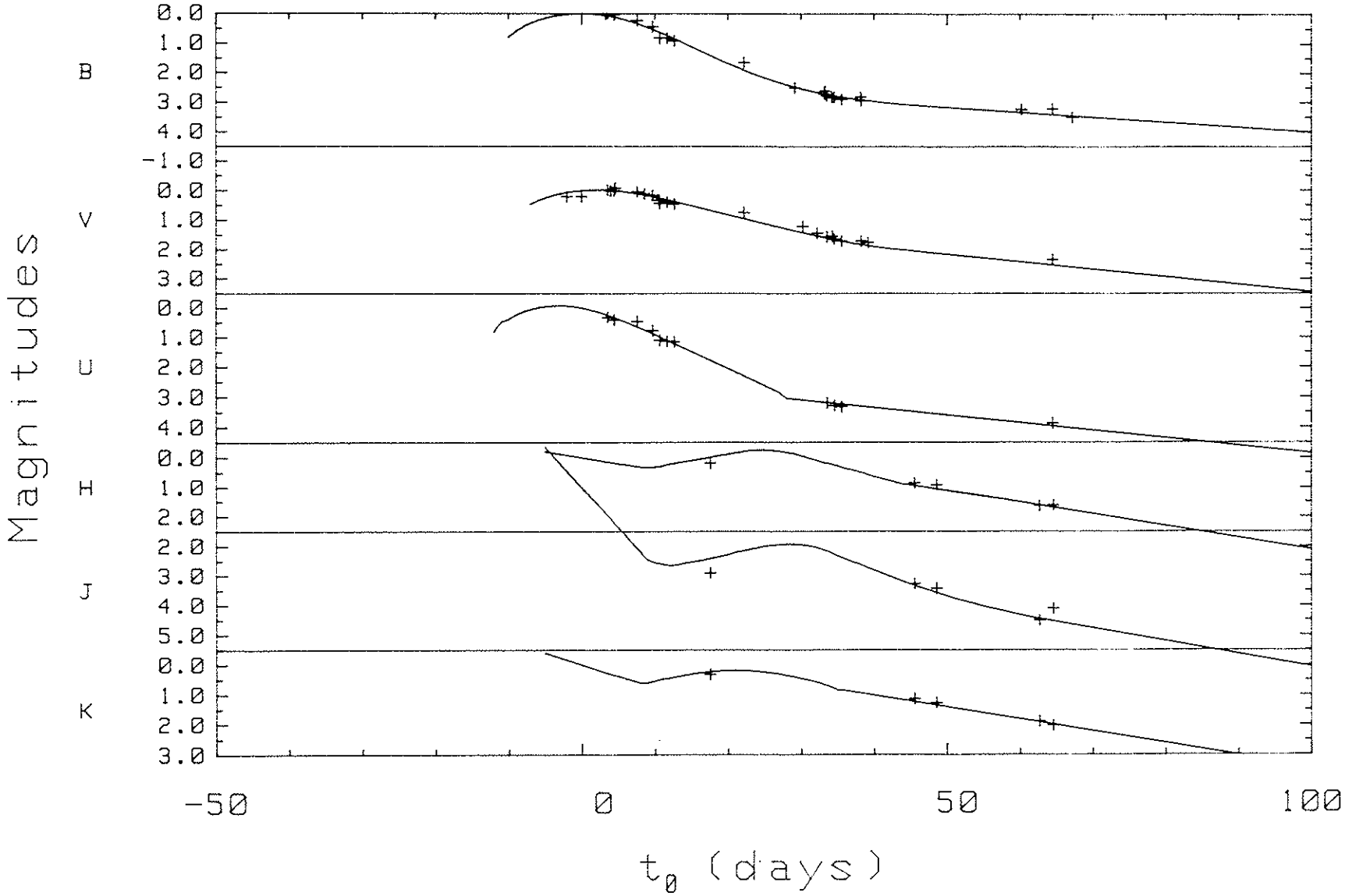
Magnitudes
B
V
U
H
J
K
0.0
1.0
2.0
3.0
4.0
-1.0
0.0
1.0
2.0
3.0
0.0
1.0
2.0
3.0
4.0
0.0
1.0
2.0
2.0
3.0
4.0
5.0
0.0
1.0
2.0
3.0
-50
0
50
100
t_0 (days)

Figure 7

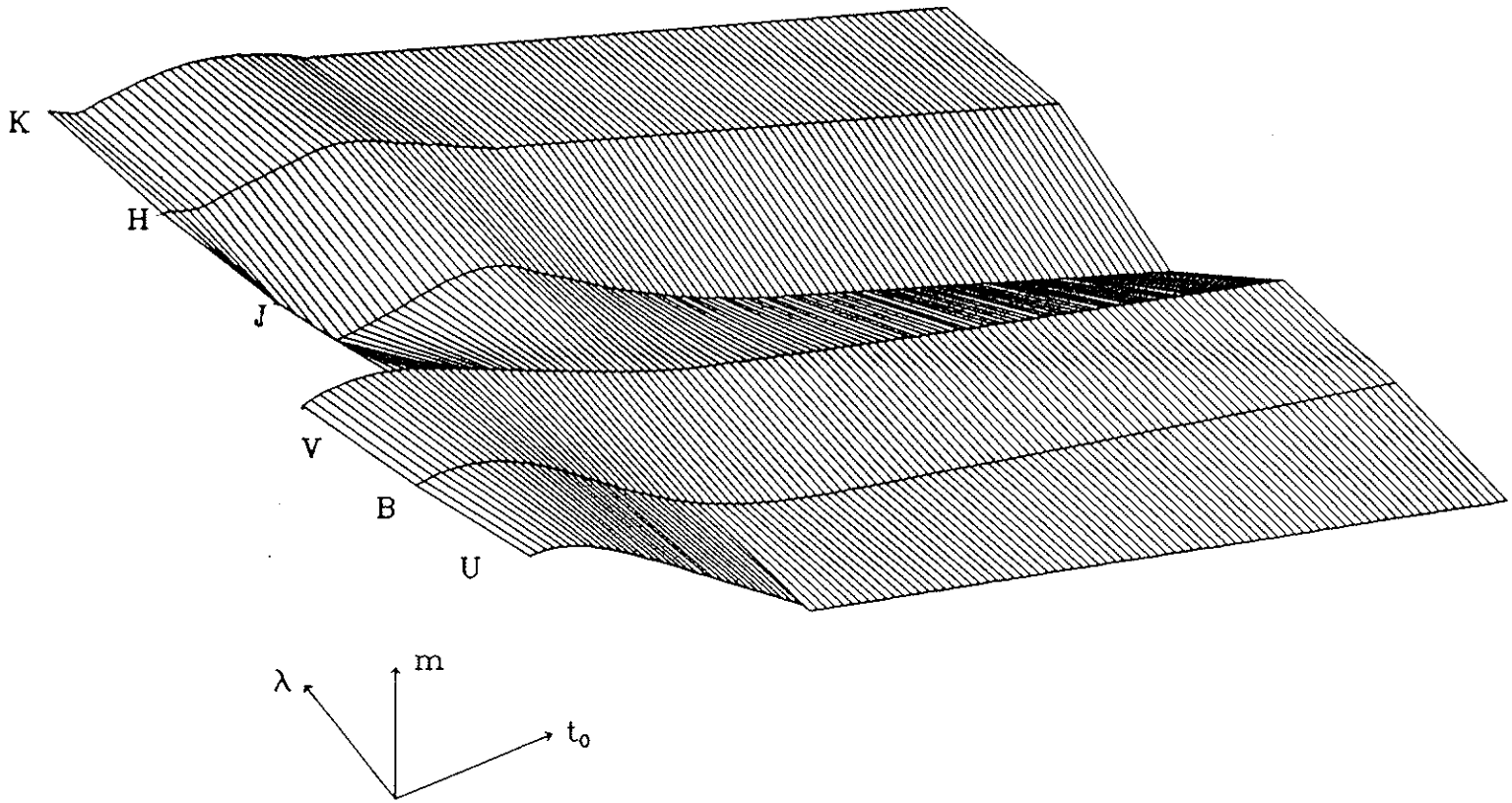

Figure 8

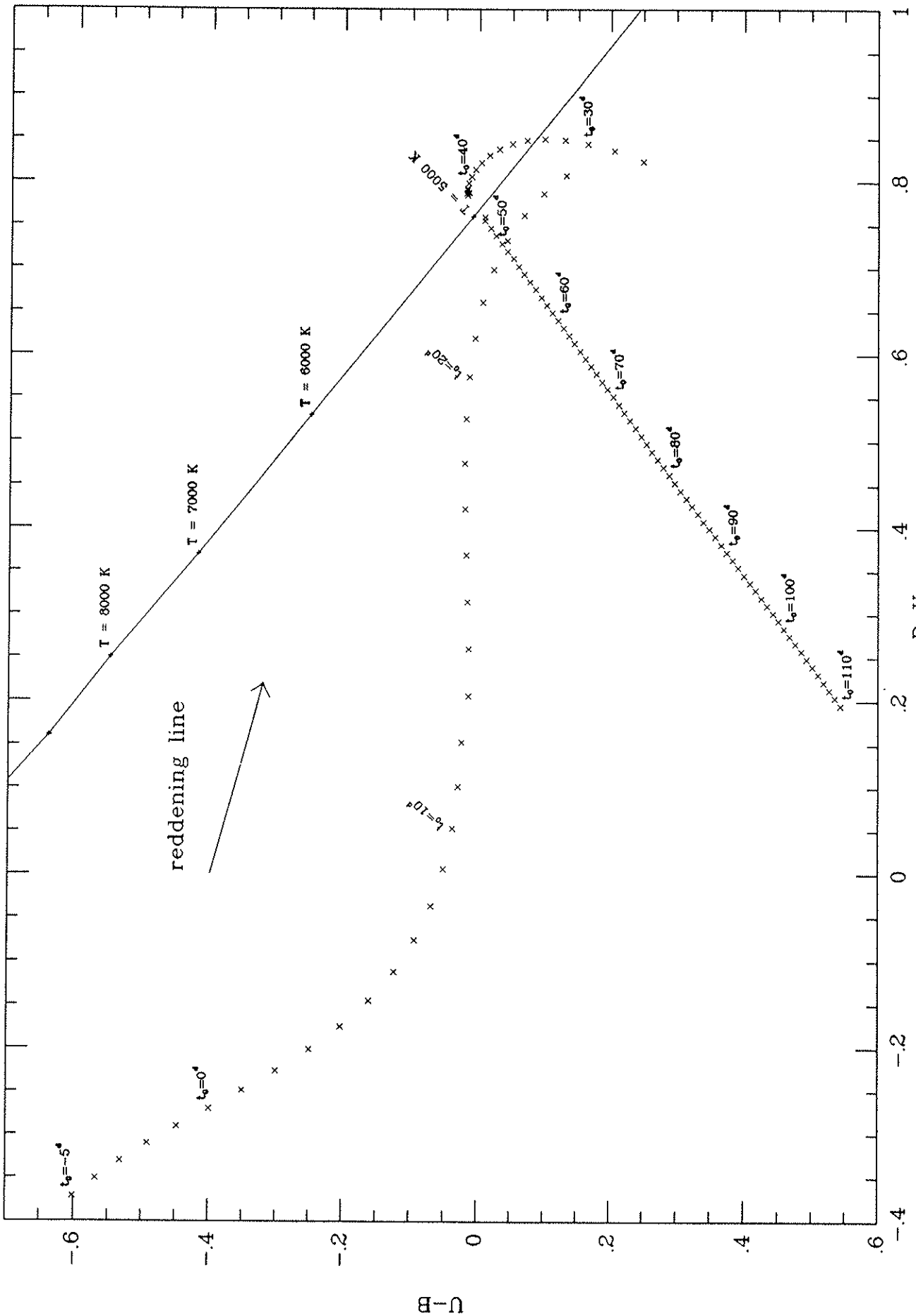
T = 5000 K
T = 6000 K
T = 7000 K
T = 8000 K
reddening line
t_0=-5^d
t_0=0^d
t_0=10^d
t_0=20^d
t_0=30^d
t_0=40^d
t_0=50^d
t_0=60^d
t_0=70^d
t_0=80^d
t_0=90^d
t_0=100^d
t_0=110^d
U−B
B−V
-.6
-.4
-.2
0
.2
.4
.6
-.4
-.2
0
.2
.4
.6
.8
1

Figure 9

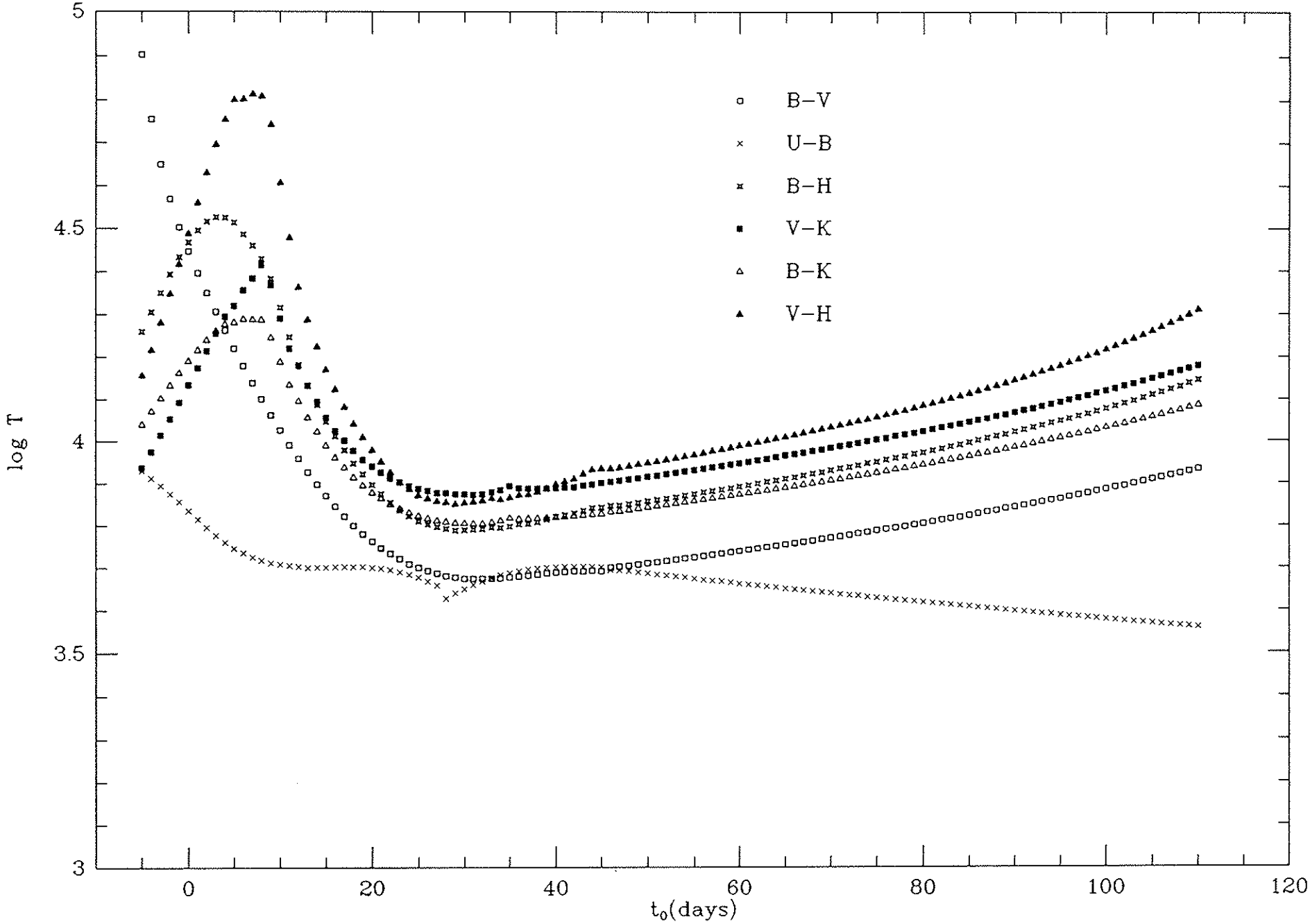

Figure 10

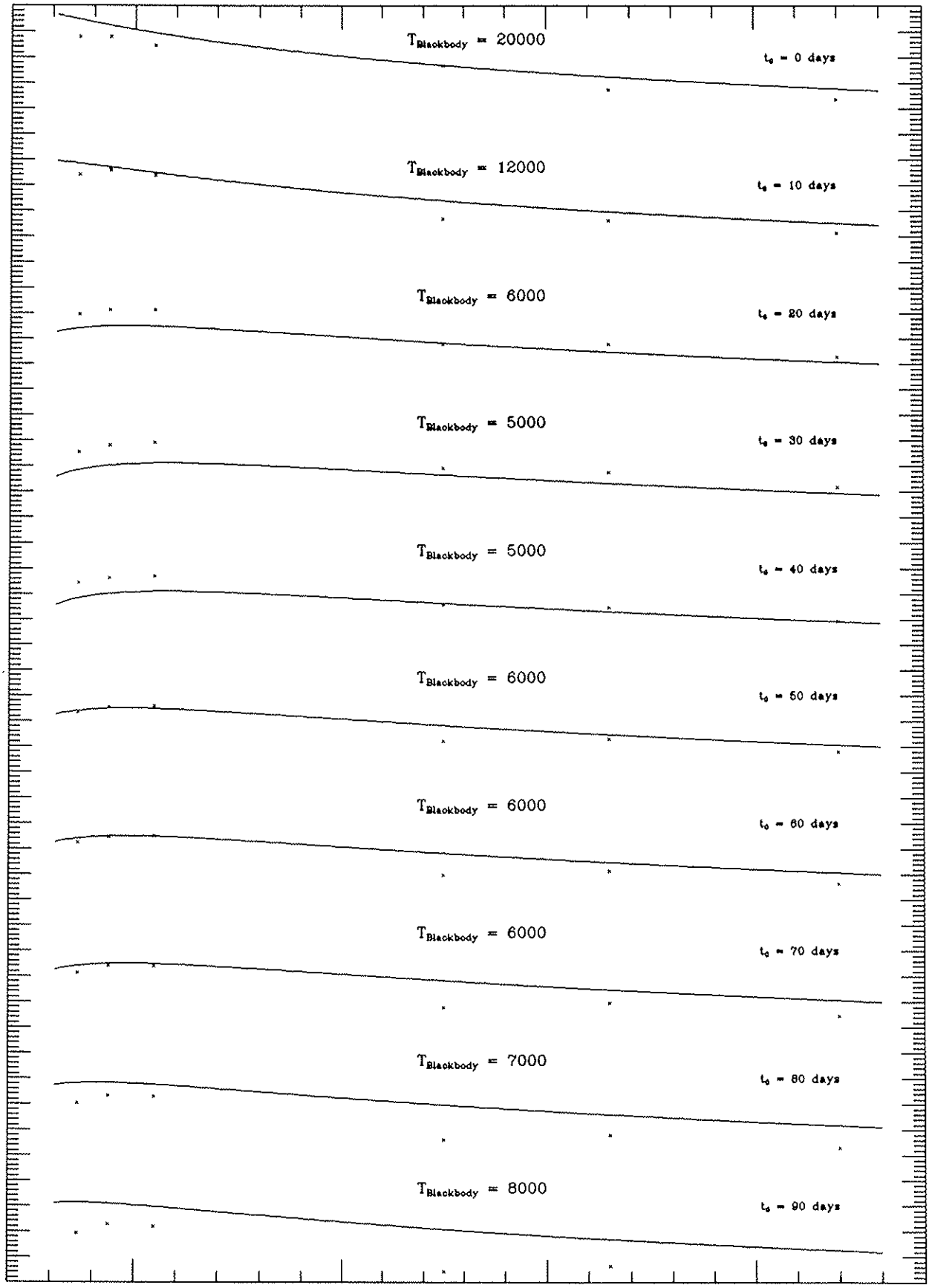
$T_{Blackbody}$ = 20000
t_0 = 0 days
$T_{Blackbody}$ = 12000
t_0 = 10 days
$T_{Blackbody}$ = 6000
t_0 = 20 days
$T_{Blackbody}$ = 5000
t_0 = 30 days
$T_{Blackbody}$ = 5000
t_0 = 40 days
$T_{Blackbody}$ = 6000
t_0 = 50 days
$T_{Blackbody}$ = 6000
t_0 = 60 days
$T_{Blackbody}$ = 6000
t_0 = 70 days
$T_{Blackbody}$ = 7000
t_0 = 80 days
$T_{Blackbody}$ = 8000
t_0 = 90 days
5000
10000
15000
20000
Angstroms
log (rel. flux)

Figure 11

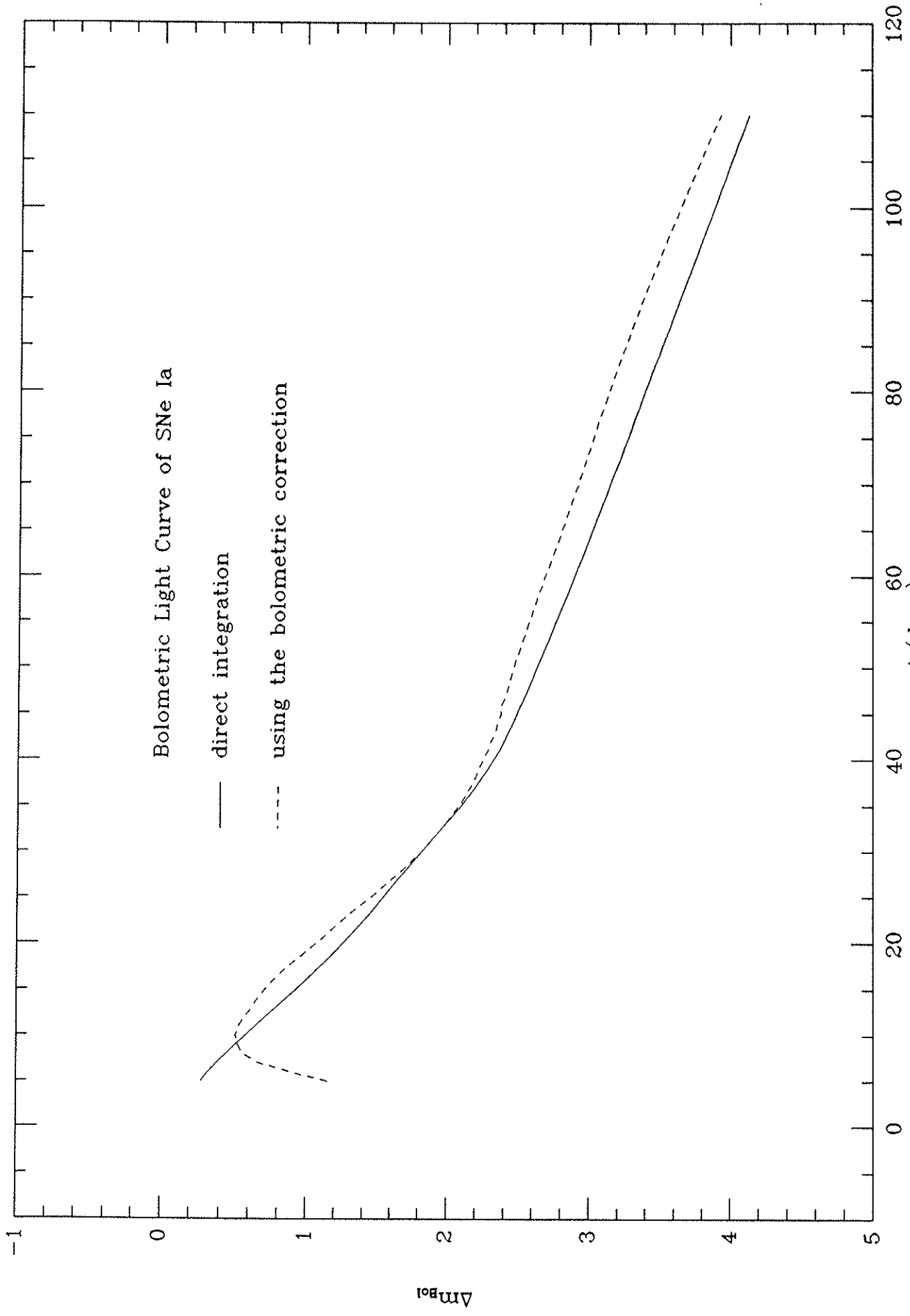
Bolometric Light Curve of SNe Ia
direct integration
using the bolometric correction
Δm_{bol}
t_0(days)
−1
0
1
2
3
4
5
0
20
40
60
80
100
120

Figure 12

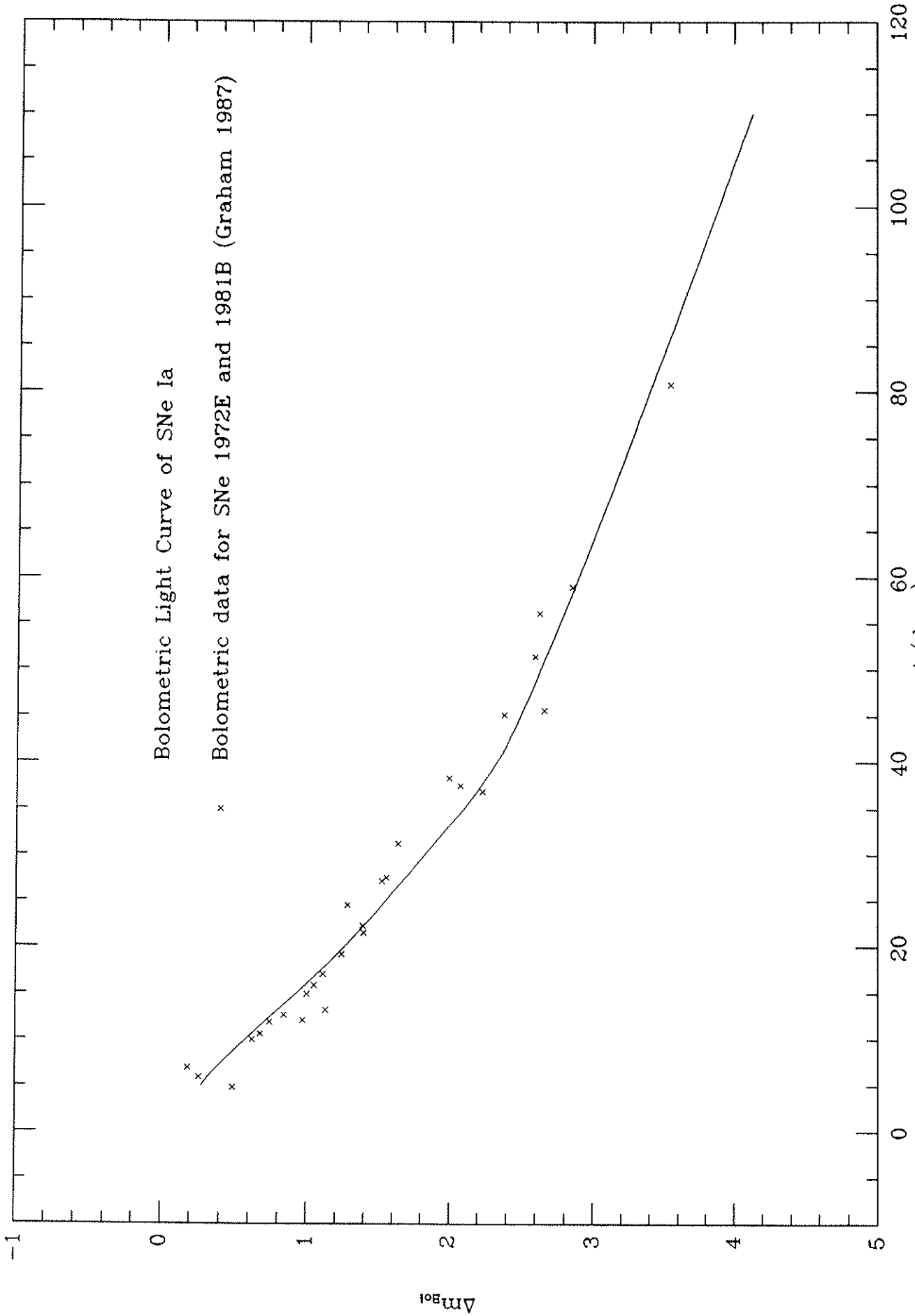
Bolometric Light Curve of SNe Ia
Bolometric data for SNe 1972E and 1981B (Graham 1987)
Δm_{bol}
t_o(days)
−1
0
1
2
3
4
5
0
20
40
60
80
100
120

Figure 13

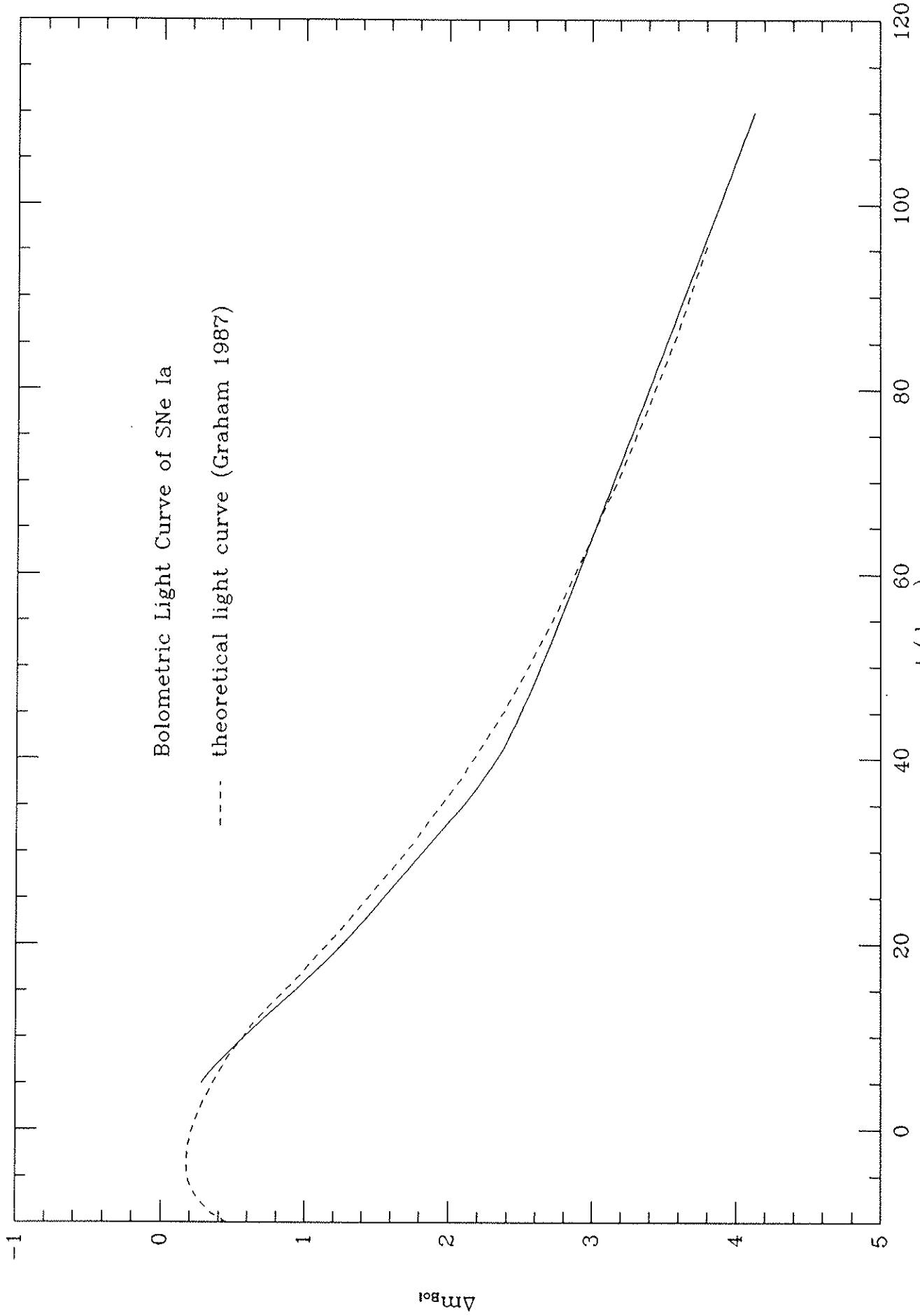
Bolometric Light Curve of SNe Ia
---- theoretical light curve (Graham 1987)
Δm_{bol}
t_o(days)
-1
0
1
2
3
4
5
0
20
40
60
80
100
120

Figure 14

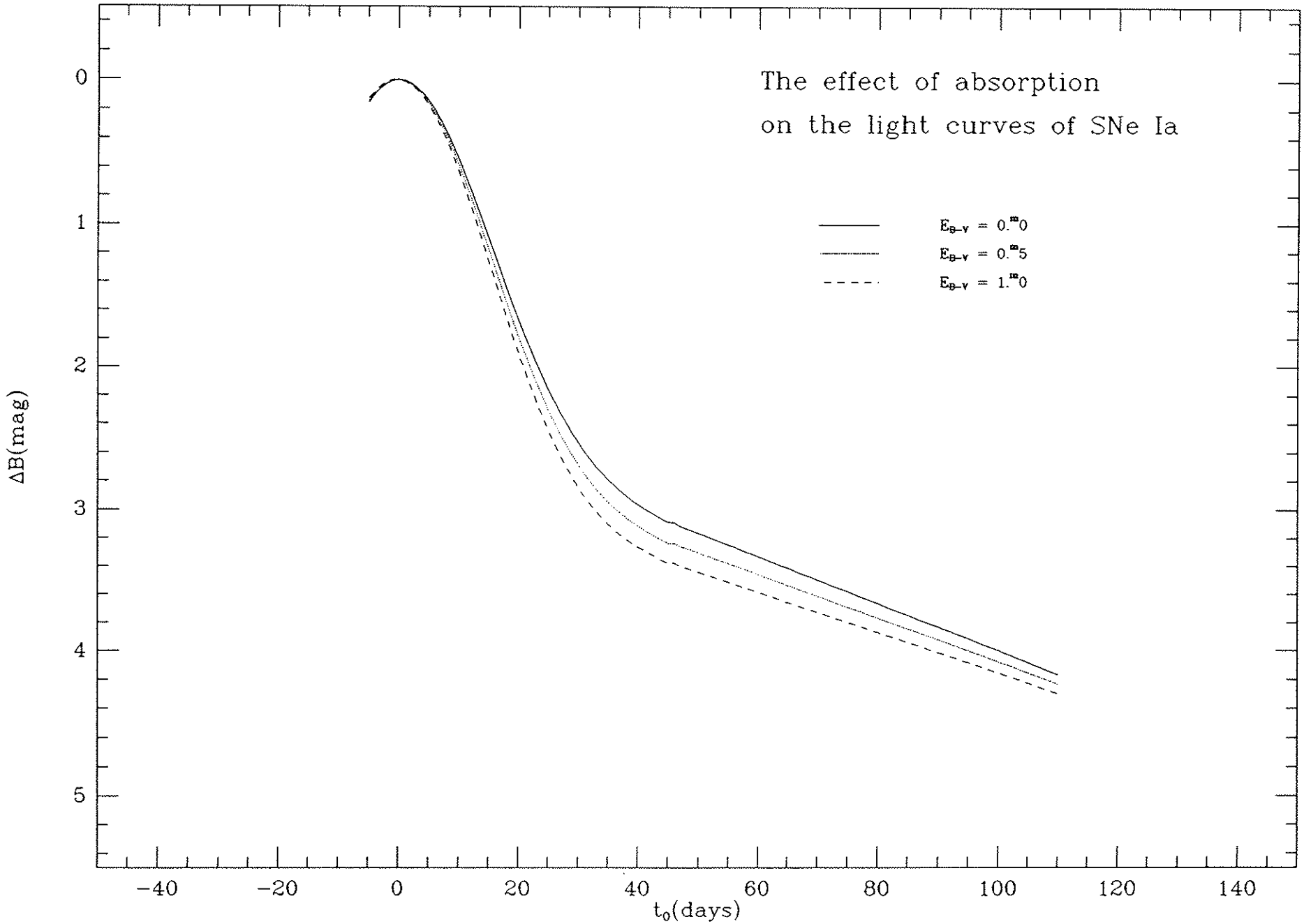
The effect of absorption
on the light curves of SNe Ia
E_{B-V} = 0.^{m}0
E_{B-V} = 0.^{m}5
E_{B-V} = 1.^{m}0
ΔB(mag)
0
1
2
3
4
5
−40
−20
0
20
40
60
80
100
120
140
t_0(days)

Figure 15

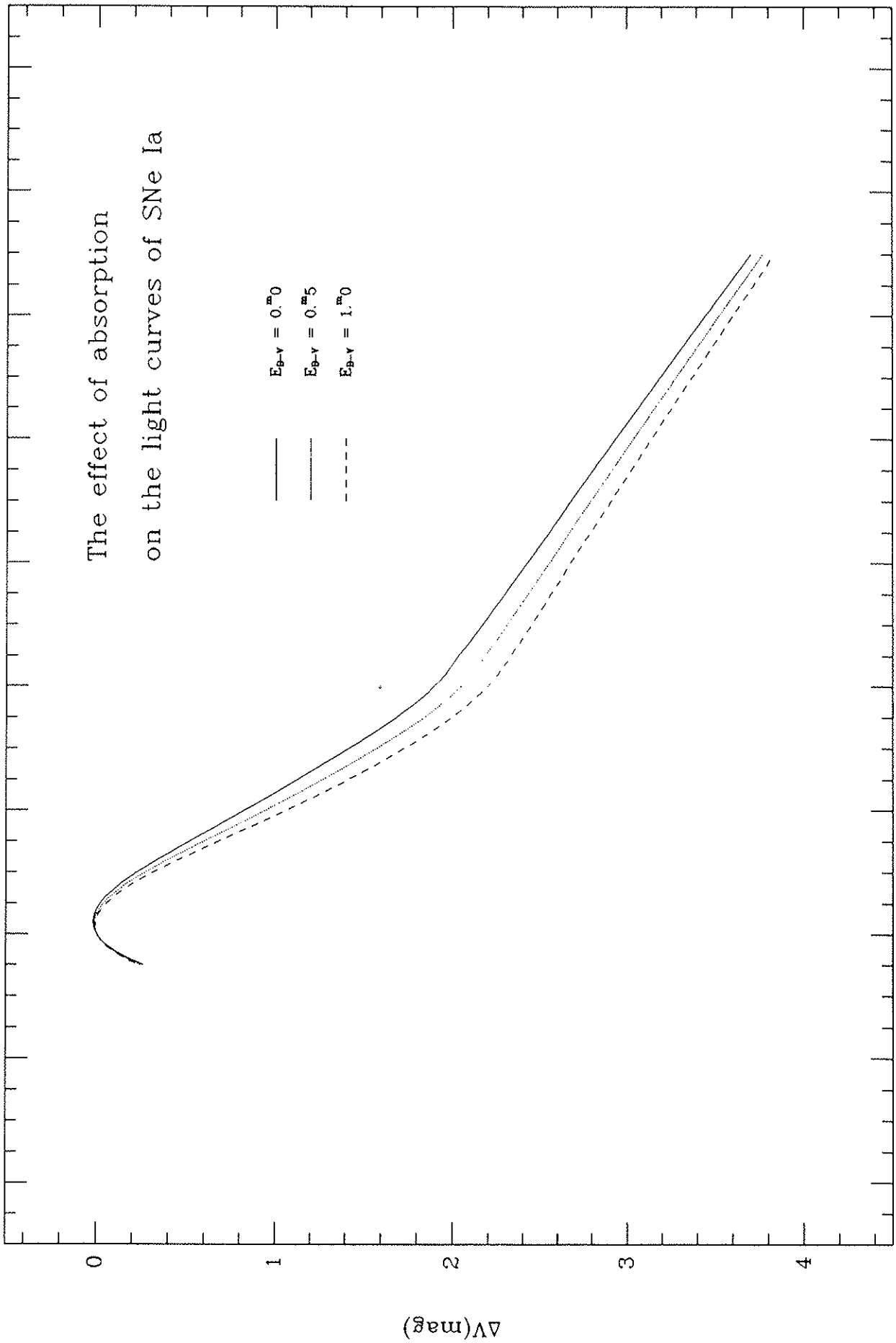
The effect of absorption
on the light curves of SNe Ia
$E_{B-V} = 0.^m0$
$E_{B-V} = 0.^m5$
$E_{B-V} = 1.^m0$
ΔV(mag)
t_o(days)
0
1
2
3
4
-40
-20
0
20
40
60
80
100
120
140

Figure 16

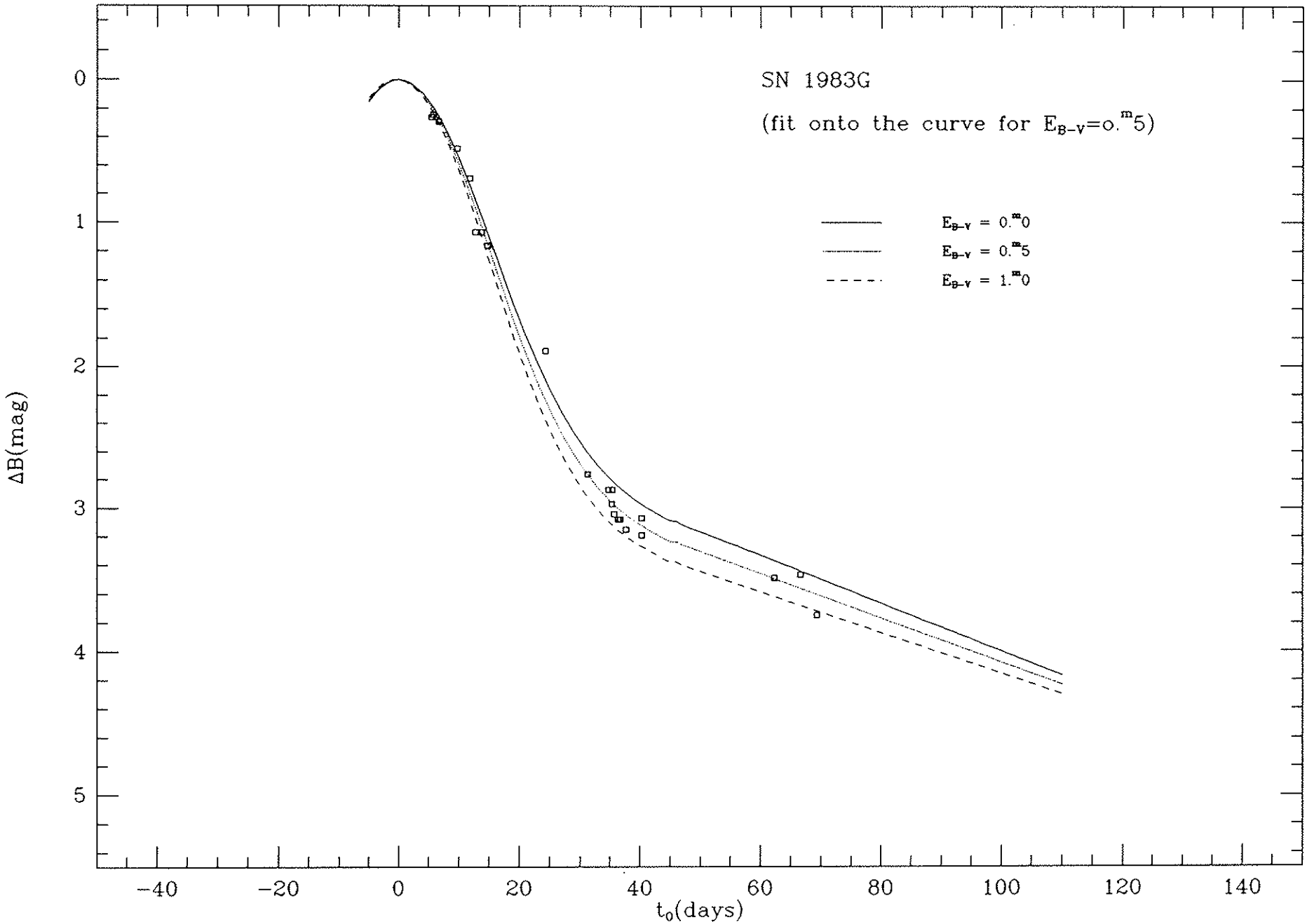
SN 1983G
(fit onto the curve for E_{B-V}=o.^{m}5)
E_{B-V} = 0.^{m}0
E_{B-V} = 0.^{m}5
E_{B-V} = 1.^{m}0
ΔB(mag)
0
1
2
3
4
5
-40
-20
0
20
40
60
80
100
120
140
t_0(days)

Figure 17

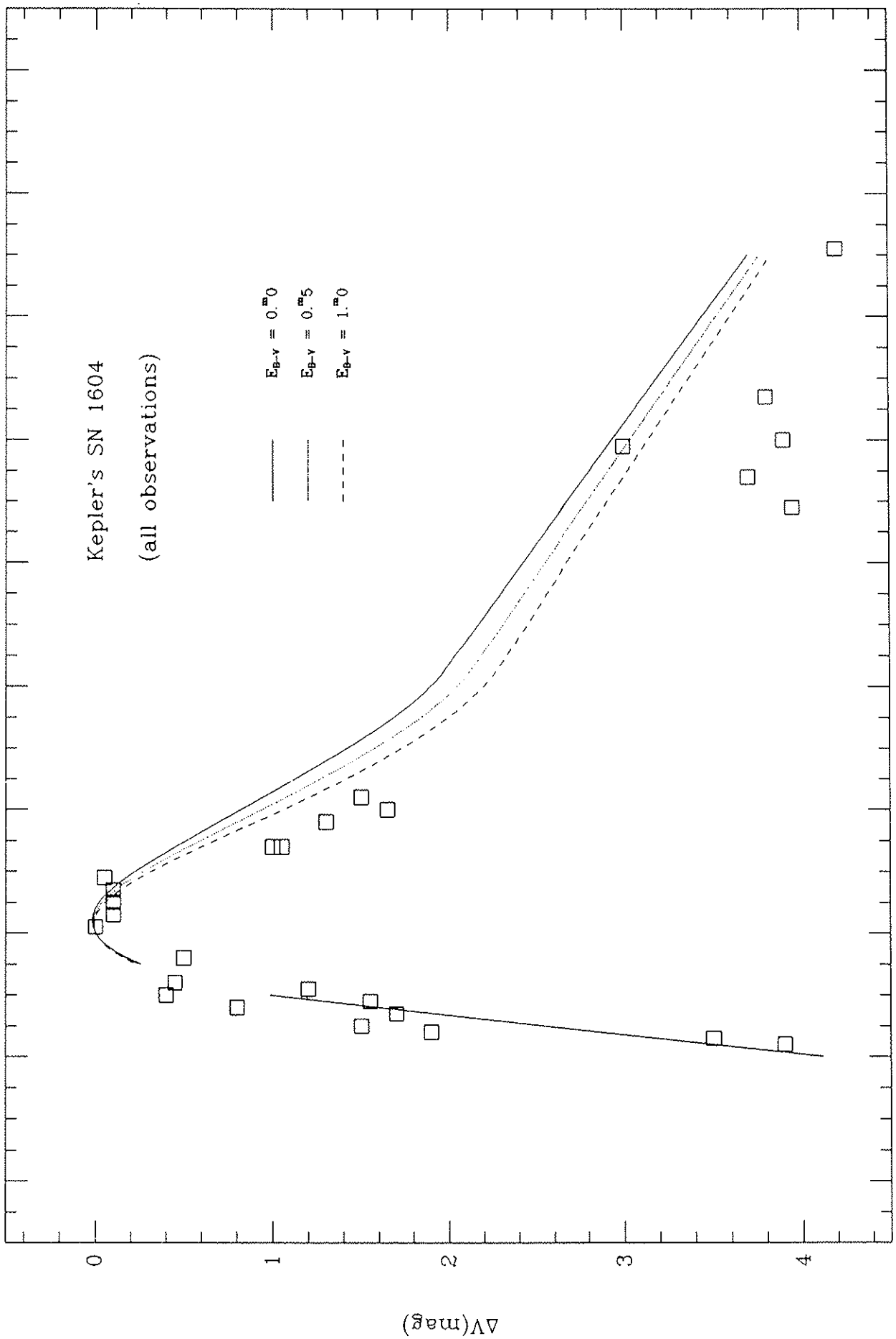
Kepler's SN 1604
(all observations)
$E_{B-V} = 0.^m0$
$E_{B-V} = 0.^m5$
$E_{B-V} = 1.^m0$
ΔV(mag)
t_0(days)
0
1
2
3
4
-40
-20
0
20
40
60
80
100
120
140

Figure 18

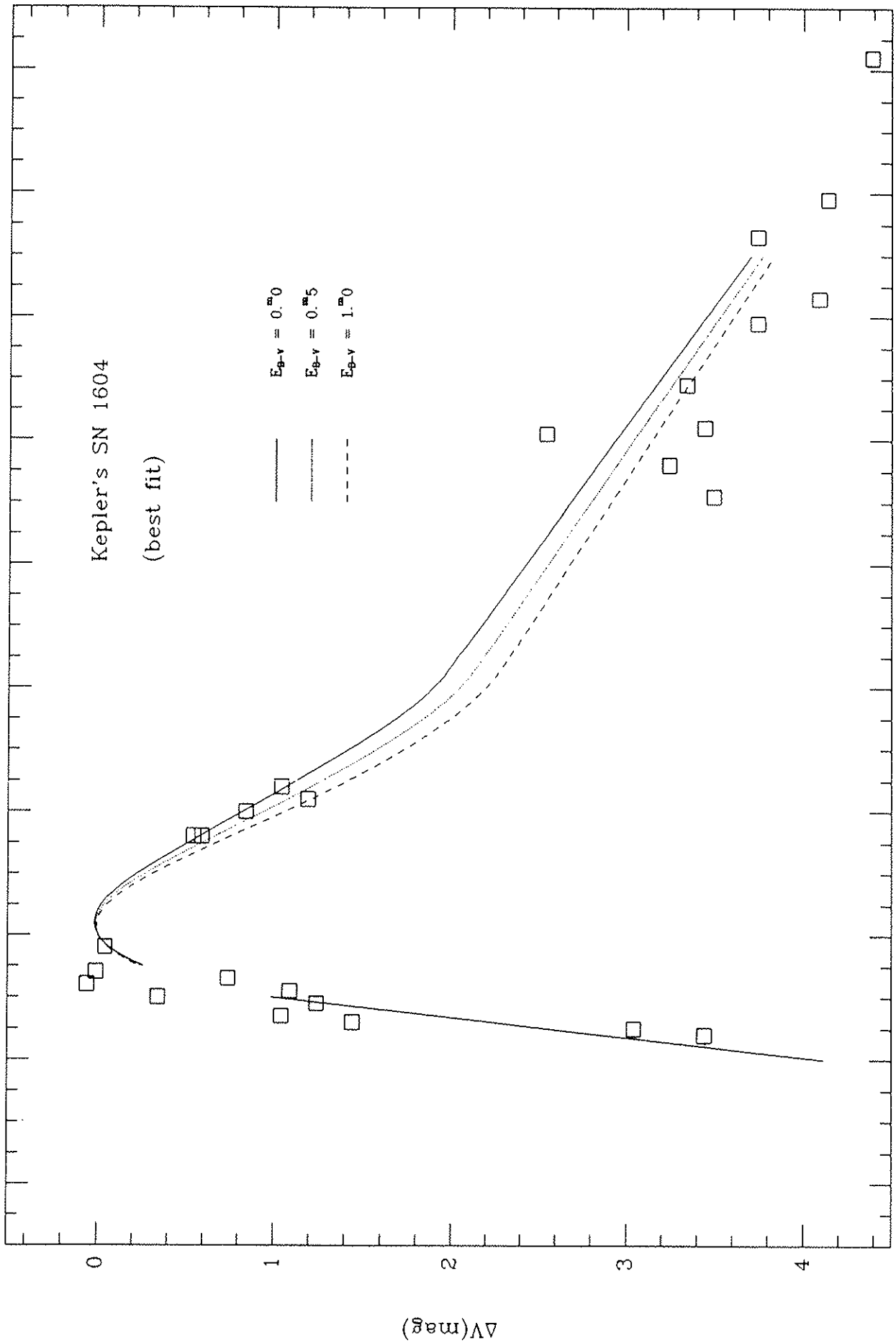
Kepler's SN 1604
(best fit)
$E_{B-V} = 0.^{m}0$
$E_{B-V} = 0.^{m}5$
$E_{B-V} = 1.^{m}0$
t_o(days)
ΔV(mag)

Figure 19

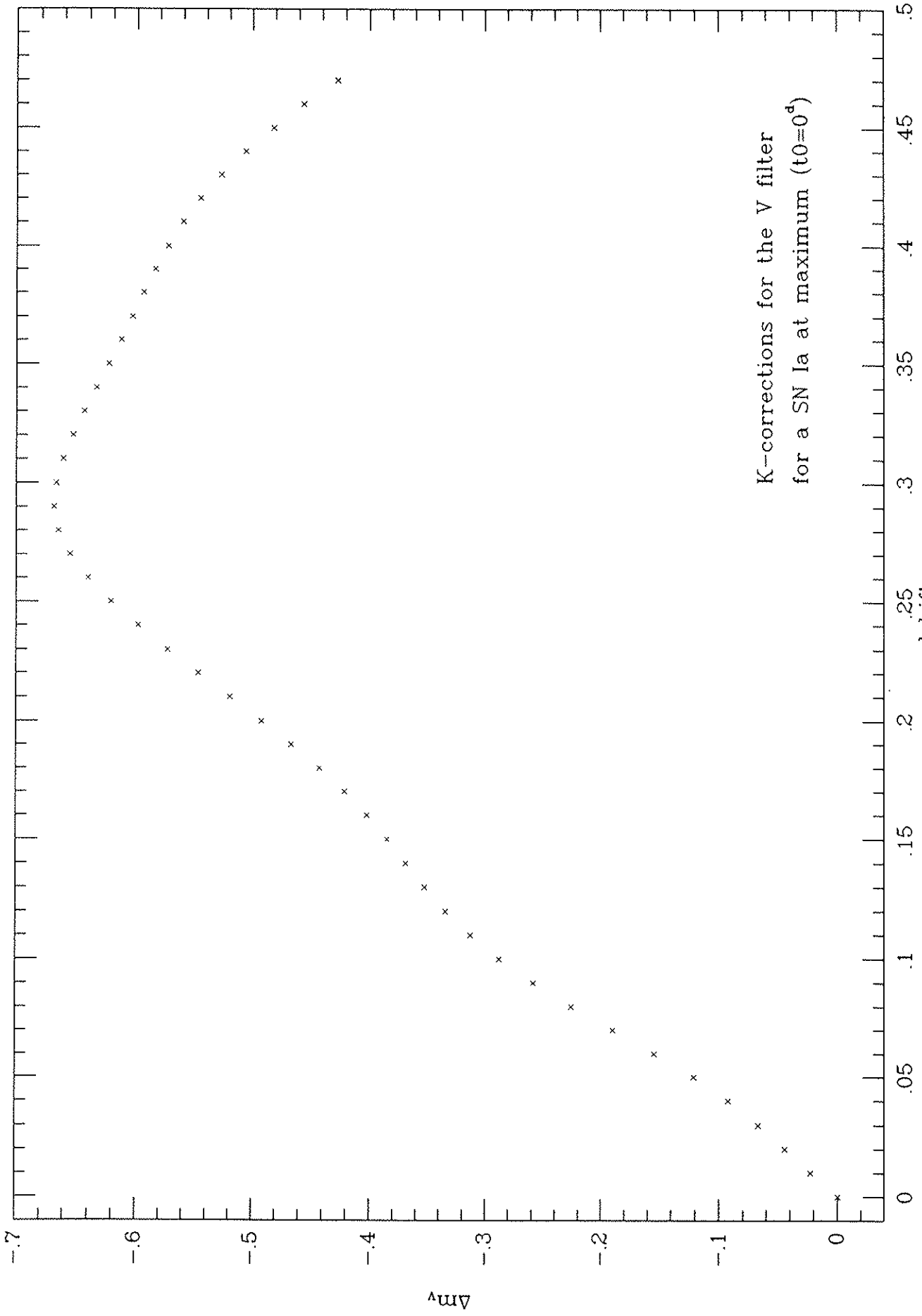
K-corrections for the V filter
for a SN Ia at maximum (t0=0d)
Δmv
redshift z
0
-.1
-.2
-.3
-.4
-.5
-.6
-.7
.05
.1
.15
.2
.25
.3
.35
.4
.45
.5

Figure 20

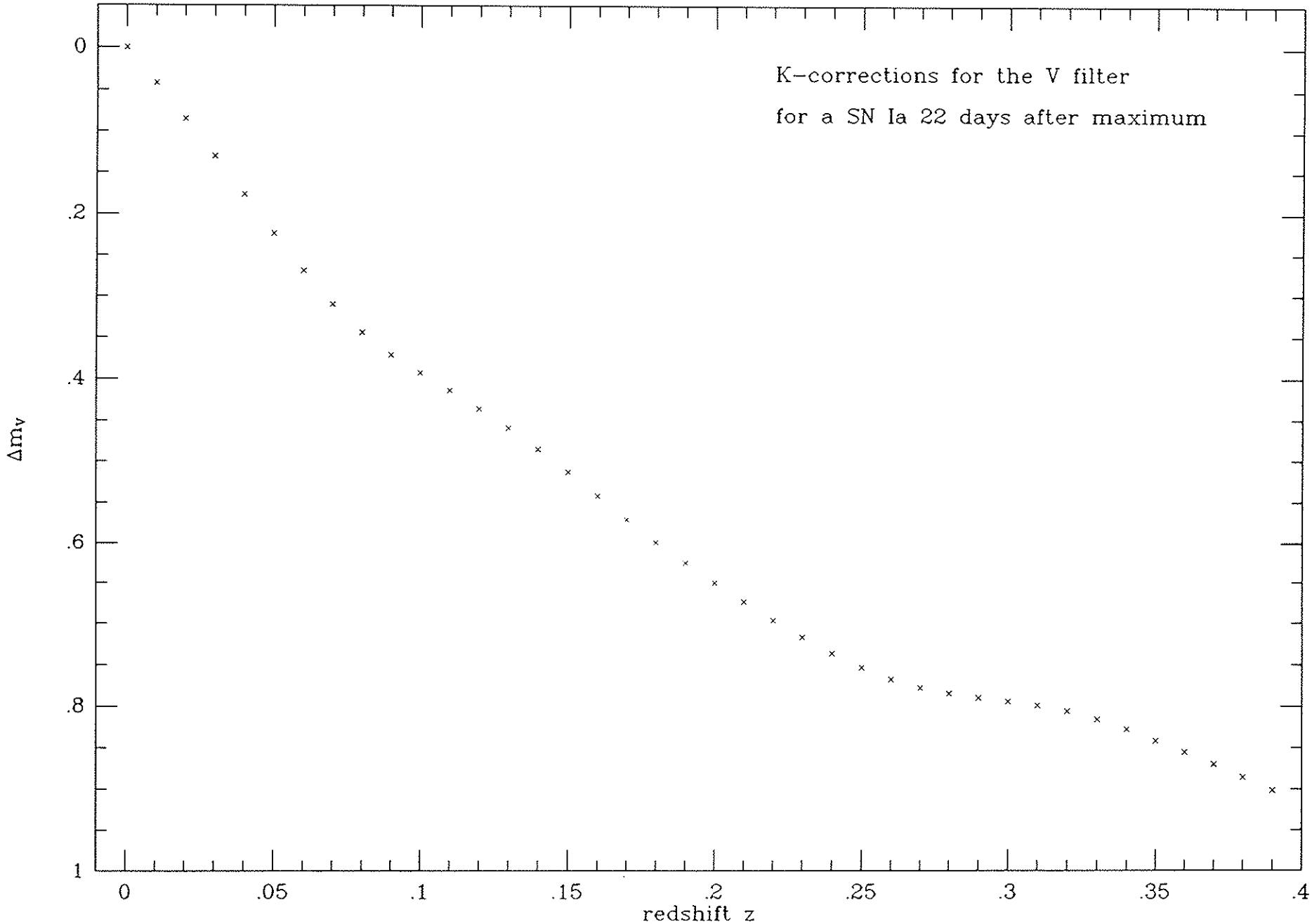
K-corrections for the V filter
for a SN Ia 22 days after maximum
Δm_V
0
.2
.4
.6
.8
1
0
.05
.1
.15
.2
.25
.3
.35
.4
redshift z

Figure 21

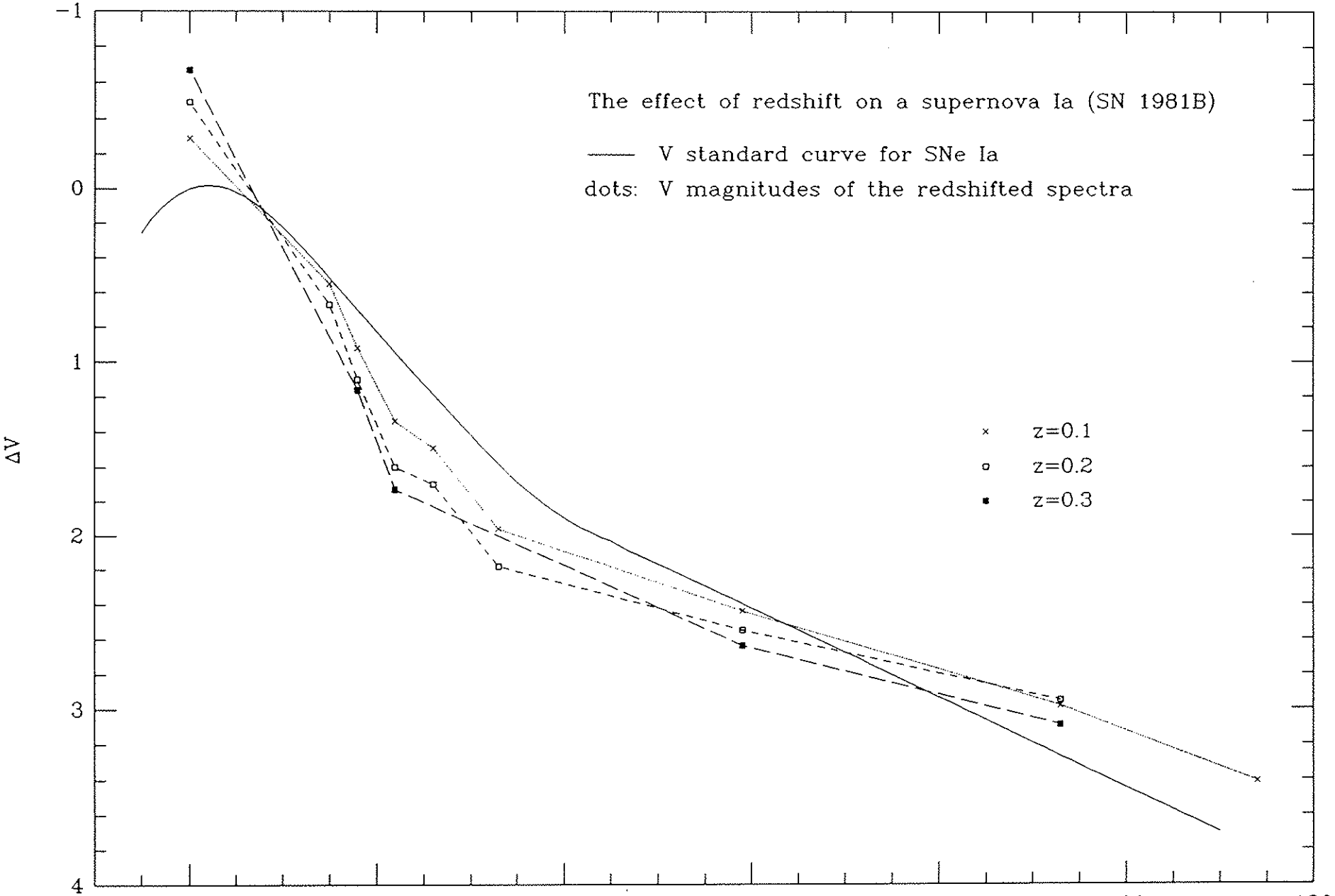
The effect of redshift on a supernova Ia (SN 1981B)
—— V standard curve for SNe Ia
dots: V magnitudes of the redshifted spectra
z=0.1
z=0.2
z=0.3
ΔV
−1
0
1
2
3
4
0
20
40
60
80
100
120
t_0(days)

Figure 22

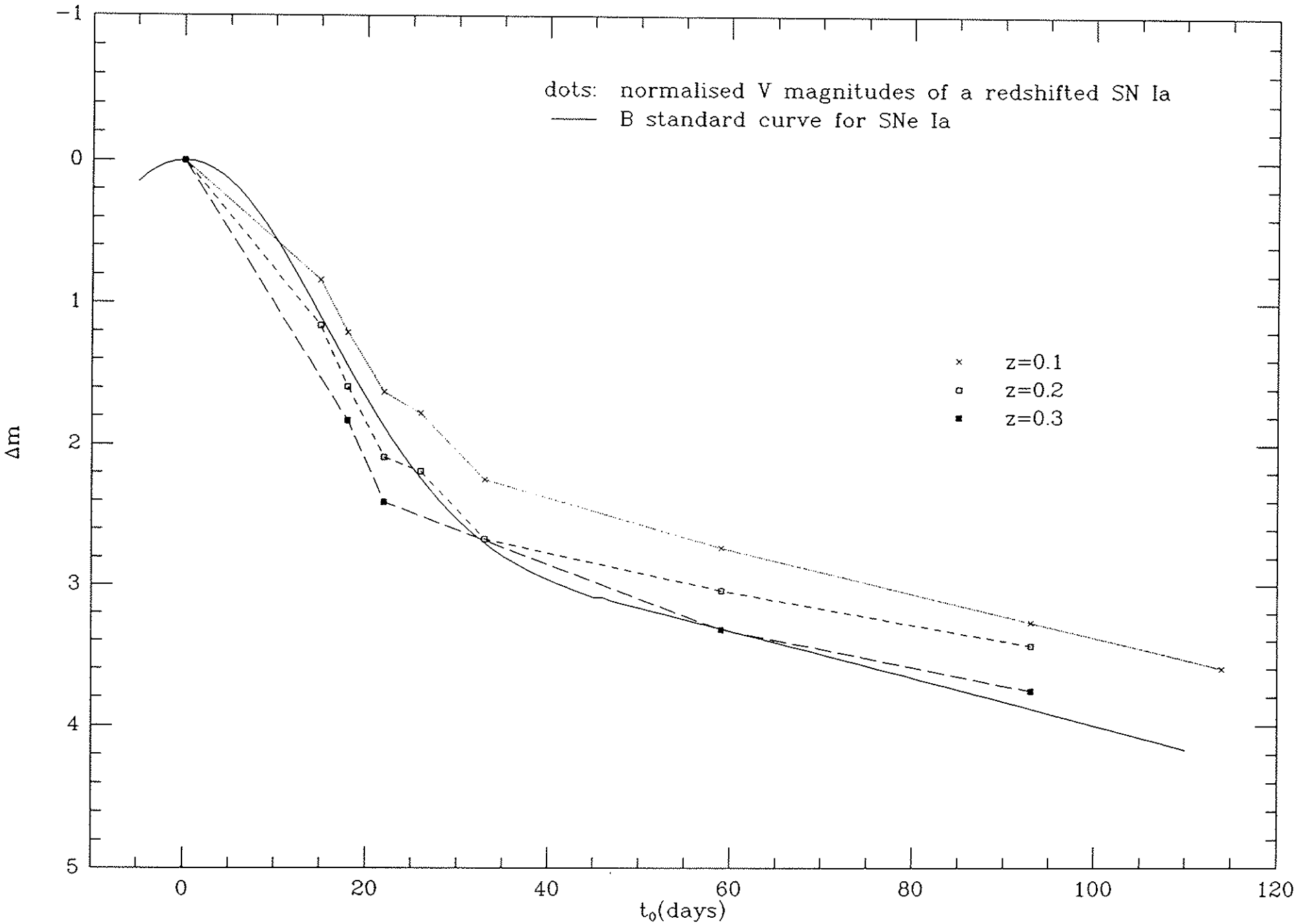
dots: normalised V magnitudes of a redshifted SN Ia
B standard curve for SNe Ia
z=0.1
z=0.2
z=0.3
Δm
−1
0
1
2
3
4
5
0
20
40
60
80
100
120
t_0(days)

Figure 23

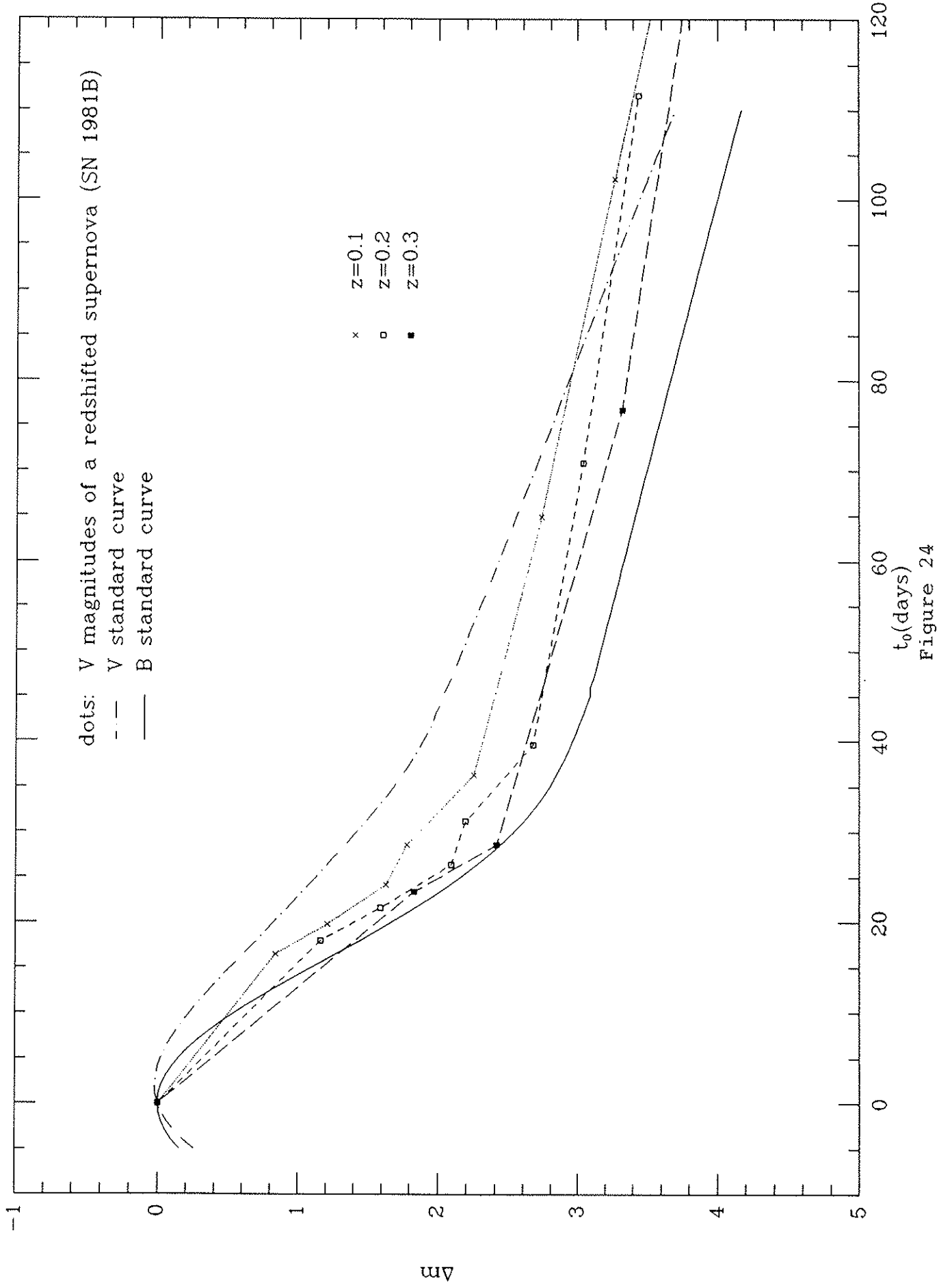
dots: V magnitudes of a redshifted supernova (SN 1981B)
V standard curve
B standard curve
z=0.1
z=0.2
z=0.3
Δm
t_o(days)
−1
0
1
2
3
4
5
0
20
40
60
80
100
120

Figure 24

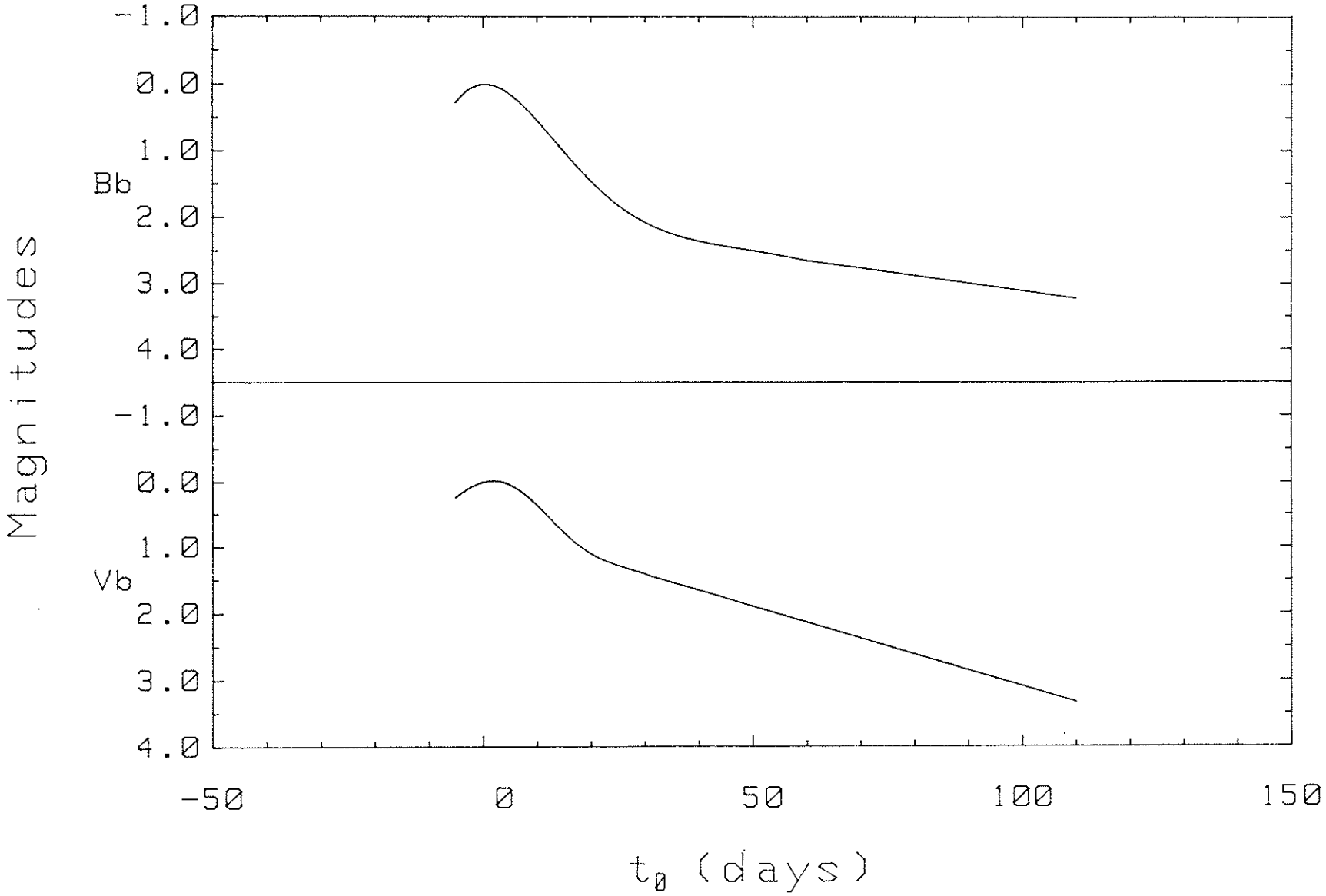

Figure 25

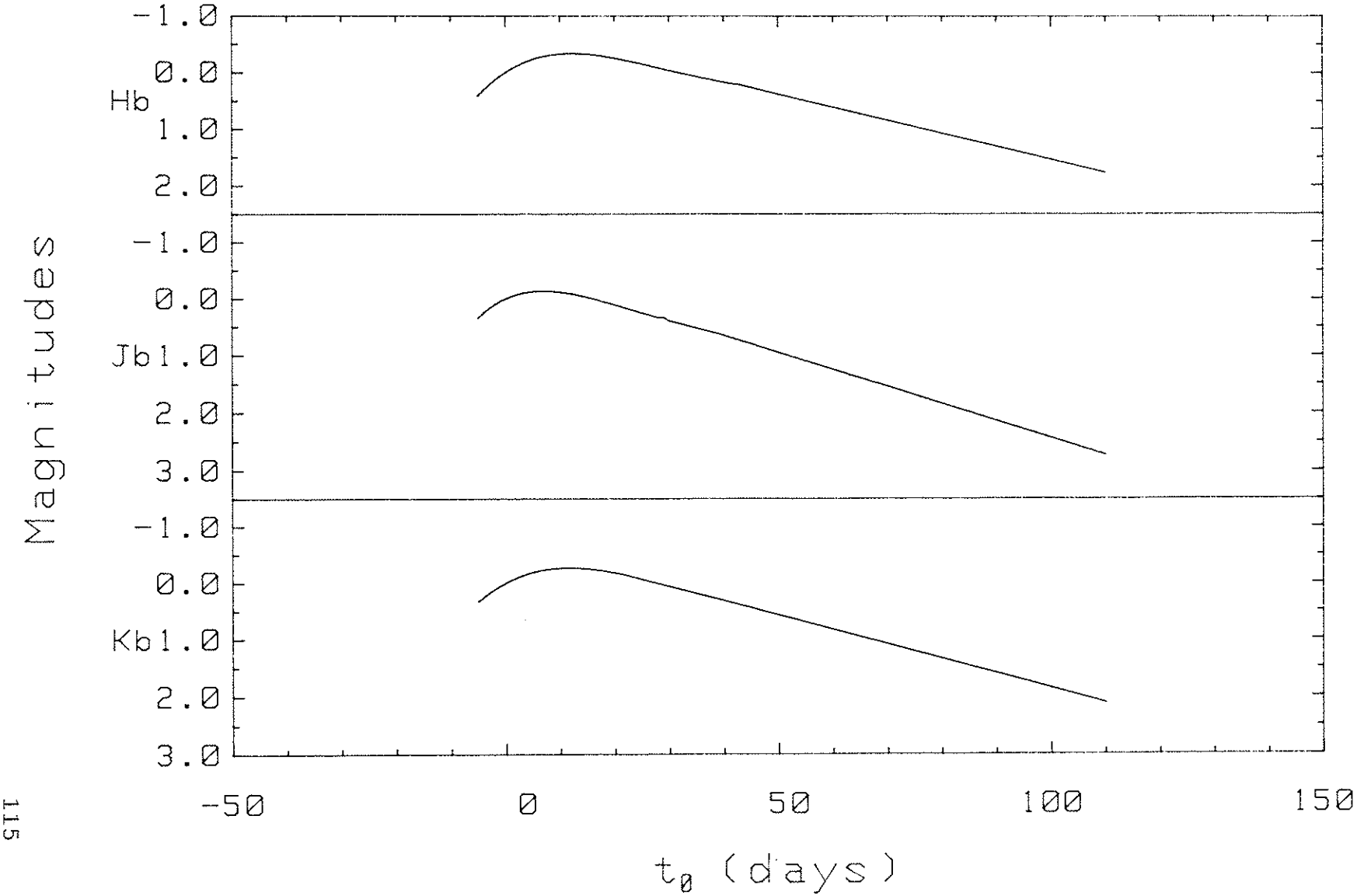

Figure 26

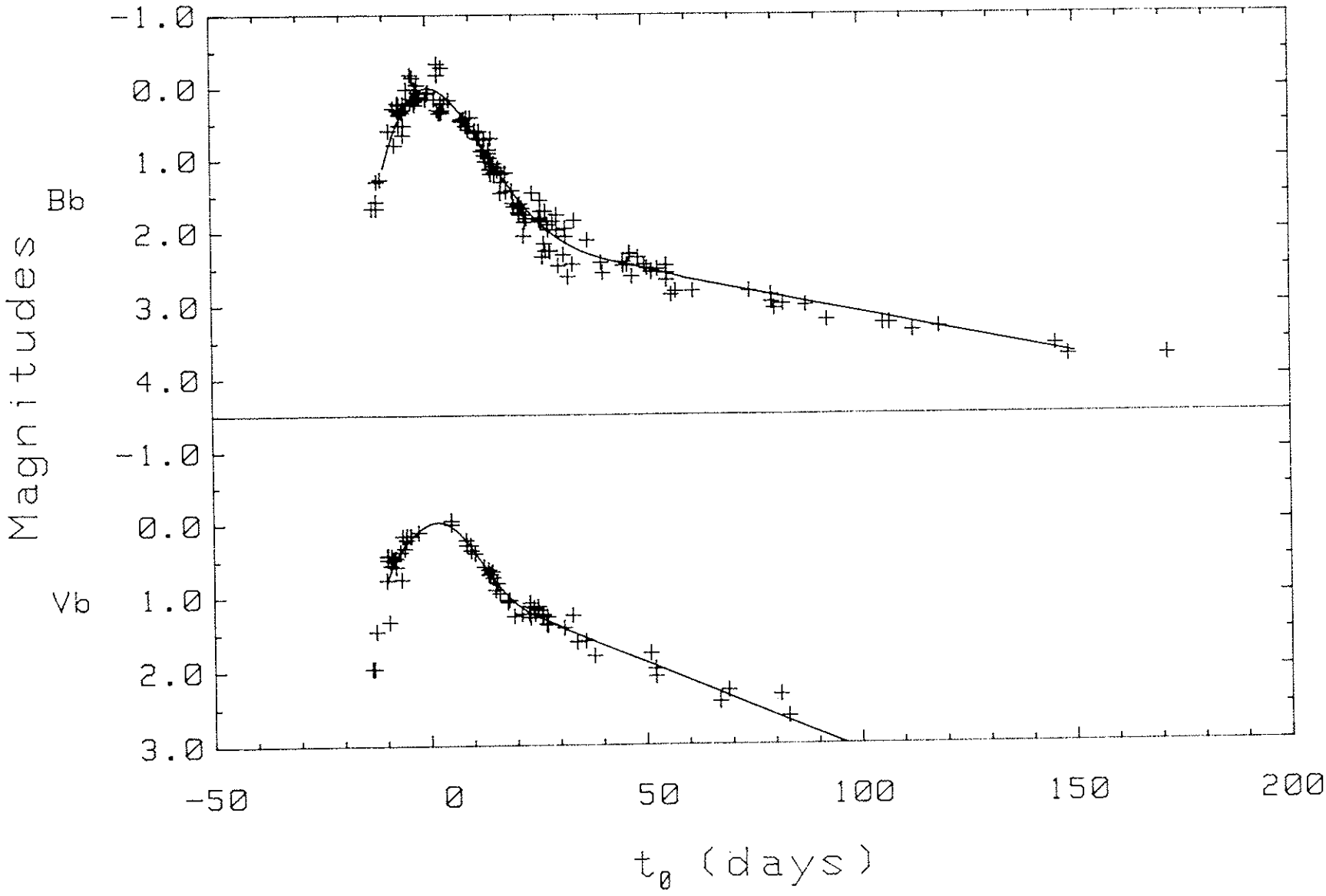
Magnitudes
Bb
Vb
-1.0
0.0
1.0
2.0
3.0
4.0
-1.0
0.0
1.0
2.0
3.0
-50
0
50
100
150
200
t_0 (days)

Figure 27

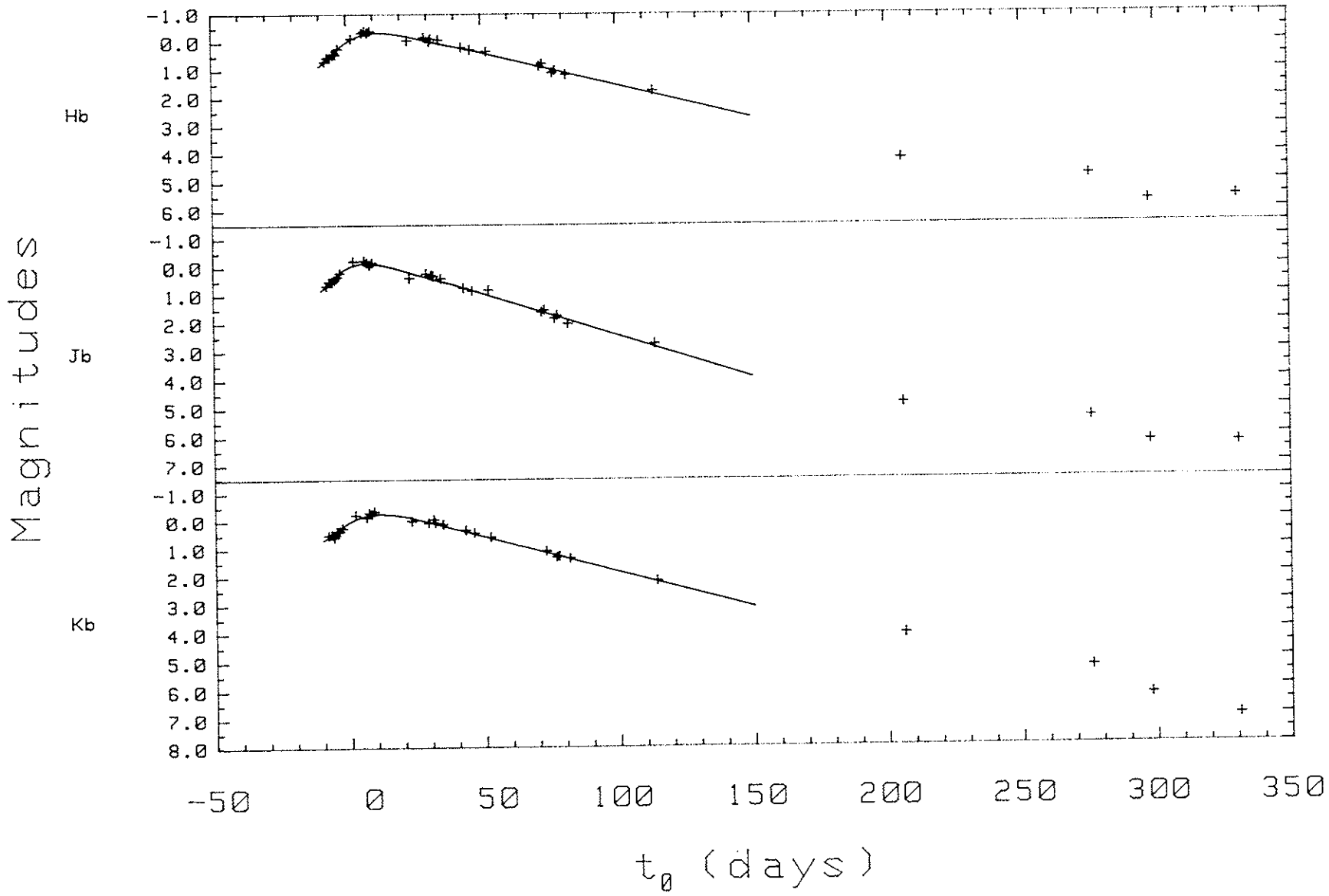
Magnitudes
Hb
Jb
Kb
-1.0
0.0
1.0
2.0
3.0
4.0
5.0
6.0
7.0
8.0
-50
0
50
100
150
200
250
300
350
t_0 (days)

Figure 28

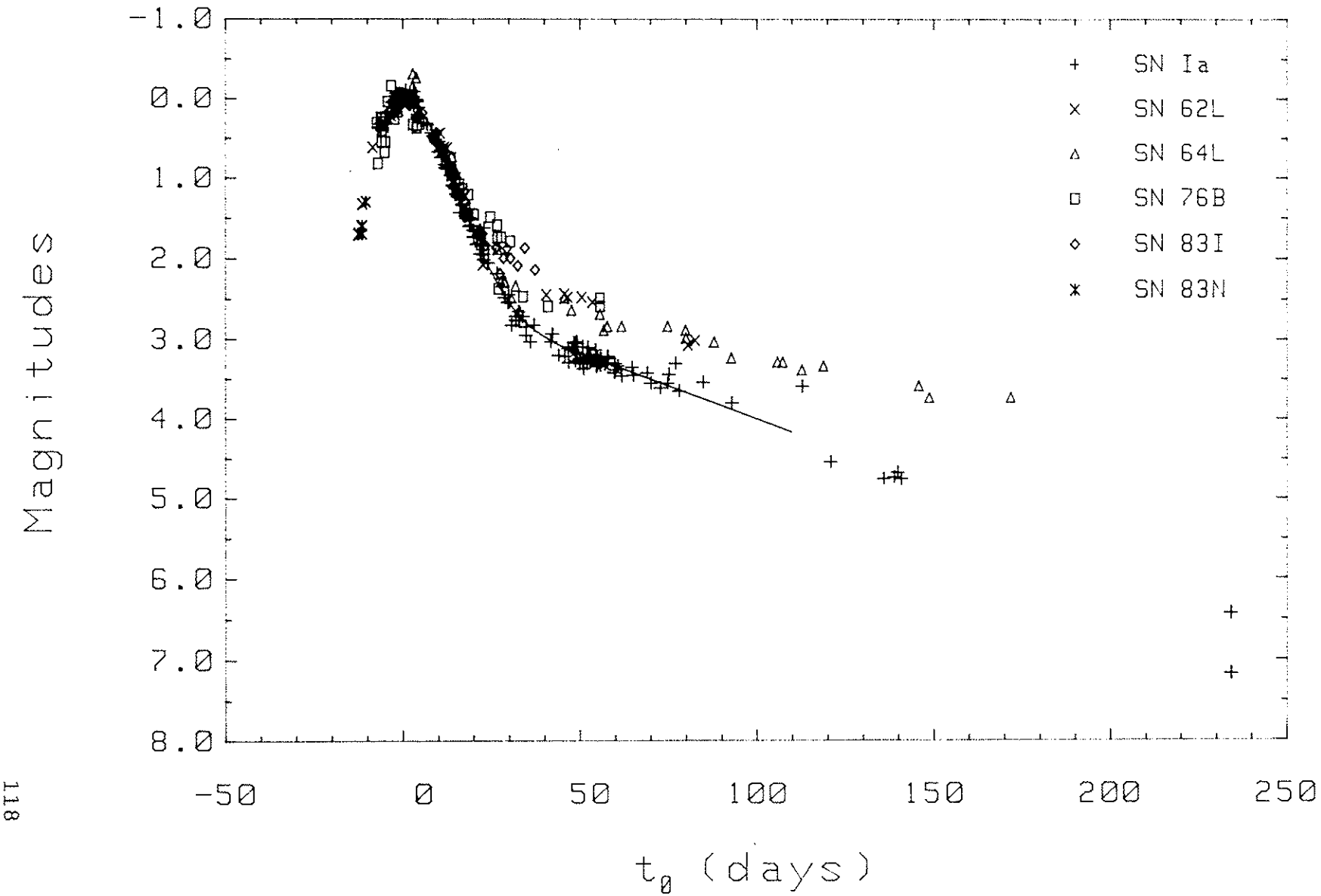
-1.0
0.0
1.0
2.0
3.0
4.0
5.0
6.0
7.0
8.0
Magnitudes
-50
0
50
100
150
200
250
t_0 (days)
SN Ia
SN 62L
SN 64L
SN 76B
SN 83I
SN 83N

Figure 29

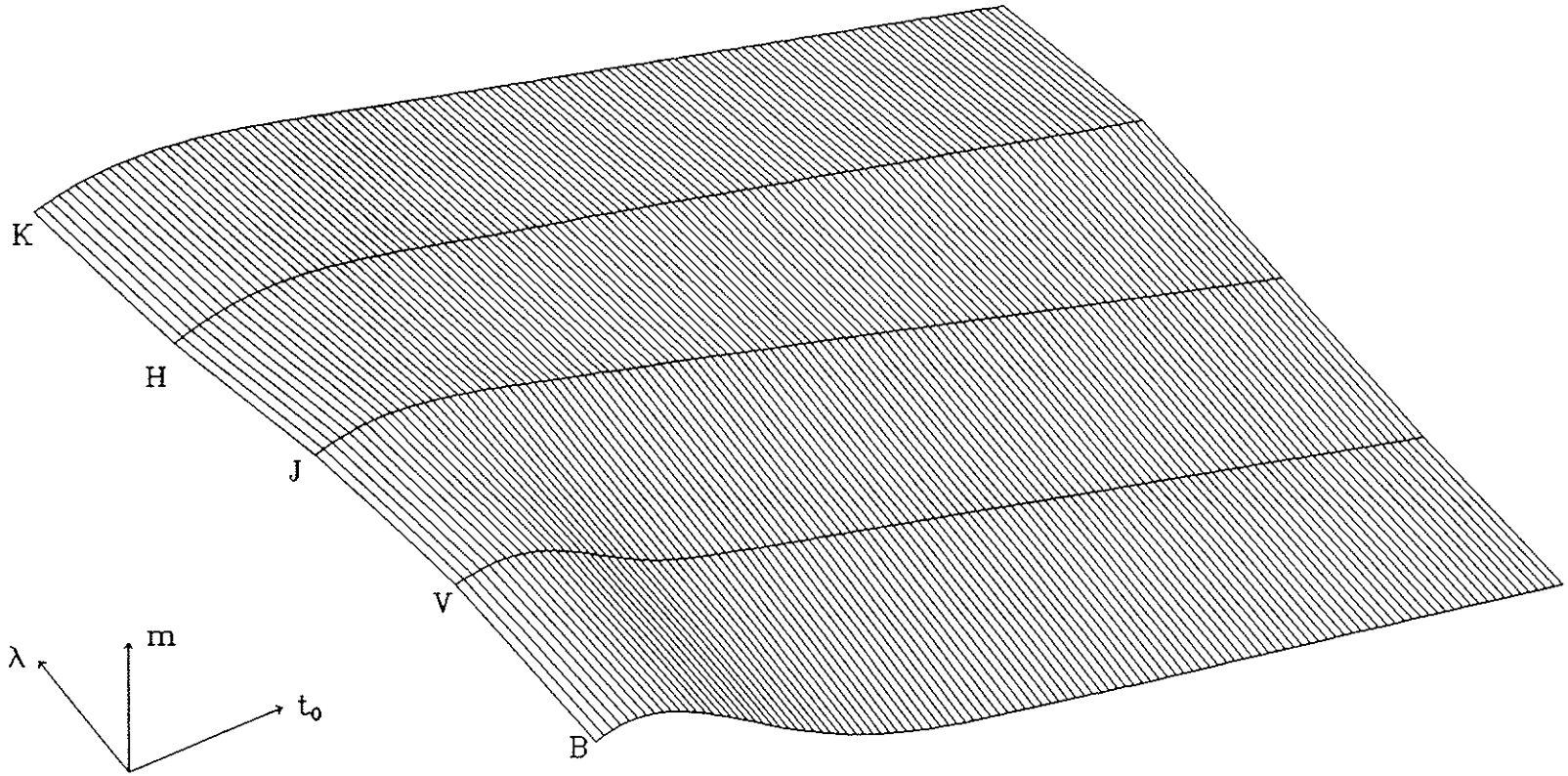

Figure 30

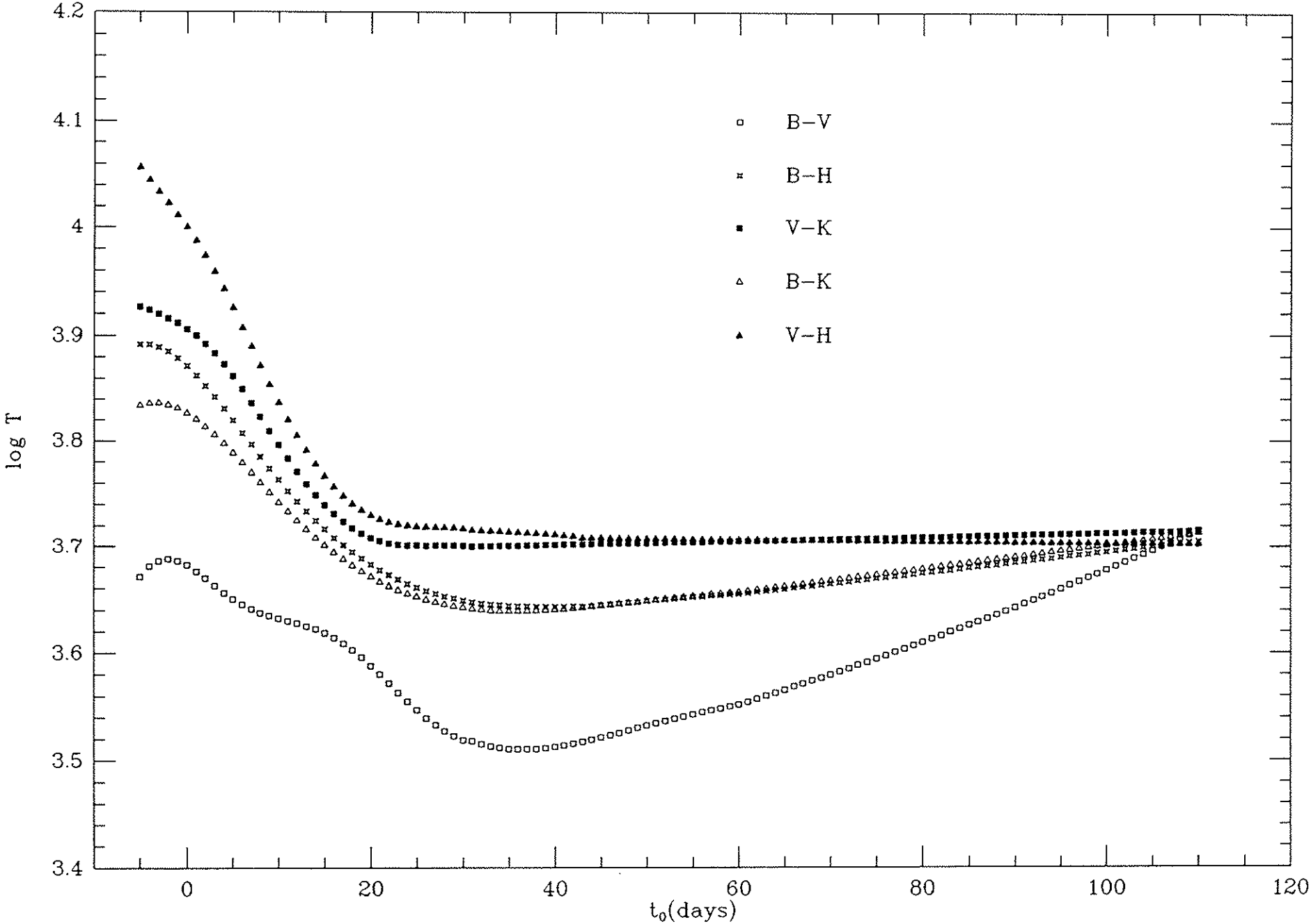
4.2
4.1
4
3.9
3.8
3.7
3.6
3.5
3.4
log T
B−V
B−H
V−K
B−K
V−H
0
20
40
60
80
100
120
t_0(days)

Figure 31

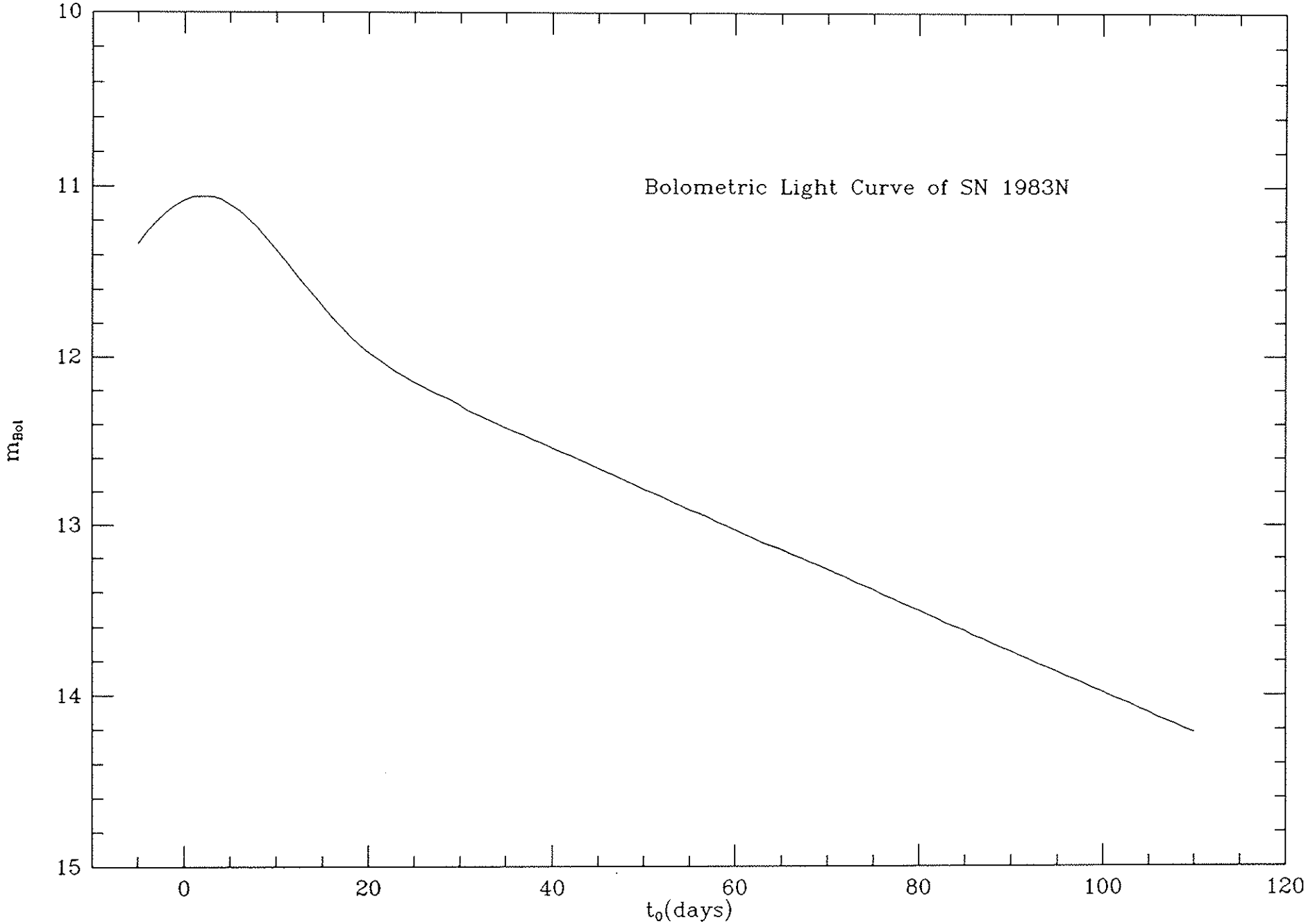
Bolometric Light Curve of SN 1983N
10
11
12
13
14
15
m_{Bol}
0
20
40
60
80
100
120
t_0(days)

Figure 32

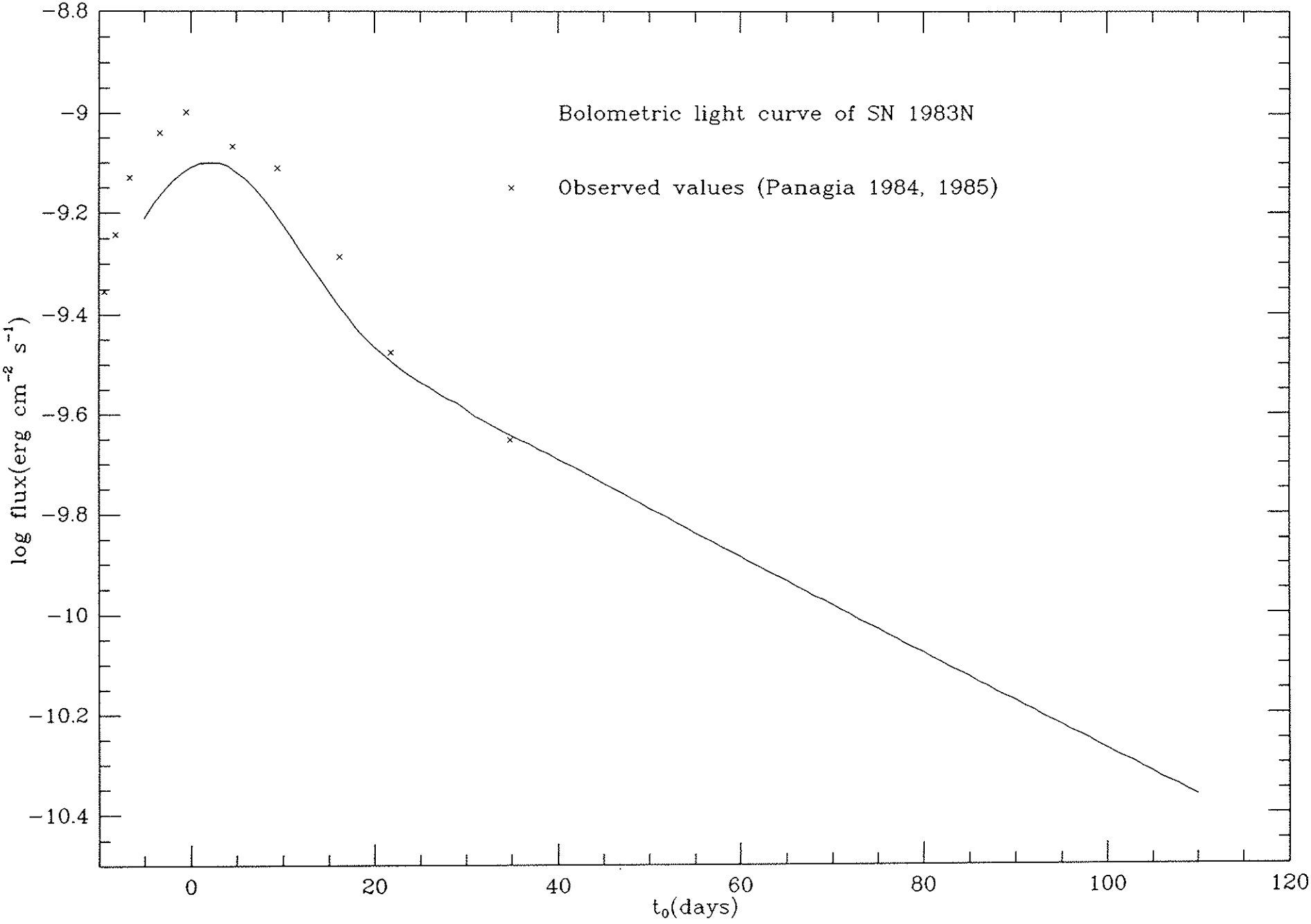
Bolometric light curve of SN 1983N
Observed values (Panagia 1984, 1985)
log flux(erg cm^{-2} s^{-1})
−8.8
−9
−9.2
−9.4
−9.6
−9.8
−10
−10.2
−10.4
0
20
40
60
80
100
120
t_0(days)

Figure 33

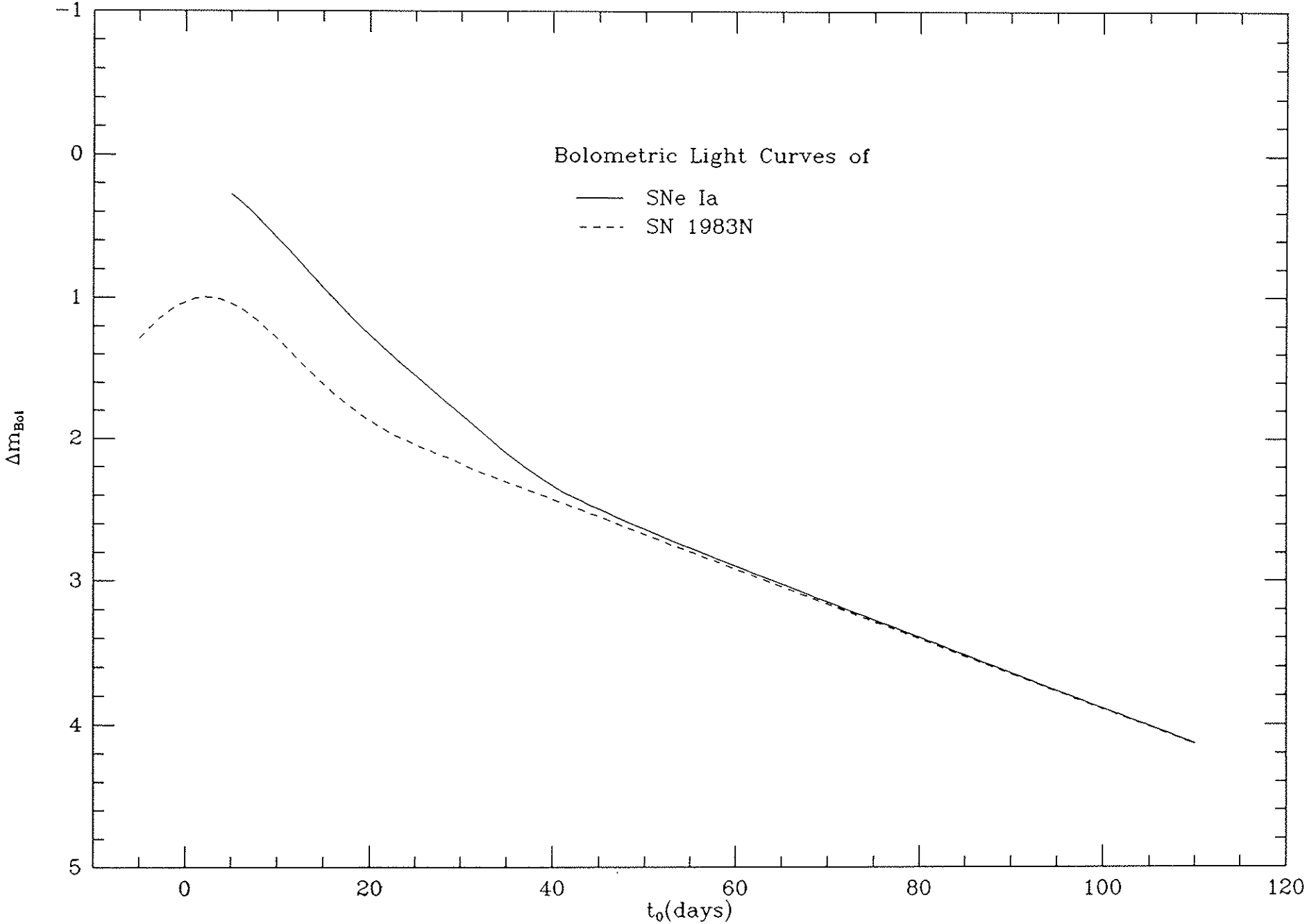
Bolometric Light Curves of
SNe Ia
SN 1983N
Δm_{Bol}
t_0(days)
−1
0
1
2
3
4
5
0
20
40
60
80
100
120

Figure 34

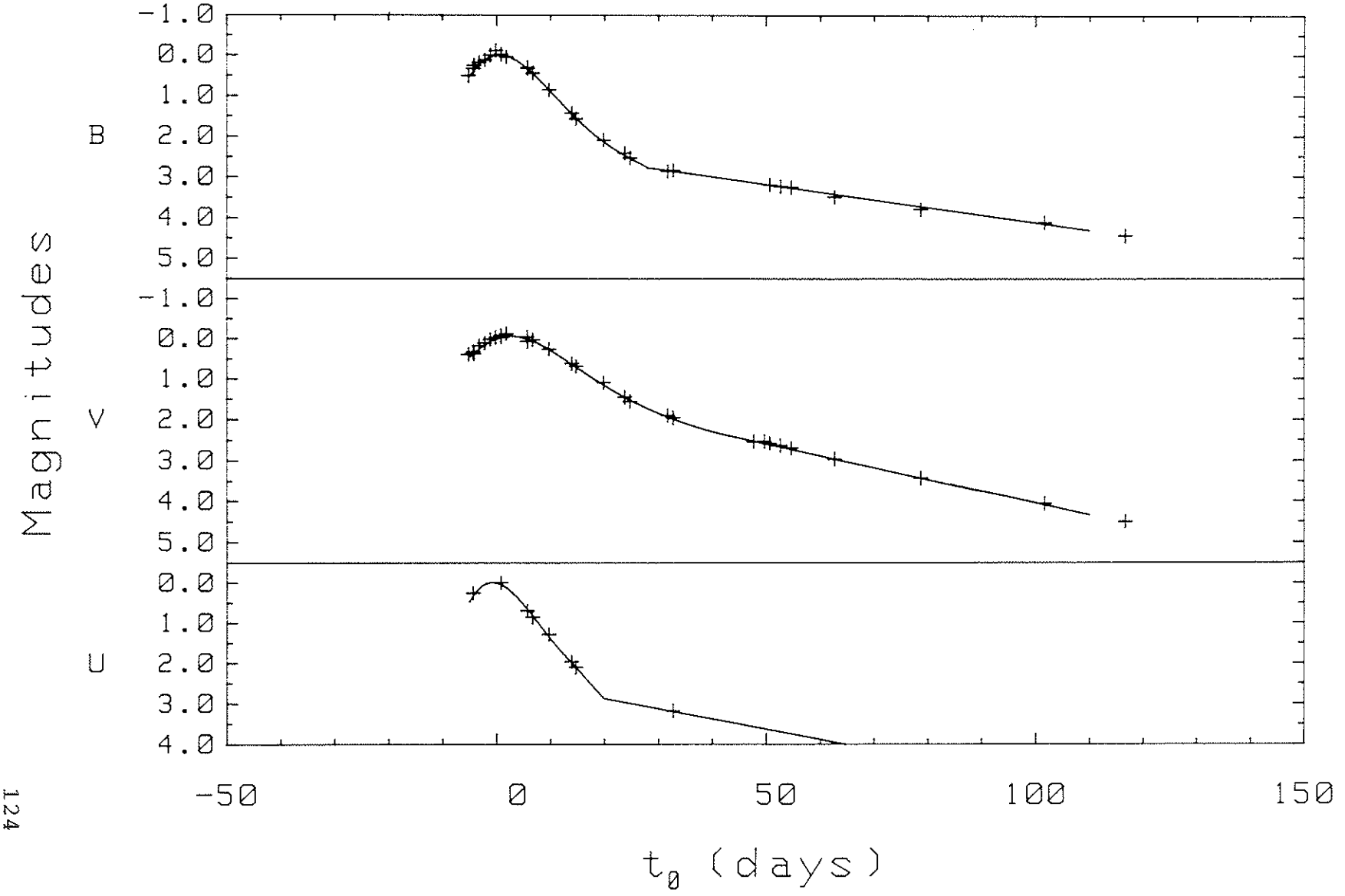

Figure 35

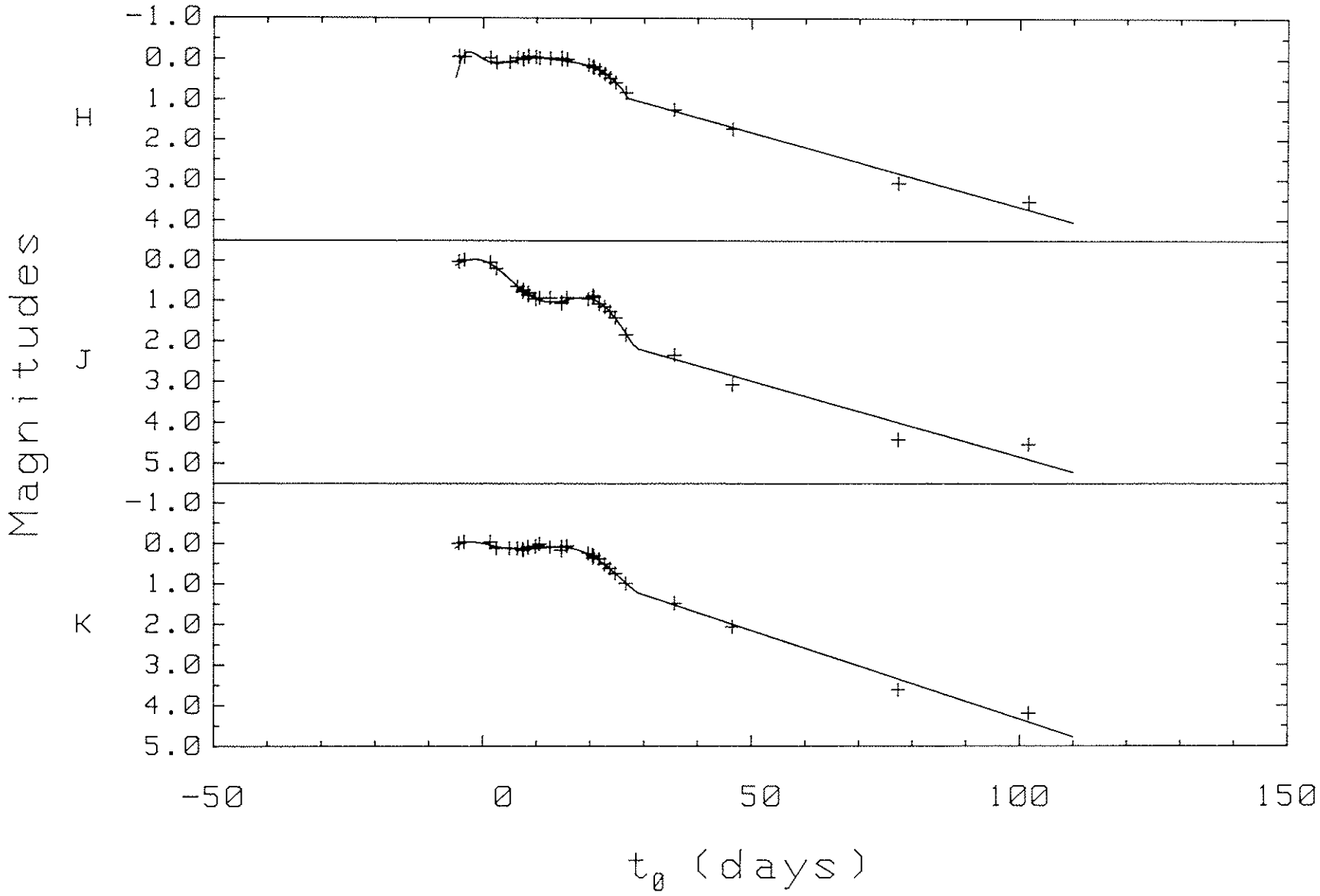

Figure 36

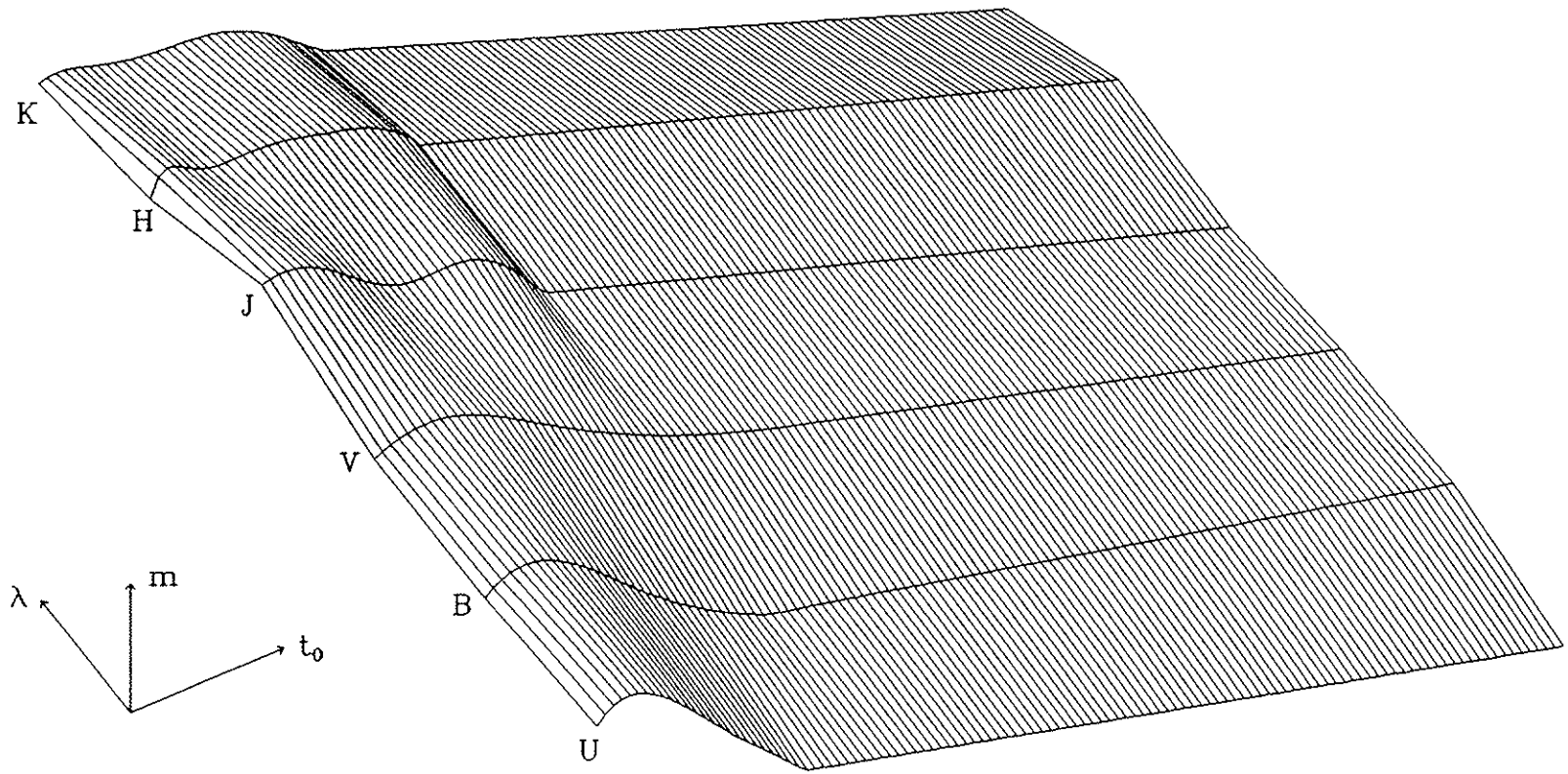

Figure 37

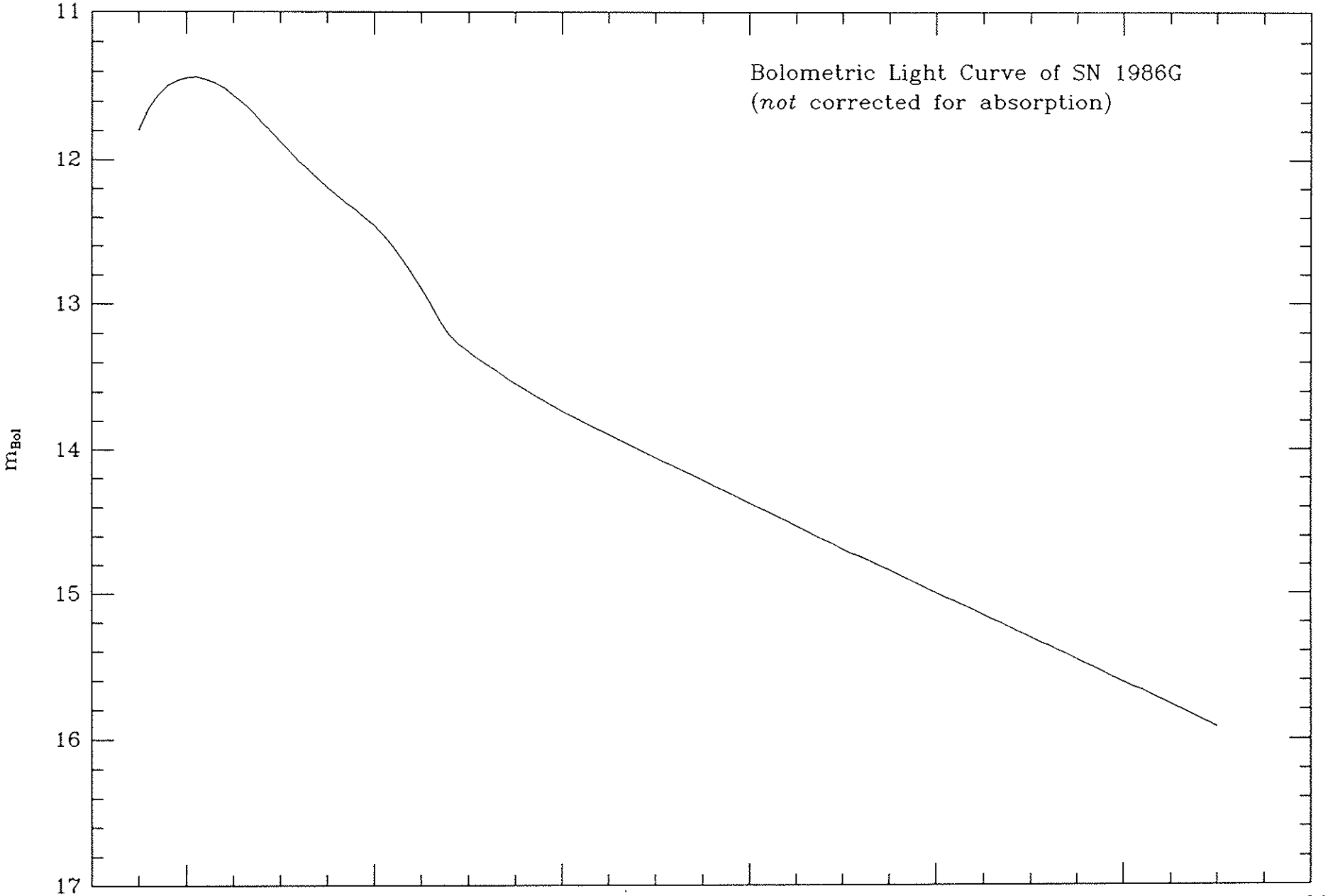
Bolometric Light Curve of SN 1986G
(*not* corrected for absorption)
m_{Bol}
11
12
13
14
15
16
17
0
20
40
60
80
100
120
t_0(days)

Figure 38

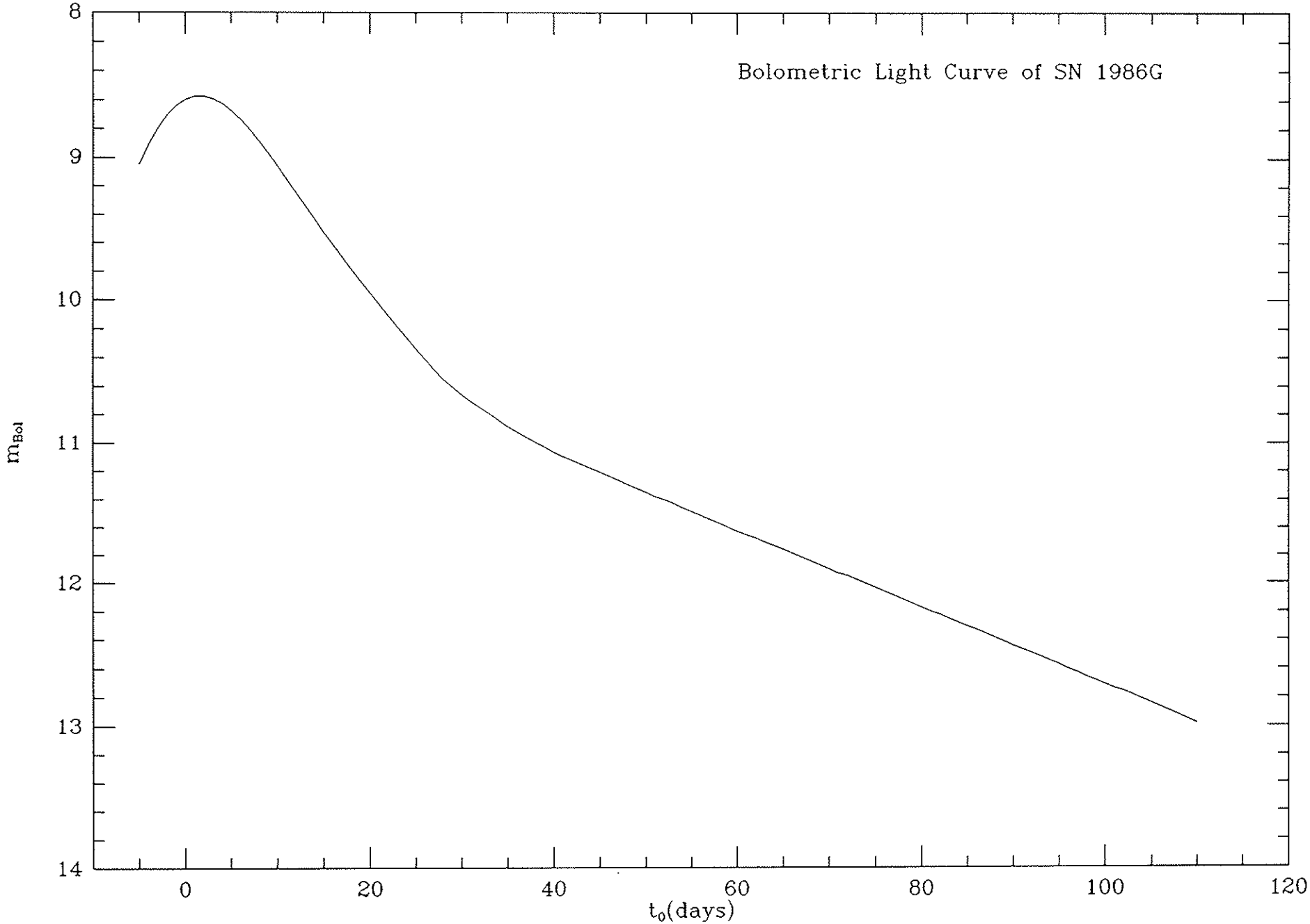
Bolometric Light Curve of SN 1986G
8
9
10
11
12
13
14
m_{Bol}
0
20
40
60
80
100
120
t_0(days)

Figure 39

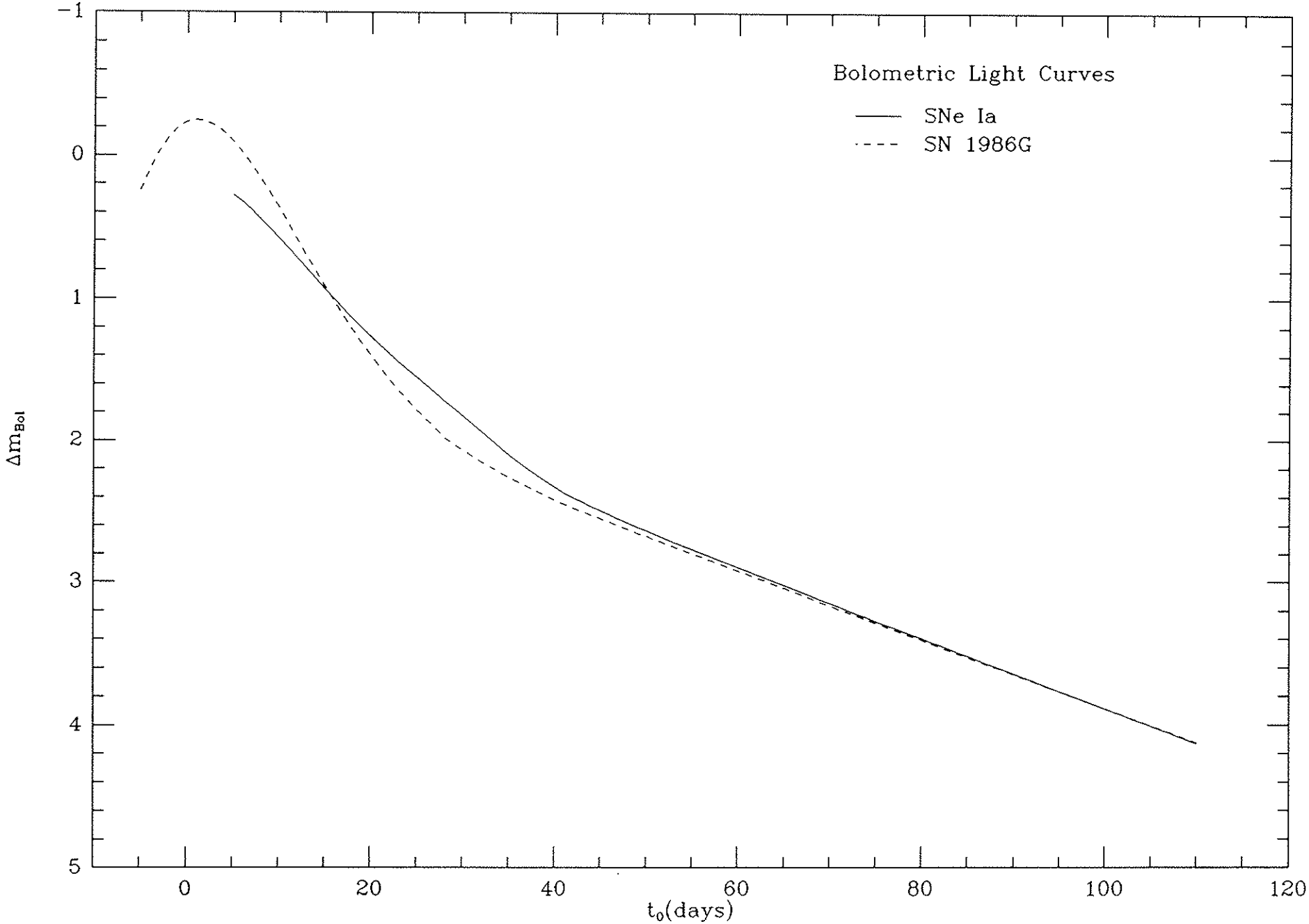
Bolometric Light Curves
SNe Ia
SN 1986G
Δm_{Bol}
t_0(days)
−1
0
1
2
3
4
5
0
20
40
60
80
100
120

Figure 40

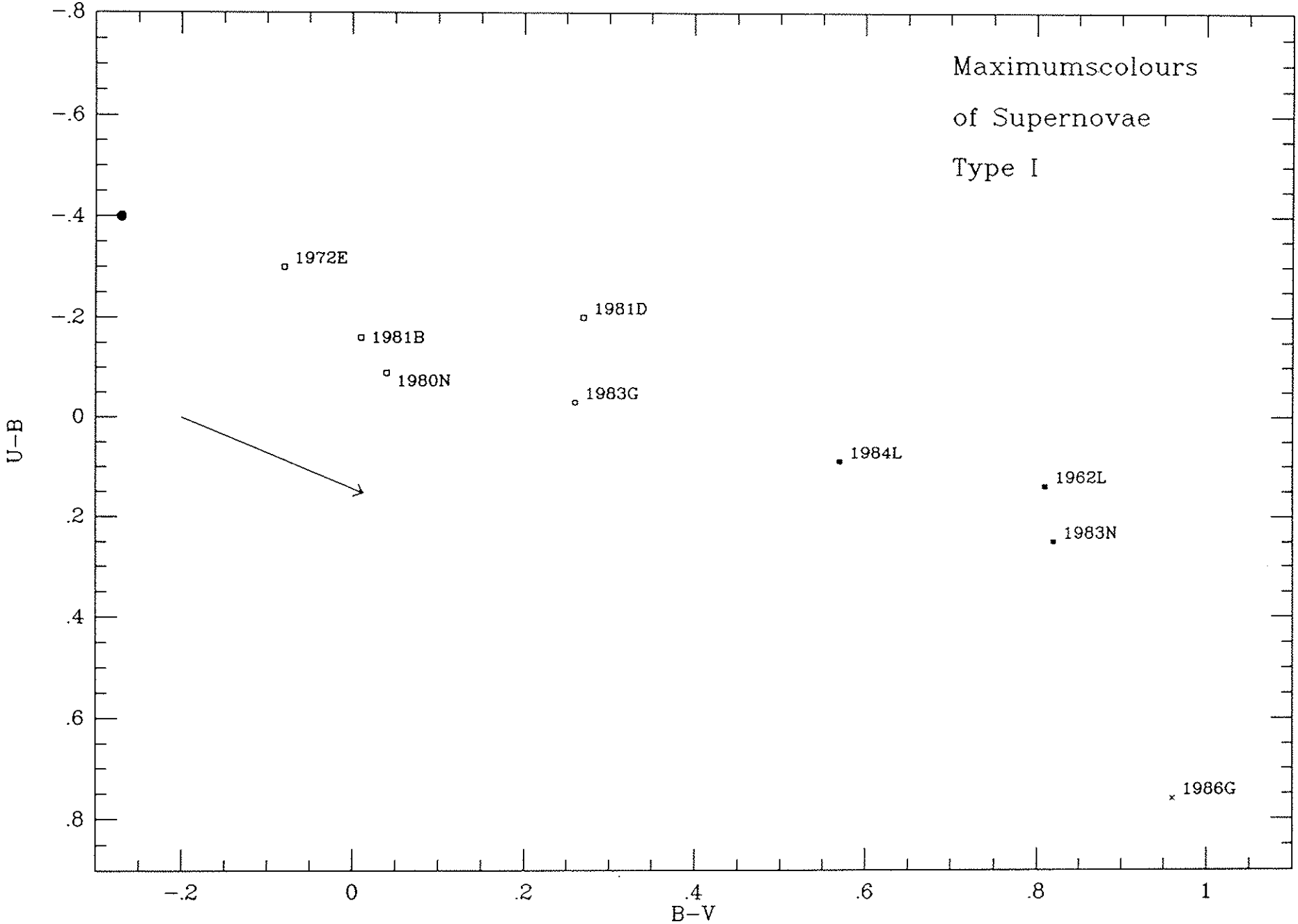
Maximumscolours
of Supernovae
Type I
1972E
1981D
1981B
1980N
1983G
1984L
1962L
1983N
1986G
U-B
B-V
-.8
-.6
-.4
-.2
0
.2
.4
.6
.8
-.2
0
.2
.4
.6
.8
1

Figure 41

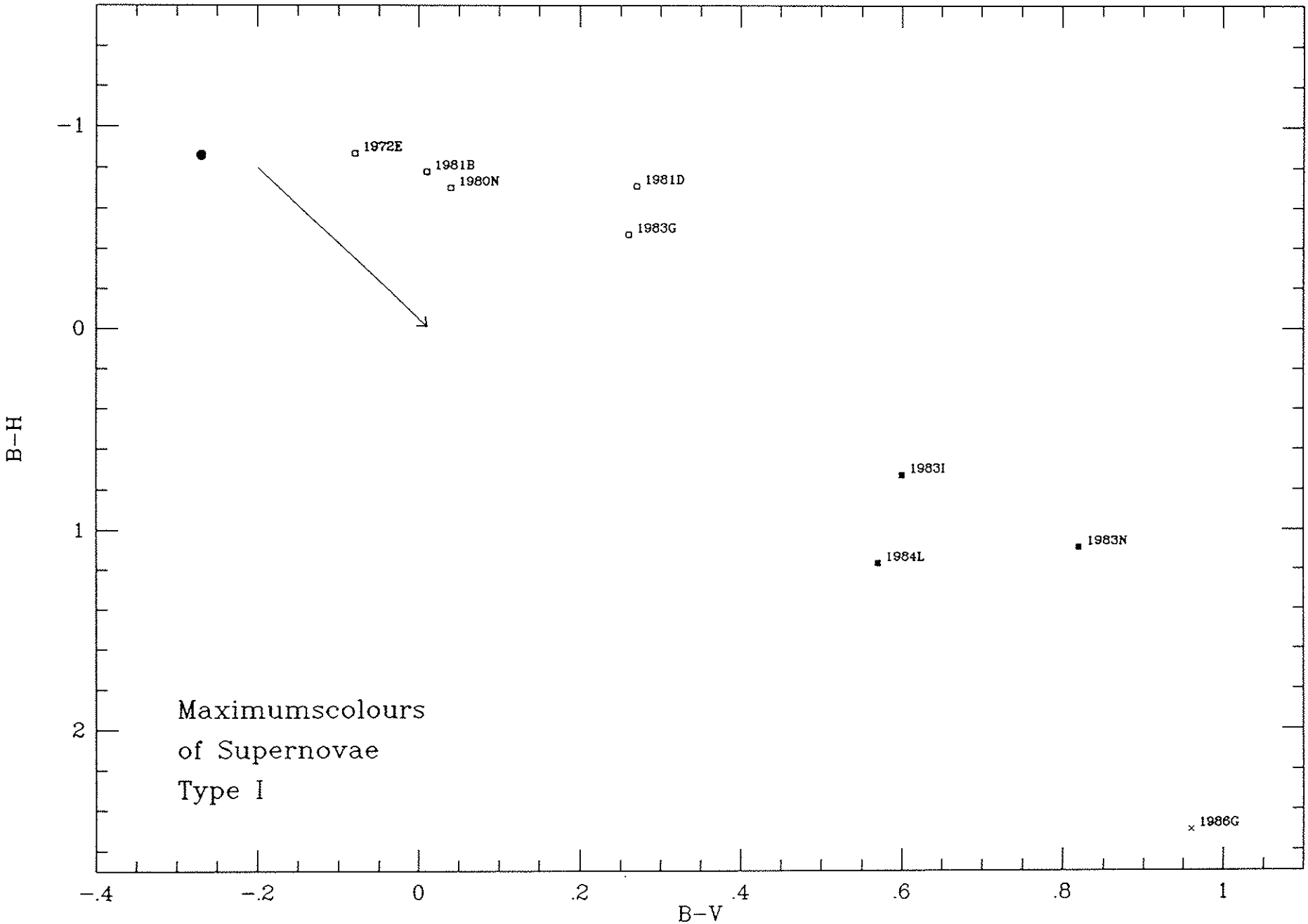
1972E
1981B
1980N
1981D
1983G
1983I
1983N
1984L
1986G
Maximumscolours
of Supernovae
Type I
B-H
B-V
−1
0
1
2
−.4
−.2
0
.2
.4
.6
.8
1

Figure 42

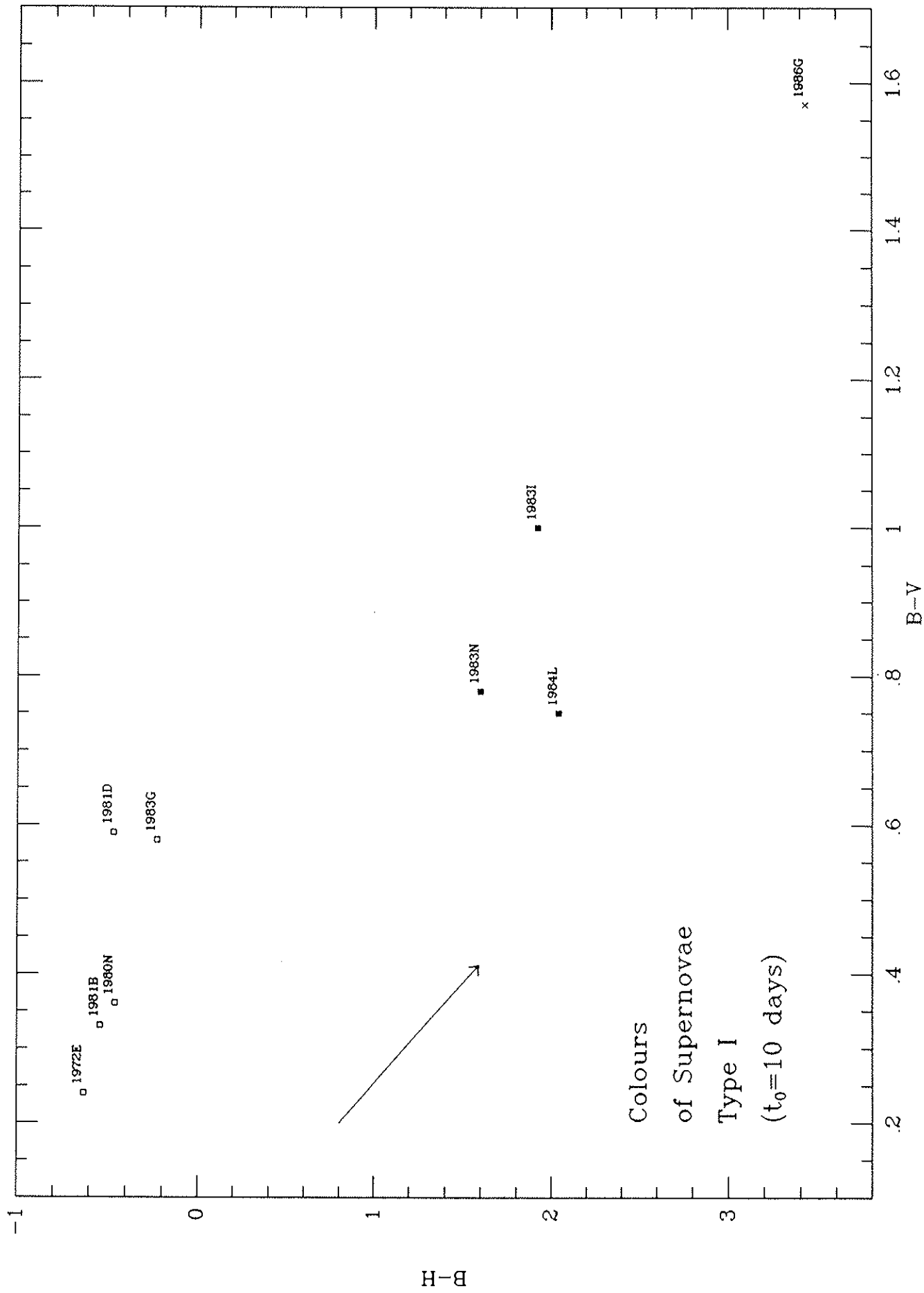
B−H
B−V
−1
0
1
2
3
.2
.4
.6
.8
1
1.2
1.4
1.6
1972E
1981B
1980N
1981D
1983G
1983N
1964L
1983I
1986G
Colours
of Supernovae
Type I
(t_0=10 days)

Figure 43

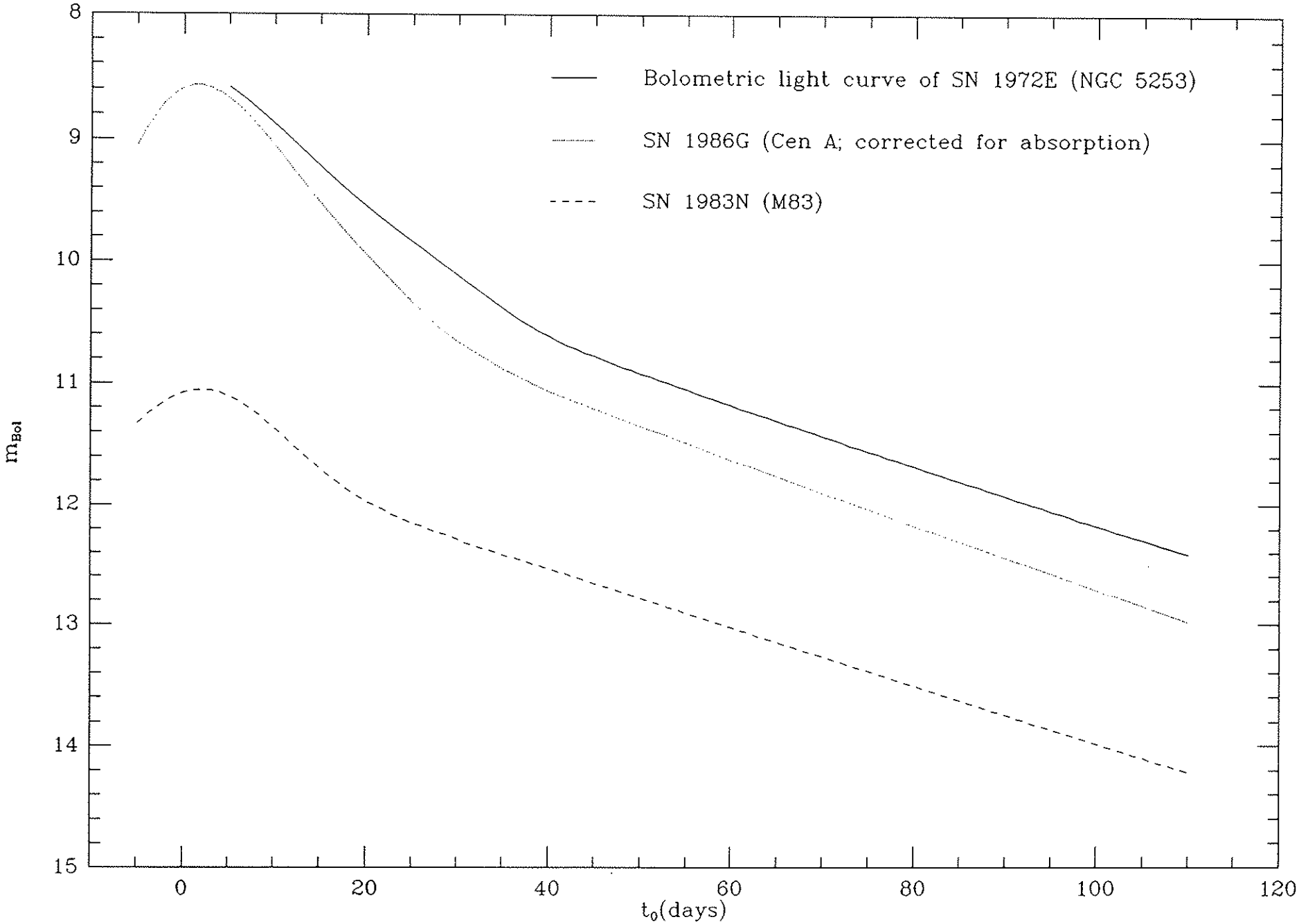
Bolometric light curve of SN 1972E (NGC 5253)
SN 1986G (Cen A; corrected for absorption)
SN 1983N (M83)
m_{Bol}
t_0(days)
8
9
10
11
12
13
14
15
0
20
40
60
80
100
120

Figure 44

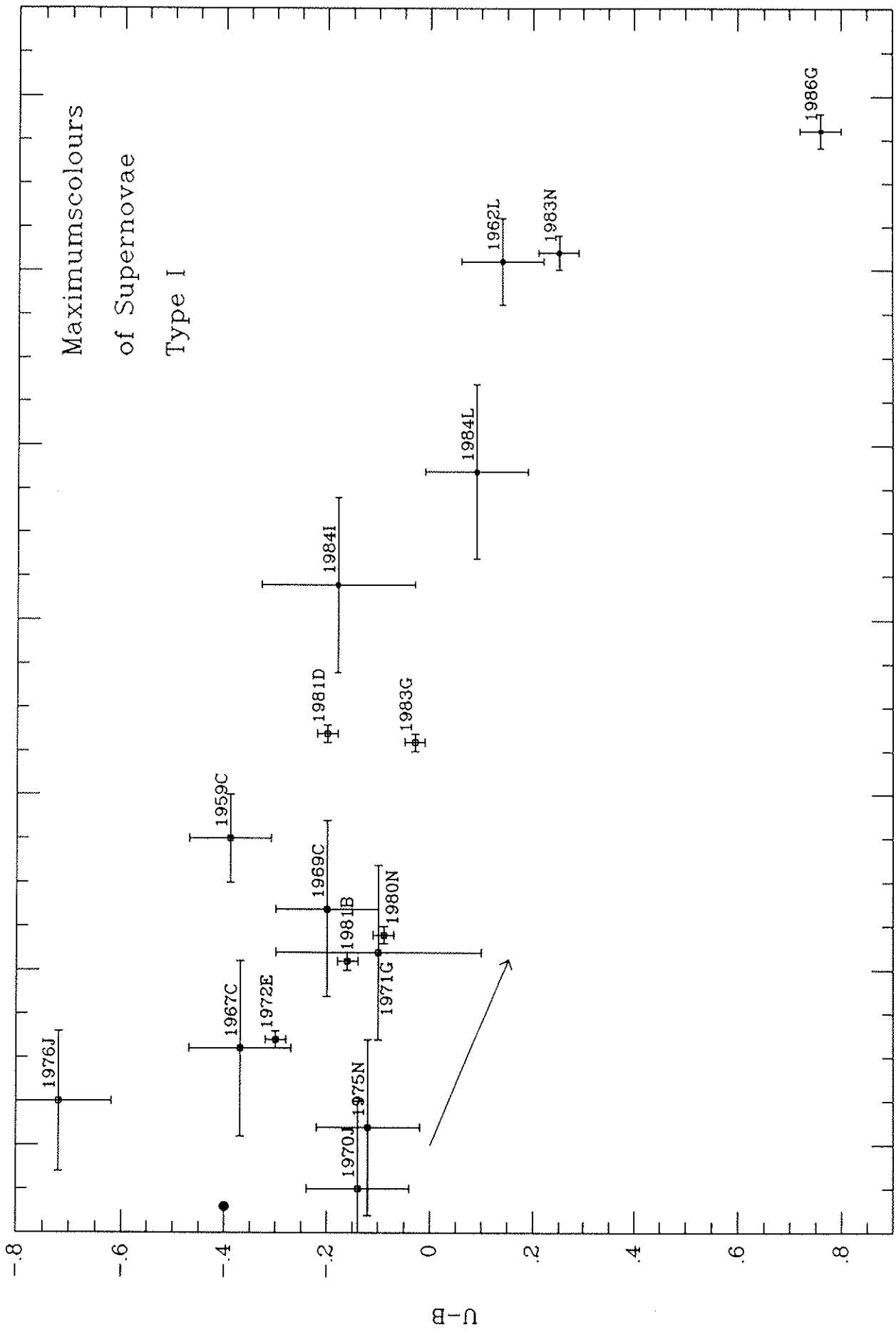
Maximumscolours
of Supernovae
Type I
1986G
1962L
1983N
1984L
1984I
1981D
1983G
1959C
1969C
1981B
1980N
1971G
1967C
1972E
1976J
1975N
1970J
U-B
B-V
-.8
-.6
-.4
-.2
0
.2
.4
.6
.8
1
-.2
0
.2
.4
.6
.8

Figure 45

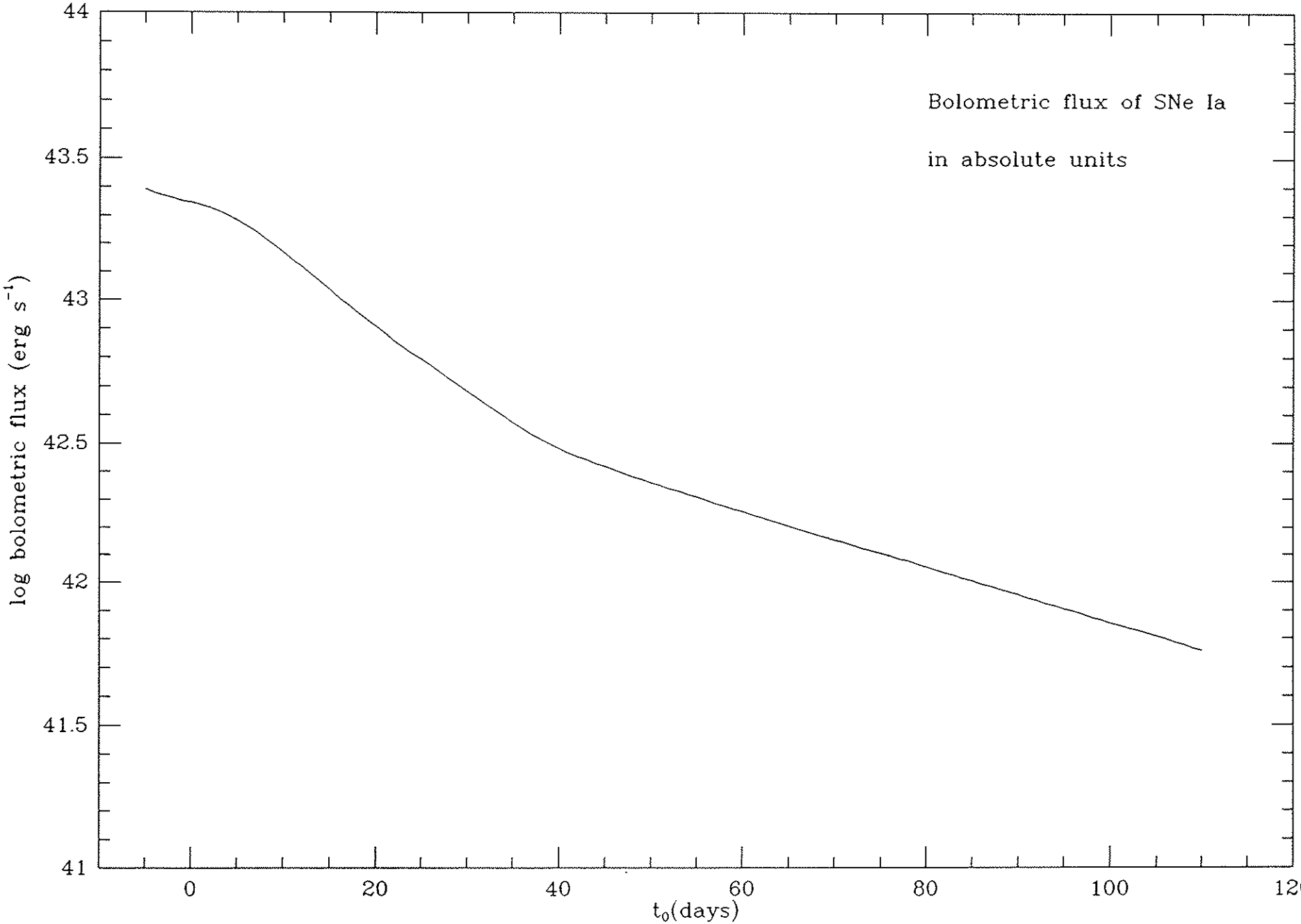
Bolometric flux of SNe Ia
in absolute units
log bolometric flux (erg s^{-1})
44
43.5
43
42.5
42
41.5
41
0
20
40
60
80
100
120
t_0(days)

Figure 46

Verdankungen

Zu besonderem Dank verpflichtet bin ich Herrn Prof.Dr. G.A. Tammann, der mit Geduld und Wohlwollen meine Arbeit unterstützte. Aus den anregenden und intensiven Diskussionen sind viele Ideen in diese Arbeit eingeflossen. Dank schulde ich auch meinen Arbeitskollegen und -kolleginnen am Astronomischen Institut, die immer ein offenes Ohr für meine Probleme hatten und viel Zeit opferten.

Dem Kanton Basel-Stadt und dem Schweizerischen Nationalfonds zur Förderung der Wissenschaft seien die finanzielle Unterstützung während der Erstellung dieser Arbeit gedankt.

Curriculum Vitae

Geboren wurde ich, Bruno Leibundgut, Bürger von Affoltern im Emmental (Bern), als Sohn des Paul Leibundgut und der Hermine, geborene Hauser, am 1. April 1960 in Basel. Hier besuchte ich auch die Primarschule, von der ich 1971 ins Humanistische Gymnasium Basel wechselte. 1979, nach Bestehen der Maturitätsprüfungen (Typus B) im Frühjahr, immatrikulierte ich mich an der Philosophisch-Naturwissenschaftlichen Fakultät der Universität Basel, wo ich im Hauptfach Theoretische Physik und in den Nebenfächern Experimentalphysik, Mathematik und Astronomie belegte. Nach Ausarbeitung einer Diplomarbeit unter Anleitung von Herrn Prof.Dr. D. Trautmann, schloss ich das Physikstudium mit Erlangung des Diploms für Theoretische Physik im Herbst 1983 ab. Mit Beginn des Jahres 1984 trat ich als wissenschaftlicher Assistent in das Astronomische Institut der Universität Basel ein, wo ich unter Betreuung von Herrn Prof.Dr. G.A. Tammann mit der Ausarbeitung meiner Dissertation über Supernovae begann. Während den Jahren 1984-1986 war ich hauptsächlich in einem Supernovasuch-Programm der Herren Tammann und Sandage (Pasadena) in Chile beschäftigt.

Am 2. Dezember 1988 habe ich Veronica Elisabeth, geborene Fergusson, geheiratet.

Meine Lehrer und Lehrerinnen an der Universität Basel waren folgende Professoren un Dozenten:

R. Buser, R.P. Fenkart, W. Mattig, U.W. Steinlin, G.A. Tammann (Astronomie); C. Bandle, W. Habicht, H. Huber, H. Kraft, B. Scarpellini (Mathematik); K. Alder, G. Backenstoss, E. Baumgartner, G. Baur, J. Fünfschilling, H.-J. Güntherodt, G.-R. Plattner, H. Rudin, R. Schilling, T.H. Schucan, F. Seiler, I. Sick, H. Thomas, D. Trautmann, R.D. Viollier, R. Wagner, I. Zschokke-Gränacher (Physik)